TID-4500, UC-48

ACRH-29

ARGONNE CANCER RESEARCH HOSPITAL
950 EAST FIFTY-NINTH STREET • CHICAGO • ILLINOIS 60637

Semiannual Report to
THE ATOMIC ENERGY COMMISSION

MARCH 1968

ALEXANDER GOTTSCHALK, M.D.
Editor

MARGOT DOYLE, Ph.D.
Associate Editor

OPERATED BY THE UNIVERSITY OF CHICAGO
UNDER
CONTRACT AT-(11-1)-69

DISCLAIMER

LEGAL NOTICE

This report was prepared as an account of Government sponsored work. Neither the United States, nor the Commission, nor any person acting on behalf of the Commission:

A. Makes any warranty or representation, express or implied, with respect to the accuracy, completeness, or usefulness of the information contained in this report, or that the use of any information, apparatus, method, or process disclosed in this report may not infringe privately owned rights; or

B. Assumes any liabilities with respect to the use of, or for damages resulting from the use of any information, apparatus, method, or process disclosed in this report.

As used in the above, "person acting on behalf of the Commission" includes any employee or contractor of the Commission to the extent that such employee or contractor prepares, handles or distributes, or provides access to, any information pursuant to his employment or contract with the Commission.

Printed in the U.S.A.
Available from the Clearinghouse for Federal Scientific and Technical Information, National Bureau of Standards, U.S. Department of Commerce, Springfield, Virginia 22151

Price: Printed copy $3.00; Microfiche $0.65

TID-4500, UC-48 ACRH-29

ARGONNE CANCER RESEARCH HOSPITAL
950 EAST FIFTY-NINTH STREET • CHICAGO • ILLINOIS 60637

Semiannual Report to

THE ATOMIC ENERGY COMMISSION

MARCH 1968

ALEXANDER GOTTSCHALK, M.D.
Editor

MARGOT DOYLE, Ph.D.
Associate Editor

OPERATED BY THE UNIVERSITY OF CHICAGO
UNDER
CONTRACT AT-(11-1)-69

TABLE OF CONTENTS

FLUORESCENT THYROID SCANNING: A NEW METHOD OF IMAGING THE THYROID*

By

P. B. Hoffer,† W. B. Jones,‡ R. B. Crawford,† R. Beck, and A. Gottschalk

A method has been developed for imaging the thyroid gland through the use of K-shell fluorescence. This work was stimulated by the pioneer efforts of Jacobson,[1] Edholm,[2] MacKay,[3] Heedman,[4] and Roy et al,[5] whose studies demonstrated the feasibility of radiologic detection of in vivo thyroidal iodine. Although it is well known that the thyroid gland selectively traps and incorporates significant amounts of iodine, it is not generally appreciated that the iodine content of the average thyroid gland is only .04 per cent by weight.[6] Nevertheless, this quantity is sufficient to act as the target in the system to be described.

The technique for imaging the thyroid gland presented in this communication incorporates the basic scheme of an x-ray fluorescent spectrometer. The equipment is a modification of the TMC Model 331 photon spectrometer used in conjunction with a dysprosium-159 radiation source. The dysprosium is placed in the flanges of a collimator, and a lithium drifted silicon crystal (30 mm^2 with 3 mm depleted region) is located behind the collimator in a low temperature vacuum chamber. A human thyroid gland, embedded in a plastic neck phantom serves as the target in this study, and is placed in front of the source detector system. The experimental set-up is illustrated in Figures 1 and 2.

Dysprosium-159 is used as the radiation source because it produces a reasonably monochromatic 44.5 KeV x-ray. This energy is above the K-shell edge of iodine which is 33.2 KeV. It is also high enough above the characteristic radiation of iodine not to interfere as background. When the 44.5 KeV source x-ray interacts with a K-shell electron in the iodine atom, a photoelectron is produced and a vacancy is created in the K-shell. An electron falls from one of the outer shells to replace it, and a characteristic x-ray is produced. The probability of this occurring is 87 per cent. When the electron is from the L-shell, the 28.5 KeV K_α characteristic x-ray is generated. When the x-ray is from the M-shell, the 32.3 K_β characteristic x-ray is generated. Production of K_α x-rays predominates over the production of K_β x-rays in a ratio of 7.5/1.[7] It is the K_α x-ray with a half-value layer in soft tissue of $\approx$ 2 cm that is used to produce the thyroid image in this system. The detector is a 30 mm^2 lithium-drifted silicon crystal with a depleted layer of 3 mm. The energy resolution of this crystal in the energy range of 30 KeV is better than 500 eV full width at one-half maximum at 78° K. The efficiency of collection is $\approx$ 66 per cent.

The target phantoms in this study consisted of normal thyroid glands (obtained at autopsy) fixed in formalin and embedded in a plastic (lucite) cylinder 9 cm in diameter. At no point was

---

*This report was presented before the Radiological Society of North America, Chicago, November, 1967, and appears in Radiology, 90:342, 1968.

†Department of Radiology, The University of Chicago.

‡Special Products Division of the Technical Measurements Corporation, San Mateo, California.

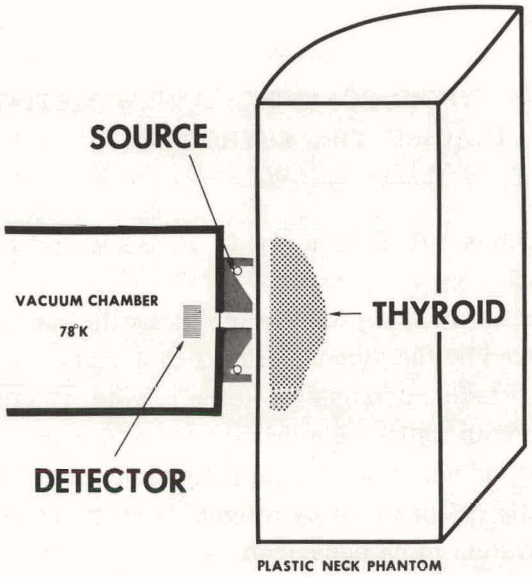

Figure 1. A diagrammatic representation of the fluorescent scanner. The source consists of two 0.3 microcurie dysprosium-159 encapsulated pellets; the detector is a lithium-drifted silicon crystal; and the collimator a single 1/8-inch straight bore hole.

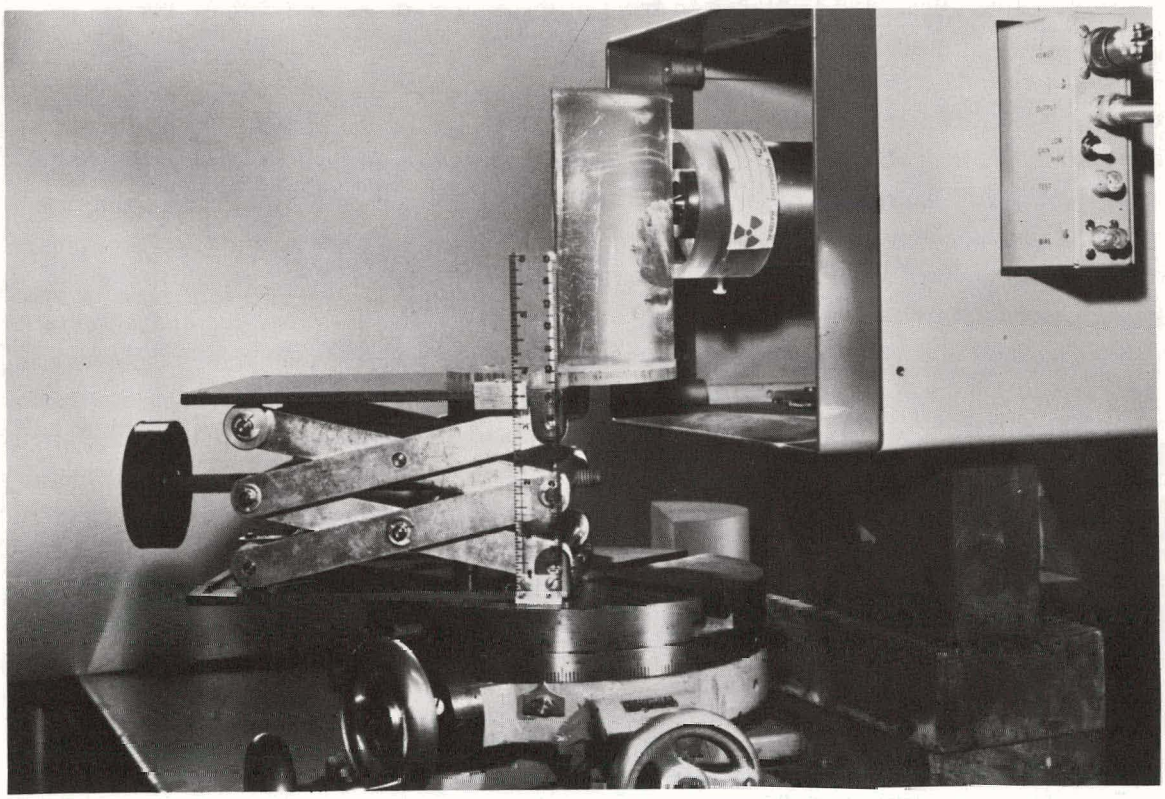

Figure 2. Actual photograph of the experimental set-up. The target phantom is made from a human thyroid gland imbedded in lucite.

the gland closer than 3 mm to the surface of the phantom, and the average thyroid mass had 1 cm of tissue equivalent over it. The neck phantom was then placed against the source-detector system and an image was obtained. Because a weak 0.6 millicurie dysprosium source was used, counts were collected at 7 mm intervals across the gland with a 7 mm vertical line separation rather than by a continuous scan. The time required for each interval count was 40 minutes. The signal from the crystal was amplified and recorded in a 400 channel analyzer. An x-y plotter was used to store information from each 7 mm interval. Figure 3 demonstrates an x-y plot

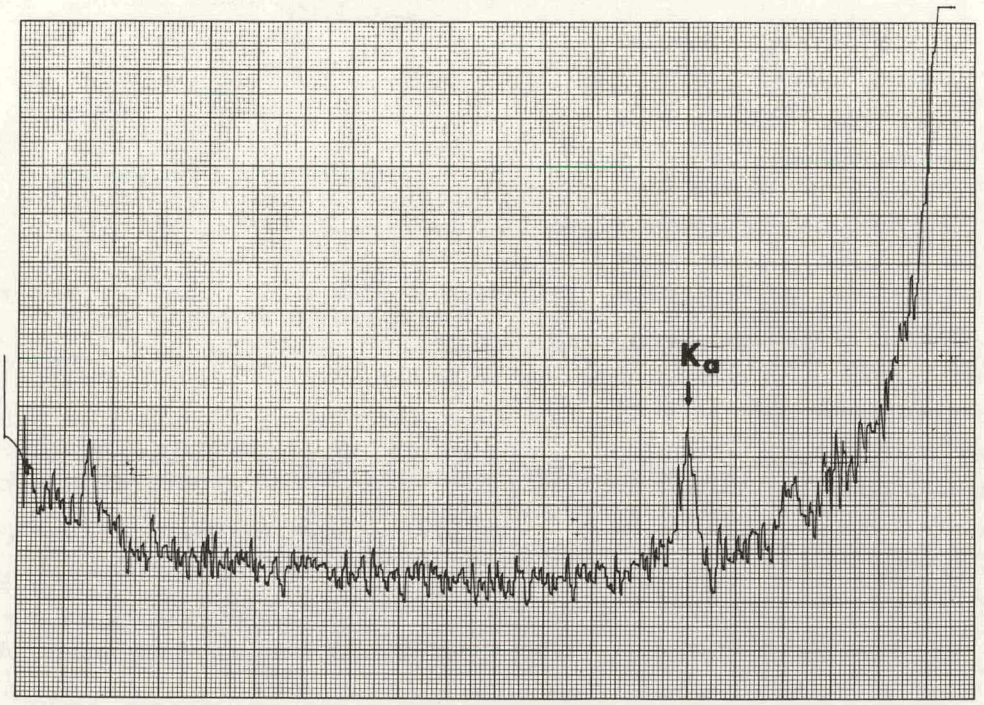

Figure 3. x-y plot derived from the multichannel analyzer. This matrix point was near the center of one lobe of the gland. The K_α peak (28.5 KeV) is easily identified above background.

of the multichannel recording from one of these interval points near the center of one lobe. The K_α peak is clearly seen above the background scatter radiation. The counts from the five channels centered at the K_α peak were integrated from the multichannel plot (12.2 channels per KeV). The five channels immediately above and immediately below the iodine peak were also integrated and subtracted as background from the peak counts. A numerical matrix was thus produced which represents the counts above background at each point. From this matrix, an isobar map of the thyroid was constructed (see Figure 4).

To determine the spatial resolution of the crude collimator used, a .002 inch molybdenum wire was placed in the phantom at a depth of 3 mm and scanned at 1 mm intervals. The curve produced had a full width at one-half maximum of 3 mm.

This system offers several advantages over conventional thyroid scanning. Patient irradiation is incurred only during the examination since no radioactivity is injected in the subject. The examination time is consequently dependent only on the strength of the dysprosium source

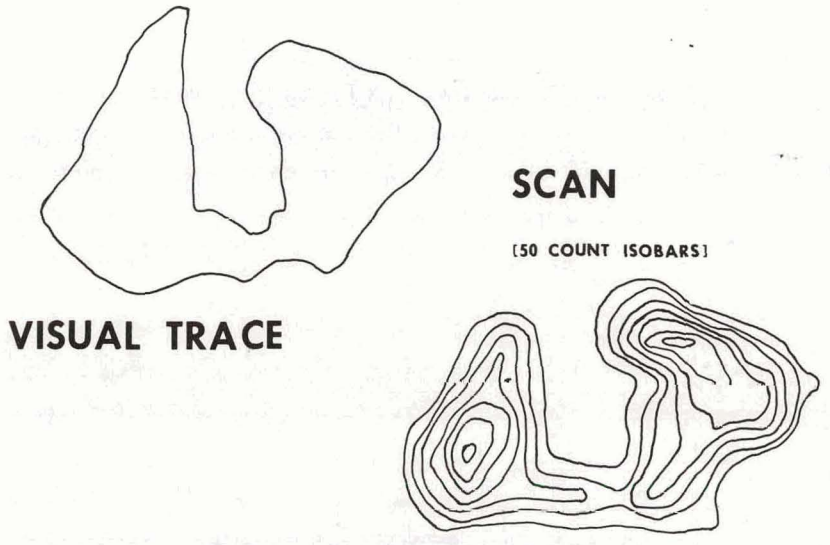

Figure 4. A comparison of the fluorescent scan with a visual outline of the thyroid gland in the phantom. The isobars are drawn at 50 count intervals above background.

used. These preliminary studies demonstrate that a thyroid image containing more than 8,000 total counts (maximum count density 700 per cm^2) can be obtained with a dose of but 500 m rads to the gland (see Appendix).

The potential of this technique seems particularly exciting because it adds a unique parameter to thyroid imaging. The fluorescent scan will provide information about the distribution of iodine in the thyroid, but gives only indirect information about gland function. As a result, it may prove to be most valuable when used in conjunction with conventional scanning. A battery of images utilizing the technetium pertechnetate scan, the radioiodine scan, and the fluorescent scan would thus provide information about thyroid trapping, hormone formation, and overall iodine distribution. It is even possible that the fluorescent scans of "cold" nodules would show differences in iodine distribution that might be characteristic enough to permit accurate diagnosis of the various etiologies responsible for these lesions.

Although no scans have yet been carried out on humans or animals, a scanner that will be suitable for such studies is in the process of construction.

APPENDIX

The anterior surface of the thyroid gland was chosen for dosimetry calculations because it is the portion of the gland closest to the radiation source, and therefore receives the highest dose. The measured air dose at the surface of the phantom was 700mR/hr. Since each point count required forty minutes of exposure, the surface air dose was 467 mR. The 3 mm of tissue between the phantom surface and anterior gland surface produced approximately 9 per cent attenuation. Backscatter was calculated to be less than 16 per cent. The dose at the surface of the thyroid gland was therefore approximately 500 m rads. Because a crude collimator system was used, the areas receiving the highest dose were those outside of the field of view of the collimated crystal. With an improved collimator, it should be possible to maintain a uniform 1 cm source to skin distance, thereby reducing the gland surface dose to 175 m rads.

Since both dose and count rates are directly proportional to source strength x time, increasing the source strength will allow a proportional decrease in counting time with no change in dose. To illustrate, our current counts were accomplished with a 0.6 millicurie source in forty minutes, giving an exposure of 0.4 millicurie-hours. It is feasible to increase the source strength to 160 millicuries. The counting time per point could then be reduced to about ten seconds, and the exposure would remain approximately 0.4 millicurie-hours. The matrix density we have used in our phantom is one point per 49 mm^2 or about 2 points per cm^2. Assuming a 100 cm^2 area to be scanned, 200 point scans would be required. With a 160 millicurie source, the counting time for the entire area would be 33 minutes. Since the points are not overlapping, the exposure would again be 0.4 millicurie-hours or approximately 500 m rads to the anterior thyroid gland surface.

ACKNOWLEDGMENT

We are especially grateful to Dr. Leonard Goodman of the Argonne National Laboratories for his invaluable assistance.

LITERATURE CITED

1. Jacobson, B. Acta Radiologica, 39:431, 1953.
2. Edholm, P., and B. Jacobson. Acta Radiologica, 52:337, 1959.
3. MacKay, R. S. I.R.E. Transactions on Bio-Medical Electronics, ME-7:77, 1960.
4. Heedman, P., and B. Jacobson. J. Clin. Endocrinol. and Metab., 24:246, 1964.
5. Roy, O. L., R. A. Beique, and G. L. D'Ombrain. I.R.E. Transactions on Bio-Medical Electronics, ME-9:50, 1962.
6. McGavack, B. A. The Thyroid. St. Louis, Mo., C. V. Mosby, 1951.

MODULATION TRANSFER FUNCTION FOR RADIOISOTOPE IMAGING SYSTEMS*

By

R. N. Beck

The modulation transfer function, MTF(ν), describes the response of a linear image-forming system to a sinusoidal object with spatial frequency ν[cycles/cm]. This is analogous to the temporal frequency response of an electronic amplifier or filter. The rationale for this description arises in a natural manner from the fact that any object and its image can be described in terms of the amplitudes and phases of their respective frequency components;[1] the MTF(ν) is simply a measure of the efficiency with which the modulation at each frequency ν is transferred by the imaging system from the object to the image, and is unaffected by the average or "DC component" of the object.

The MTF(ν) has been used in optics,[2] photography,[3] and diagnostic radiology[4] as a measure of spatial resolution which is more general than a single number, such as the resolving power for line patterns. The latter may be thought of as indicating the highest spatial frequency to which a system responds adequately. The need for this more general measure of resolution exists because image quality is not necessarily correlated with resolving power, since the high frequency response does not indicate how well an imaging system responds to object components of lower frequency.[5] In short, the intuitive notion that the system which best reproduces the small structures (high frequency components) in an object will certainly reproduce the large structures best, is false.

When applied to radioisotope imaging devices,[6,7] the MTF(ν) can be used to describe the response of a collimated radiation detector to a planar source of radioactivity (located at a distance z from the collimator face) in which the concentration varies sinusoidally with spatial frequency ν[cycles/cm] = $1/\lambda$, where λ[cm] is the wave length. Using the notation of Figure 1, the typical object component† is a plane-wave distribution, uniform in the y direction, described by

$$\sigma(x)\left[\frac{\text{photons emitted}}{\text{sec-cm}^2}\right] = \bar{\sigma} + \tilde{\sigma}(\nu)\sin 2\pi\nu x. \tag{1}$$

The (true mean) object modulation or contrast, $m_o(\nu)$, is defined by

$$m_o(\nu) \equiv \frac{\tilde{\sigma}(\nu)}{\bar{\sigma}} = \frac{\sigma_t - \sigma_o}{\sigma_t + \sigma_o} \tag{2}$$

When the detector axis is at the point x, this object structure gives rise to a detector count rate

---

*This report appears in part as a chapter in Handbook of Radionuclides ed. by John Cameron, published by the Chemical Rubber Co., Cleveland, Ohio.

†More explicit notation would indicate that this source is the differential element of a volume distribution of radioactivity, $\rho(x,y,z)\left[\frac{\text{photons emitted}}{\text{sec-cm}^3}\right]$, at a distance z from the collimator and at a depth z_o below the tissue surface, with effective source strength given by $d\sigma(x,y,z) = \rho(x,y,z)e^{-\mu z_o}dz$. In addition, it is assumed here that the frequency spectra for the x and y directions are identical, so that a one-dimensional treatment suffices.

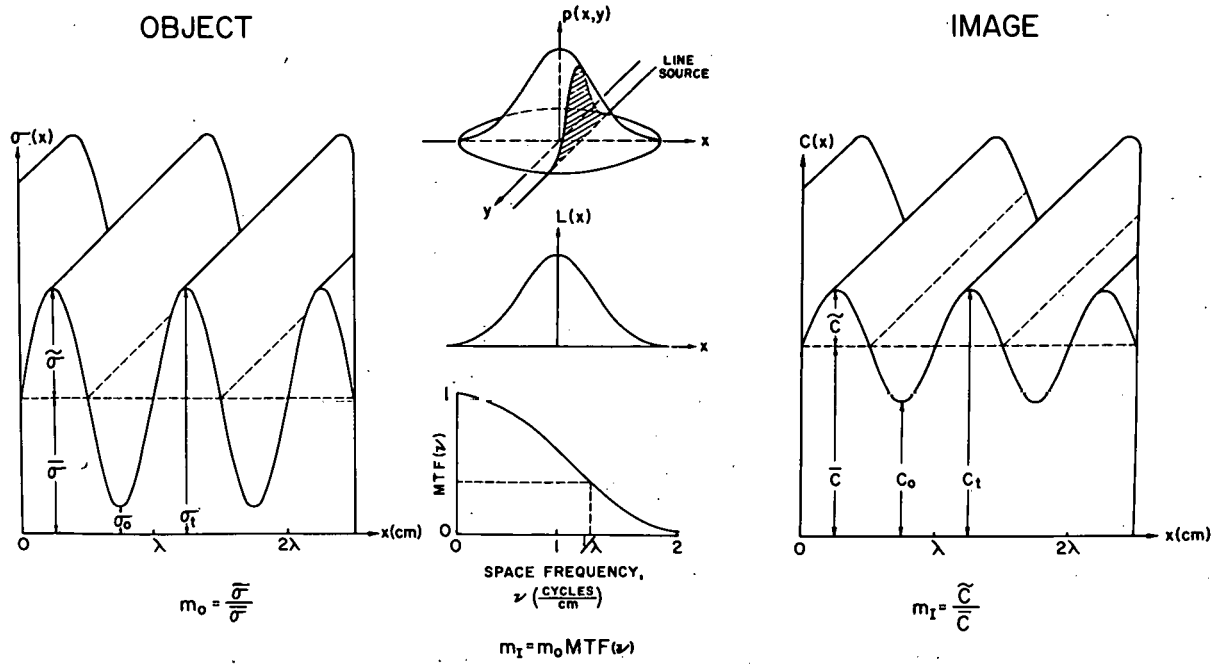

Figure 1.

with a true mean value C(x), which is also sinusoidal and described by

$$C(x)[\frac{\text{counts}}{\text{sec}}] = \bar{C} + \tilde{C}(\nu)\sin 2\pi\nu x. \tag{3}$$

Since this count rate gives rise to an image, the (true mean) image modulation or contrast, $m_I(\nu)$, is defined by

$$m_I(\nu) \equiv \frac{\tilde{C}(\nu)}{\bar{C}} = \frac{C_t - C_o}{C_t + C_o}. \tag{4}$$

The modulation transfer function is simply the ratio of image modulation to object modulation, defined by

$$MTF(\nu) \equiv \frac{m_I(\nu)}{m_o(\nu)}. \tag{5}$$

From equations (2) and (5) it is clear that MTF(ν) can be determined directly by measuring $m_I(\nu)$, described by equation (4), with a sinusoidal source for which $\sigma_o = 0$ and $m_o(\nu) = 1$ (or with any other sinusoidal source for which $m_o(\nu)$ is known). For these measurements, it is convenient to use as a test object a sinusoidal sunburst pattern of radioactivity which contains the useful range of ν.[6,7]

Alternatively, it has been shown[2,3,7] that the MTF(ν) can be determined from the line spread function, L(x), which describes the response to a uniform line source of radioactivity, parallel to the y-axis, and at a distance z from the collimator face (see Figure 2). In this case, MTF(ν) is equal to the Fourier transform of L(x), normalized so that MTF(o) = 1; that is,

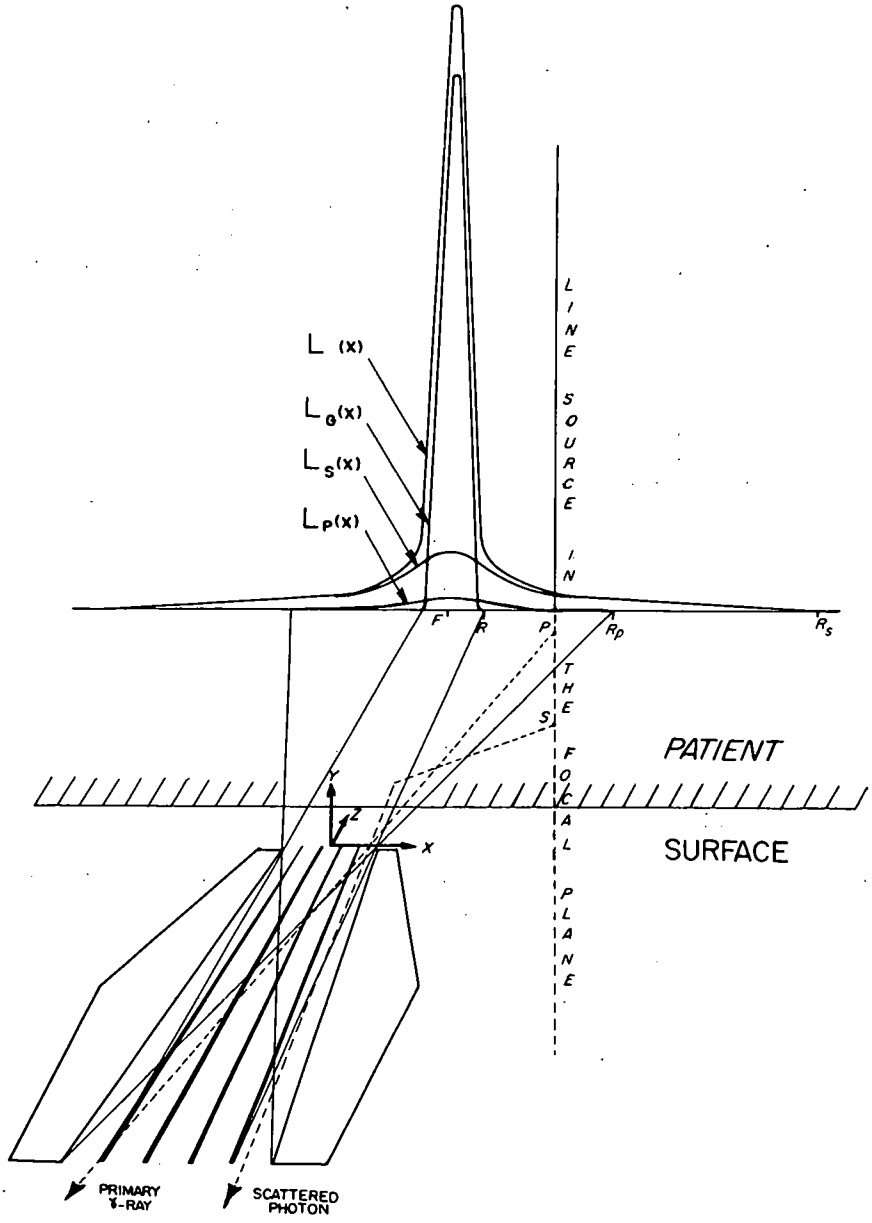

Figure 2. The line spread function, L(x), (depicted here for a line source in the focal plane at a distance z = F from the collimator face) consists of three principal components: (1) $L_G(x)$, due to properly collimated γ-rays emitted within the field of view with radius R. (2) $L_p(x)$, due to primary γ-rays emitted within the region with radius R_p, which penetrate the collimator septa, and (3) $L_S(x)$, due to γ-rays emitted within the region with radius R_S, which are scattered within the patient or collimator.

$$MTF(\nu) = \frac{\int_{-\infty}^{\infty} L(x) e^{-2\pi i \nu x} dx}{\int_{-\infty}^{\infty} L(x) dx}. \quad (6)$$

If L(x) is an even function, as is usually the case, equation (6) reduces to

$$MTF(\nu) = \frac{\int_{-\infty}^{\infty} L(x)\cos 2\pi\nu x\, dx}{\int_{-\infty}^{\infty} L(x) dx} \cong \frac{\sum_{j=1}^{m} L(x_j)\cos 2\pi\nu x_j}{\sum_{j=1}^{m} L(x_j)} \quad (7)$$

where $x_j = (j-1)\Delta x$, $j = 1,2,3 \ldots m$.

The approximation given in equation (7) provides a useful basis for computing MTF(ν) from measured values of L(x). To measure L(x), a line source in a small diameter polyethylene tubing 30 cm in length is recommended,[8] L(x) being measured over the range -15 cm $\leq x \leq$ + 15 cm. Because septal penetration and scattering within the collimator are energy-dependent phenomena, and both affect L(x), the measurements should be made with the isotope to be used in clinical practice. If scattering within the tissue is to be taken into account, the measurements are made with the line source in a suitable tissue-equivalent scattering medium. The result is an effective MTF for the particular isotope, scattering medium, collimated detector, and pulse height analyzer window setting. In this case the object is described simply by distribution of radioactivity, which also describes the distribution of emission of primary, unscattered, photons. Thus, the object is weakly self-luminous and embedded in a medium which both absorbs and scatters primary photons. The relative numbers of scattered and unscattered photons that emerge from the tissue-equivalent medium depend on the energy of the primary radiation, the dimension of the scattering medium, the depth of the radioactivity within this medium, et cetera. The radiation that enters the detector consists of both unscattered photons and a continuous spectrum of scattered photons with reduced energy. The portion of this radiation that ultimately contributes to the image depends on the collimator solid angle of view, the detector sensitivity and energy resolution, as well as the setting of the pulse height analyzer window. The net overall effect of any particular choice of this complex set of parameters can be described in terms of the response to a point source of radioactivity. This is called the point spread function, and is proportional to the sum of probabilities that a photon emitted at the point (x,y) in the z plane will enter the detector: (1) properly, or "geometrically"; (2) by penetrating the collimator septa or side walls; and (3) by scattering in the tissue or collimator. With these components indicated by subscripts $_G$, $_p$, and $_s$ respectively, the shape of the point spread function is given by

$$p(x,y) = p_G(x,y) + p_p(x,y) + p_s(x,y) \quad (8)$$

The shape of the line spread function is then given by

$$L(x) = \int_{-\infty}^{\infty} p(x,y)dy = L_G(x) + L_p(x) + L_s(x) \quad (9)$$

The total response to a uniform sheet distribution is proportional to

$$\int_{-\infty}^{\infty}\int_{-\infty}^{\infty} p(x,y)dydx = \int_{-\infty}^{\infty} L(x)dx = \int_{-\infty}^{\infty}[L_G(x) + L_p(x) + L_s(x)]dx = G(1 + P + S) \quad (10)$$

which defines G, the "geometrical efficiency" of the collimator,[7,9] and the penetration and scat-

ter fractions, P and S. The latter are measures of the responses due to penetration and scatter, respectively, relative to the geometrical response. [See Figure 1 for the relation between p(x,y) and L(x); Figure 2 for components of L(x) in relation to the collimator; Figure 3 for MTF components.]

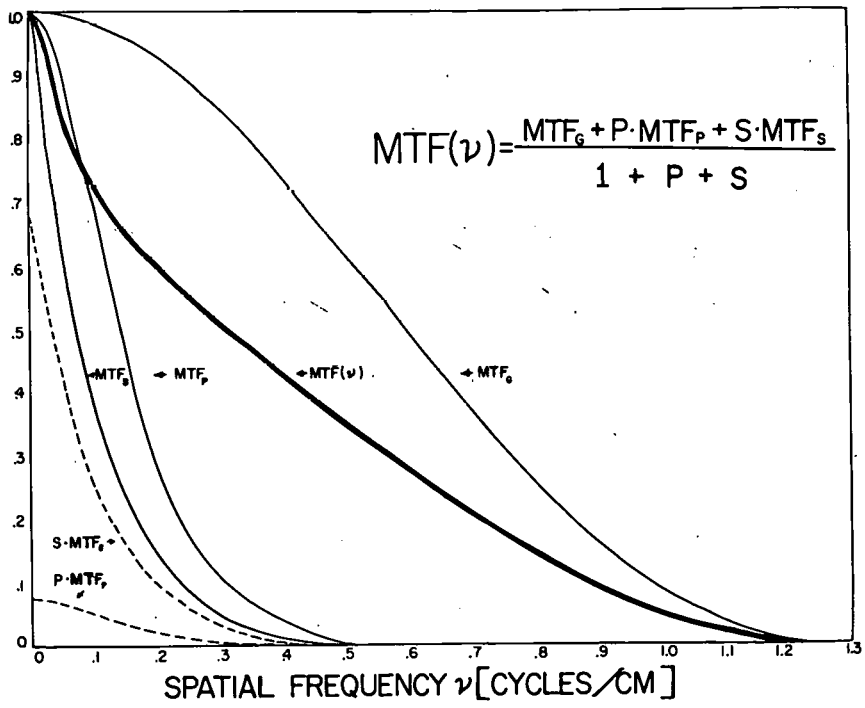

Figure 3. Large structures are partially resolved even by radiation that enters the detector by septal penetration and scattering processes (MTF_p and $MTF_s > 0$ for $\nu < .5$ cycles/cm or $\lambda > 2$ cm). This radiation simply reduces $MTF(\nu)$ for $\nu > .5$ cycles/cm.

The MTF due to properly collimated radiation alone is defined by

$$MTF_G(\nu) = \frac{\int_{-\infty}^{\infty} L_G(x) e^{-2\pi i \nu x} dx}{\int_{-\infty}^{\infty} L_G(x) dx} = \frac{\int_{-\infty}^{\infty} L_G(x) e^{-2\pi i \nu x} dx}{G} \tag{11}$$

Similarly, considering penetration and scatter responses separately, we can define

$$MTF_p(\nu) = \frac{\int_{-\infty}^{\infty} L_p(x) e^{-2\pi i \nu x} dx}{GP}, \tag{12}$$

and

$$MTF_s(\nu) = \frac{\int_{-\infty}^{\infty} L_s(x) e^{-2\pi i \nu x} dx}{GS} \tag{13}$$

From equations (6) and (10), the MTF due to the combination of these components of detector response is

$$MTF(\nu) = \frac{\int_{-\infty}^{\infty}[L_G(x) + L_p(x) + L_s(x)]e^{-2\pi i\nu x}dx}{G(1 + P + S)} \tag{14}$$

and using equations (11), (12), and(13), equation (14) reduces to

$$MTF(\nu) = \frac{MTF_G(\nu) + P \cdot MTF_p(\nu) + S \cdot MTF_s(\nu)}{1 + P + S} \tag{15}$$

If the collimator septa and side shielding are sufficiently thick, $P << 1$; furthermore, if the detector has good energy resolution, so that most of the scattered radiation can be eliminated by pulse height selection, $S << 1$.

In addition, the magnitude of each component $MTF_{G,\,p,\,s}$, depends on the shape, and especially the width, of the corresponding line spread component $L_{G,\,p,\,s}$, relative to the wave length $\lambda = \frac{1}{\nu}$. Near $\nu = 0$, λ is very large compared to the width of all these components, since all of them decrease at least as fast as the inverse of the distance from the detector axis. In this case, $\cos 2\pi\nu x \cong 1$ in equation (7), $MTF_{G,\,p,\,s} = 1$ in equation (15), and $MTF(\nu) = 1$.

In the mid-frequency range that is of primary interest (see Figure 3 for $\nu > .5$ cycles/cm), where λ is comparable to the width of $L_G(x)$, but small compared to $L_p(x)$ and $L_s(x)$, we find that $MTF_p(\nu)$ and $MTF_s(\nu)$ are small compared to $MTF_G(\nu)$, and equation (15) reduces to

$$MTF(\nu) \cong \frac{MTF_G(\nu)}{(1 + P + S)} \tag{16}$$

In this frequency range, penetration and scatter are essentially equivalent to background radiation* in the sense that they reduce the image contrast and contribute nothing to the formation of a structured image. In the high frequency range, $MTF_G(\nu) = 0$ also; thus the detector does not resolve very small structures.

It is clear from equation (7) that for $\nu = 0$, $\cos 2\pi\nu x = 1$ and $MTF(0) = 1$ for any line spread function $L(x)$. In addition, the normalization factor $1/\int_{-\infty}^{\infty}L(x)dx$ in equation (7) insures that $MTF(\nu)$ is independent of the magnitude of $L(x)$ [and, therefore, independent of such factors as the counting rate, counting time, concentration of radioactivity in the line source, et cetera]. On the contrary, $MTF(\nu)$ depends only on the shape of $L(x)$, which should be determined accurately, i.e., with negligible statistical error. In this way, the two main causes of poor image quality, namely distortion and noise, are separated experimentally as they are separated conceptually. In the context of scanning, distortion occurs primarily in the form of smoothing due to imperfect spatial resolution,[7] which is associated with decreasing values of $MTF(\nu)$ as ν increases. Noise, in the form of random fluctuation in the number of photons recorded per unit area, is associated with limited detector sensitivity[9] [in addition to limited source strength, scanning time, et cetera]. In practical systems, a compromise between resolution and sensitivity is required,[10] and this can be seen as a compromise between distortion and noise.

When the counting rate in equation (3) is written explicitly in terms of parameters used to describe the detector - pulse height analyzer system,[7] we obtain

*Here it is assumed that "background radiation" is independent of the source to be imaged, and is due to cosmic rays, radioactivity in the materials comprising the detector, et cetera. If C_b is the count rate due to such sources, it can be seen, by adding C_b to C_t and C_o in equation (4), that image contrast is thereby reduced.

$$C(x)\left[\frac{\text{counts}}{\text{sec}}\right] = G(1 + P + S)\eta\psi[\bar{\sigma} + MTF(\nu)\tilde{\sigma}(\nu)\sin 2\pi\nu x]. \quad (17)$$

Here, η is the photopeak crystal efficiency and ψ is the fraction of unscattered photopeak pulses passed by the pulse height analyzer.

In the mid-frequency range, where equation (16) holds, equation (17) reduces to

$$C(x)\left[\frac{\text{counts}}{\text{sec}}\right] = G\eta\psi[\bar{\sigma}(1 + P + S) + MTF_G(\nu)\tilde{\sigma}(\nu)\sin 2\pi\nu x] \quad (18a)$$

$$= \bar{C} + \tilde{C}(\nu)\sin 2\pi\nu x, \quad (18b)$$

where equation (18b) is the same as equation (3). Comparing equations (18a) and (18b), it is clear that, in the mid-frequency range, penetration and scatter contribute only to the average count rate, essentially as background radiation does.

If the scanning time per unit area is $t\left[\frac{\text{sec}}{\text{cm}^2}\right]$, the count rate in equation (18) gives rise to a true mean image defined by

$$C(x)t \equiv N(x)\left[\frac{\text{counts}}{\text{cm}^2}\right] = \bar{N} + \tilde{N}(\nu)\sin 2\pi\nu x \quad (19a)$$

$$N(x) = G\eta\psi t[\bar{\sigma}(1 + P + S) + MTF_G(\nu)\tilde{\sigma}(\nu)\sin 2\pi\nu x] \quad (19b)$$

Observed images will be distributed about N(x) with a standard deviation $S.D.[N(x)] = \sqrt{N(x)}$, or a fractional standard deviation given by

$$\varepsilon = \frac{S.D.[N(x)]}{N(x)} = \frac{1}{\sqrt{N(x)}} \quad (20)$$

The quantity ε is a measure of the statistical error or noise in the image due to random fluctuation of $\sigma(x)$. For a noise-free image, it is necessary that $\varepsilon = 0$; however, since N(x) is always finite in practice, image quality is always limited (to the extent that $\varepsilon > 0$) by noise.

Comparing equation (17) with equation (1), it is clear that C(x) can yield an undistorted image of $\sigma(x)$ only if $MTF(\nu) = 1$. From equation (16), this condition is satisfied in the mid-frequency range only if $MTF_G(\nu) = 1$, and $P = 0$ and $S = 0$. In practice, these conditions are never met, and to the extent that $MTF_G(\nu) < 1$, image quality is limited by spatial resolution.

Equation (19b) provides a useful description of the true mean image of a sine-wave distribution of radioactivity in terms that relate the noise and distortion to parameters which describe the situation. To summarize:

1. Noise in the image results from the fact that the scanning time, concentration of radioactivity, and sensitivity to properly collimated radiation are necessarily finite [$G\eta\psi t\bar{\sigma} < \infty$ implies that $\varepsilon > 0$].

2. Distortion in the image results from the limited spatial resolution for properly collimated radiation [$MTF_G(\nu) < 1$ implies that $N(x) \neq$ constant $\times\ \sigma(x)$].

3. Image contrast is further reduced by the response to essentially uncollimated radiation from the patient [P, $S \neq 0$ implies that

$$m_I = \frac{MTF_G m_O}{1 + P + S} < MTF_G m_O].$$

The total count rate due to a more complex source in the z plane is found by summing the count rates due to the average concentration of activity $\bar{\sigma}(z)$ and all frequency components

$\tilde{\sigma}(\nu,z)$. For a volume distribution of radioactivity, the total count rate is found by summing count rates from all z planes, taking attenuation into account.

The above analysis is based on the assumption that the radiation detector is linear; that is, the counting rate is proportional to the concentration of radioactivity. This assumption is valid for scintillation detectors over the range of concentrations usually encountered in scanning. Within the linear range, the same type of analysis can be carried out for a camera-type detector.[11,12]

If the recording device is also linear (and this may be the case even if film is used, provided that the object contrast is sufficiently low), the MTF of the scanning system is simply given by the product of the MTF's of the detector and recorder.

This analysis may be extended to include the MTF of the human visual system[10,13] under conditions where the latter is linear.

LITERATURE CITED

1. Elias, P., D. S. Grey, and D. Z. Robinson. J. Opt. Soc. Am., 42:127, 1952.
2. Lamberts, R. L. J. Opt. Soc. Am., 48:490, 1958.
3. Perrin, F. H. Soc. Motion Picture and Television Eng., 69:151 and 239, 1960.
4. Moseley, R. D. (ed.). Proceedings of the Second Colloquium on Radiologic Instrumentation, University of Chicago, 1964. Springfield: Charles C Thomas Publishers, 1965.
5. Blaschke, W. S. J. of Phot. Sci., Vol. 7, 1959.
6. Beck, R. N. In Medical Radioisotope Scanning, Vol. 1. Vienna: IAEA, 1964, p. 35.
7. Beck, R. N. The Scanning System as a Whole: General Considerations. In Fundamental Problems of Scanning. Springfield: Charles C Thomas Publishers, 1968.
8. Hine, G. J. Personal communication. IAEA Consultants' Meeting, Vienna, 1965.
9. Beck, R. N. Collimation of γ-Rays. In Fundamental Problems of Scanning. Springfield: Charles C Thomas Publishers, 1968.
10. Beck, R. N. Criteria for Evaluating Radioisotope Imaging Systems. In Fundamental Problems of Scanning. Springfield: Charles C Thomas Publishers, 1968.
11. Cradduck, T. D., S. O. Fedoruk, and W. B. Reid. Phys. Med. Biol., 11:423, 1966.
12. Gottschalk, A. Modulation Transfer Function Studies with a Gamma Scintillation Camera. In Fundamental Problems of Scanning. Springfield: Charles C Thomas Publishers, 1968.
13. Morgan, R. H. Am. J. Roentgenol., Rad. Therapy, and Nucl. Med., 93:982, 1965.

A VERSATILE INSTRUMENT FOR PHOTOSCAN ANALYSIS WHICH PRODUCES COLOR DISPLAY FROM BLACK AND WHITE PHOTOSCANS*

By

D. B. Charleston, R. N. Beck, J. C. Wood, and N. J. Yasillo

Over the past several years many different techniques have been devised in an attempt to present radioisotope scanning data in a form that is most useful for evaluation by a clinician. One such technique, color presentation of a scan display, has been given considerable attention and effort. Past experience has indicated that color scan displays are useful in the examination of scan pictures, provided the original data are not distorted by the color processing.

The desirability of the color scan presentation of scan readouts has been demonstrated by the many determined attempts to achieve it. The direct production of color scan readouts, the "re-scan" color method, the multiple exposure color technique, the hand-colored digital readout display, the closed circuit color television system, and the flying-spot-scanning color readout system are examples of the approaches made to achieve visual aid for scanning with the use of color.

Production of the original scan display in color has proved helpful in spite of the fact that the display is limited to a single color picture in which the colored contour intervals are fixed. The range of each color interval must be preset before the scan is made. In most clinical scanning procedures the operator is faced with the problem of preselecting the contour intervals with limited knowledge of what to expect in the way of maximum or minimum count rate. Considerable experience with patients and equipment has enabled some operators to produce useful color scans. Most systems that produce color scans directly depend on integration of count to determine rate levels for color contour selection and therefore are limited to the slower scan speeds to avoid scalloping and statistical "jitter" in color selection.

The re-scan technique proposed by Harris has been adapted to produce effective color pictures from scan data. This method involves scanning the original photoscan transparency with a device similar to an analog scanning densitometer. The amount of light transmitted through the negative is measured by means of a meter movement. As the meter moves, it inserts multicolored transparent film between a light source and the color film to be exposed. Different colors are inserted for different meter deflections. A mechanical linkage assures a one-to-one relationship between the scanned negative and the color film (usually Polaroid color film).

This process is relatively slow and the color film costs can be quite high if several rescans must be made to satisfy the observer.

Anger has produced some remarkable color scan pictures by multiple exposures of color film with light transmitted through both filters and the black and white scan transparency. The pictures certainly demonstrate the value of color scans as an aid to evaluation of scan readouts but this is not a simple routine process and the pictures are made primarily for the purposes of demonstration and exhibition.

---

*This paper was presented at an International Nuclear Medicine Symposium, Imperial College, London, England, September, 1967.

Several closed-circuit color television systems have been modified for the color analysis of black and white negatives and prints. A system of this type is simple to operate but must operate over a limited range of light intensity. If any part of the scan picture produces saturation of the vidicon tube the entire picture becomes distorted.

In an attempt to avoid the limitations of these systems, the Argonne Cancer Research Hospital group has had a flying-spot-scanning system under study for the past few years (Charleston, in press).

The system makes use of a cathode ray tube to generate a very short persistence spot which is focused by a lens onto a plane which holds a photoscan transparency. The light transmitted through the negative is collected by another lens and is projected onto the photo-cathode of a photomultiplier tube. The voltage output of this tube can be processed electronically in many ways before it is presented to the color television set (which is synchronized with the flying-spot-cathode ray tube) for display.

With the flying-spot-scanning color display technique, areas of activity can be mapped in color. Each area of equal (but different) exposure density is assigned a color to identify its relative level of activity. Many color combinations can be generated over a fairly narrow range of density levels. The system allows adjustment of the three color channels (red, green, and blue) to cover the entire range of film densities, from the most dense region just below saturation, to the least dense region just above the fog level of the film.

The color contour lines can be adjusted through this range of film densities making it possible to observe the exposure density that corresponds to the "hottest" spot of the scan. For black on white negatives the most dense region is "hot," for white on black negatives the least dense region corresponds to the "hottest spot." When these densities are established and labeled with color, it is a simple matter to normalize against this level for generation of other colored contours in regions of interest.

Three channels of continuously variable comparators with upper and lower pick-off levels are used to label (with color) "density intervals" at will. Since the colors are interchangeable and can overlap, a great number of color combinations can be achieved simply by turning knobs.

By narrowing down the "window" or range between upper and lower comparator levels for each channel it is possible to generate very sharp, fine-line contours which are identified by color.

The real impact of the technique can be realized while the operator is dynamically manipulating the enhancement and color labeling parameters. It has been our experience that an observer watching the dynamic changes as they take place will quickly notice even minor perturbations or discontinuities, although he would be hard pressed to pick out the same structure from a static display.

For direct quantitative analysis of count rates of film density, a film step-wedge of varying density can be used to quantify the various levels by matching colors on the calibration wedge with those generated from the scan film. A calibrated film step-wedge made with random pulses would probably be the most useful for these purposes.

One of the most promising features of this type of system for scan film analysis makes use of the differentiated output signal from the flying-spot-scanner. When a differentiated signal is fed to the television tube readout, the steeper density gradients within the film will be enhanced to a greater degree than the slowly changing gradients. This means that some fine structure in-

formation can be displayed (provided its gradients are significant) even though it may be partially obscured by gross structure in the film.

Variable differentiation circuitry has been built into the ACRH system to allow one to vary the degree of this type of enhancement. The differentiation of the output signal from the flying-spot-scanner produces a "shadow" effect which simulates a three-dimensional display of the photoscan. Hot spots can be made to look like hills, and cold spots like valleys, producing a topographic display.

The flying spot, as it sweeps across the scan negative, is transmitted through the film and detected by the photomultiplier, is essentially converting the spatial structure (lines per cm) within the exposed transparency to correspond to temporal signals (cycles per second) at the electrical output of the photomultiplier tube. It is therefore possible to operate on these electronic signals (cycles per second) in routine fashion with low pass electronic filtering, high pass filtering, and band pass filtering. The final display will have been subjected to spatial filtering by electronic means, similar in effect to the optical spatial filtering process suggested by Beck, Harper, Charleston, and Yasillo (1967). Band pass filtering studies are under way presently at the ACRH Hospital, and the preliminary results are most promising.

The system has additional flexibility in that magnification can be achieved electronically (by changing the flying-spot cathode-ray tube roster size) for "close-in" analysis of regions of interest to determine if there is some sub-structure information present in the magnified area. Minification, which has proved helpful for orientation, and in some cases valuable as a direct visual aid, can be achieved in the same manner as magnification.

Both the brightness control of the scanning cathode-ray tube and the variable high-voltage adjustment of the photomultiplier tube establish the central operating range of the system. It has been demonstrated that even bad photoscan negatives (either very dense or very thin), can be handled by the system as long as the film is not saturated or solarized.

Since the system generates only a single small spot at any one time, high level signals that may reach saturation in some areas do not disturb the rest of the display.

In practice this saturation effect is a most useful feature, especially in the differentiated mode of operation. The simulated peaks and valleys mentioned previously can be made to "plateau off" as the gain of the system is changed, leaving only the highest or lowest points in evidence on the display.

The system will process any film transparency, black on white, or white on black, to produce an image on a color television receiver in green, blue, red, yellow, purple, black, white, and shades of grey. The black on white can be inverted to produce an image of white on black, thus making the readout independent of the original scan polarization. Simultaneously varying amounts of differentiation, contrast, and brightness can be selected at will with or without colored contour lines, color area mapping, or spatial filtering.

At the present time this device is being used as a laboratory study tool. Past experience with the ACRH flying-spot-scanning system however, indicates that it offers considerable potential as a useful tool for clinicians.

LITERATURE CITED

Charleston, D. B. An Analog Approach to Scan Readout Data Manipulation and Enhancement. In Gottschalk, A., and Beck, R. N. (editors) Fundamental Problems in Radioisotope Scanning. Springfield, Illinois: Charles C Thomas Publishers (in press).

Beck, R. N., P. V. Harper, D. B. Charleston, and N. J. Yasillo. J. Nucl. Med., 8:286, 1967 (Abstract).

EXPERIENCE IN RADIOBIOLOGICAL DOSIMETRY WITH HIGH DOSE RATE ELECTRONS*

By

M. L. Griem, L. S. Skaggs, L. H. Lanzl, and F. D. Malkinson

In 1963, Carpender et al. reported their experiences with radiation therapy with high energy electrons using pencil beam scanning.[1] Before patients were treated, experiments to determine the lethal dose for 50 per cent death at thirty days were conducted on adult female mice with both high energy electrons and cobalt 60 gamma rays at 5 cm depth in a water phantom. The electron energy used was 30 MeV and the physical dose in the phantom was adjusted to equal both irradiation conditions for the mice. The relative biological effectiveness (RBE) was determined to be 1.00 ± 0.07, which represents the 95 per cent confidence limit. The paper also described the limited skin reaction observed in patients with this mode of electron beam therapy. In patient treatment, the 0.5 cm diameter beam is magnetically deflected in a scanning fashion over the treated area and the beam is scanned at the linear rate of 10 cm in 8.7 seconds. The beam delivers 1-microsecond pulses of electrons, and for clinical use and for the LD 50 determinations mentioned above a rate of sixty pulses per second was used. We wondered whether the lack of skin reaction observed clinically might be based on the possibility that the scan pattern, which is similar to that of a television raster, resembles treatment through a grid. Although we try to produce a nearly homogeneous surface dose, physical measurement of the inhomogeneity of the surface dose suggests that variations at the surface may be less than 10 per cent. Physical measurements with lithium fluoride dosimeters in a water phantom have been carried out near the surface and are shown in Figure 1. The lithium fluoride was placed at the bottom of a plastic unit density petri dish resting on unit density plastic. The depth of water over the lithium fluoride was varied to obtain the data plotted in Figure 1. This physical measurement does not explain the lack of skin reaction observed in the clinics. Another explanation for the lack of biological epidermal reaction at the surface might be postulated. The inhomogeneity of dose at the surface, although only about 10 per cent, might be sufficient to allow repopulation of the basal cell layer in the skin with partial reconstitution of basal cell population taking place between daily treatments. This might explain the lack of skin reaction.

We have used several biological indicators to study this lack of skin reaction. The skin of the pig was used to evaluate the erythema and other skin reactions that appeared to parallel the clinical observations.

Further evaluations of the electron beam have been carried out on the proliferating matrix cells of the mouse anagen hair. This system provides an in vivo biological method of small spatial resolution with which it is possible to measure the surface effects of radiation in vivo. By placing a tissue equivalent bolus above the skin the same system may be used to measure in vivo

*This report is taken from a paper that was presented before a Conference on High Energy Radiation Therapy sponsored by the New York Academy of Sciences, June 15-17, 1967, and will be published in the Proceedings thereof. The work was supported in part by U. S. Public Health Service Grant number RH-00280 and Research Career Development Award 5-K3-CA19415.

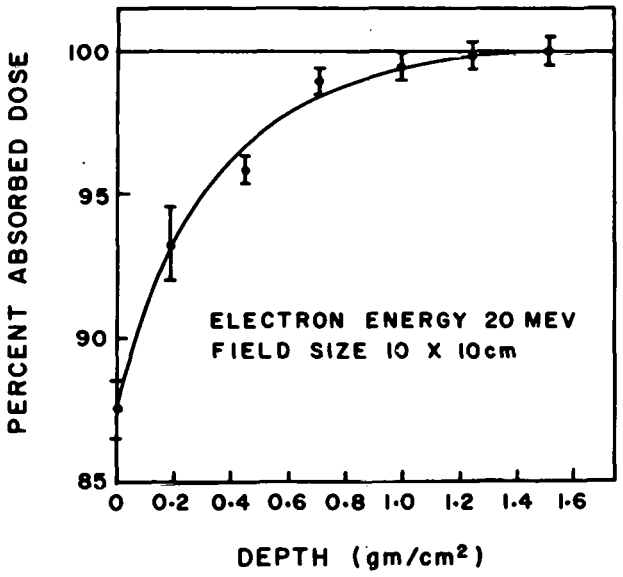

Figure 1. Physical dose measurements as a function of depth in a water phantom.

radiation effects in the tissue depth. The matrix cells in the hair bulb divide and differentiate to produce hair. We have scored the injury to regrowing rodent hair by counting the number of damaged or dysplastic hairs produced following irradiation of an anagen hair coat.[2] Unfortunately this system shows a rather large variation between individual animals. We have also reported on the use of tensile strength measurements of irradiated rat whiskers as a means of biological intercomparison of different types of ionizing radiation.[3]

Recently we have been using the incorporation of radioactive serine into hair keratin as a measurement of hair shaft production, and have found that irradiation of hair depresses this system, the depression being dose dependent.[4]

All studies were carried out in three-month-old Carworth Farms #1 female mice according to the following technique.[5] In this strain of mouse the active phase of hair growth or anagen lasts from seventeen to twenty days, and can be induced by plucking. Following the active growth period the follicles are inactive for a variable length of time. Twenty-four days after initial plucking, when the hairs have entered the inactive phase, the mice were again plucked to induce the active phase of growth. Twelve days later, on the twelfth day of anagen, groups of mice received a single dose of irradiation under sodium pentabarbitol anesthesia. During irradiation the anesthetized animal was positioned with its left flank in a hollow in a block of uniform density material. The right flank was thus exposed to the source of radiation, the electron beam entering the right flank and emerging from the left flank. Two days after the single irradiation, on the fourteenth day of anagen, all animals were given 3 to 5 microcuries of tritiated serine (specific activity 25 millicuries per millimole) intravenously. On the twenty-fourth day, when the hair was again in the resting phase, both flanks of each mouse were plucked for study. Hair samples were weighed and placed in a combustion apparatus in the presence of oxygen. The tritiated water produced by the combustion was assayed in a liquid scintillation spectrometer by a modification of the method described by Schöninger.[6] Hair samples from control and

irradiated sites were counted individually. By proper experimental design the data could be analyzed on a computer using a second order of analysis of variance. The data in Table 1 were obtained at exposures of 300 rads, 500 rads, and 600 rads.[7] At the low dose of 300 rads, serine uptake in the hair was depressed equally at both exit and entry portals. At moderate doses of 500 and 600 rads, the ratios of right to left sides were respectively 1.18 and 1.13. Averaging these determinations, one obtains a figure of 1.15. Comparing data obtained at the surface of the right flank, and at 2.5 cm through the mouse on the left flank, with the graph presented in Figure 1, the difference between the surface dose and plateau dose would be a factor of 1.12 or a build-up factor of 12 per cent.

Table 1

REDUCED LEVELS OF ^{3}H-DL-SERINE IN MOUSE HAIR FOLLOWING ELECTRON BEAM IRRADIATION IN ANAGEN

(Percentages are expressed as an average ratio of DPM/mg of the beam entry side (R) to the beam exit side (L) for each individual animal.)

Dose (rads)	Animals	DPM/mgL (beam exit side)	DPM/mgR (beam entry side)	R/L%	Standard error of the mean
300	8	2340	2044	95	13
500	9	2619	2978	118	12
600	26	322	365	113	4
No radiation (control group)	7	3131	3097	100	4

These effects may be entirely due to the depopulation of the matrix cells, but inflammation and changes in the vascular dermal papilla and vascular changes in the deeper structures of the dermis may also play a part. Since the mouse was lying in the phantom, the left flank through which the beam emerged might have been in a slightly anoxic state, which might "understate" the scored injury at the site of exit.

A second series of experiments has been conducted in vitro in mammalian cells using a line of Chinese hamster cells grown in tissue culture. This cell line was obtained from Dr. Warren Sinclair of the Argonne National Laboratory. These cells have been used as an asynchronous population and survival curves have been determined at 250 keV and with the electron beam. We have been interested in exploring the use of the scanning electron beam in two modes of operation. The usual mode of operation consists of 1-microsecond pulses of radiation delivered at a rate of sixty pulses per second as the beam traverses the irradiated area. In a second mode, with the same scanning speed, and 1-microsecond pulses, a rate of six pulses per second was used. The beam current was adjusted to provide equal average physical doses at the surface of a unit density phantom. That surface dose was measured with lithium fluoride and compared with calorimetric and current measurements of the beam. All measurements compared favorably with each other. Absorbed doses at the surface of the phantom of 200, 600, 1000, 1300, 1800, and 2200 rads were then used in the tissue culture experiments. Petri dishes of unit density plastic were suspended over the electron beam which was directed vertically upward. The tissue culture cells lie on the bottom of the petri dish, covered with a 0.5 cm layer of nutrient medium.

Above this is a small air space, and the petri dish is then covered with 3 cm of tissue equivalent plastic. Figure 2 gives data from three experiments carried out in this manner. The solid line represents one experiment and is the survival curve for graded doses of radiation using sixty 1-microsecond pulses of radiation per second. The dotted line represents two experiments

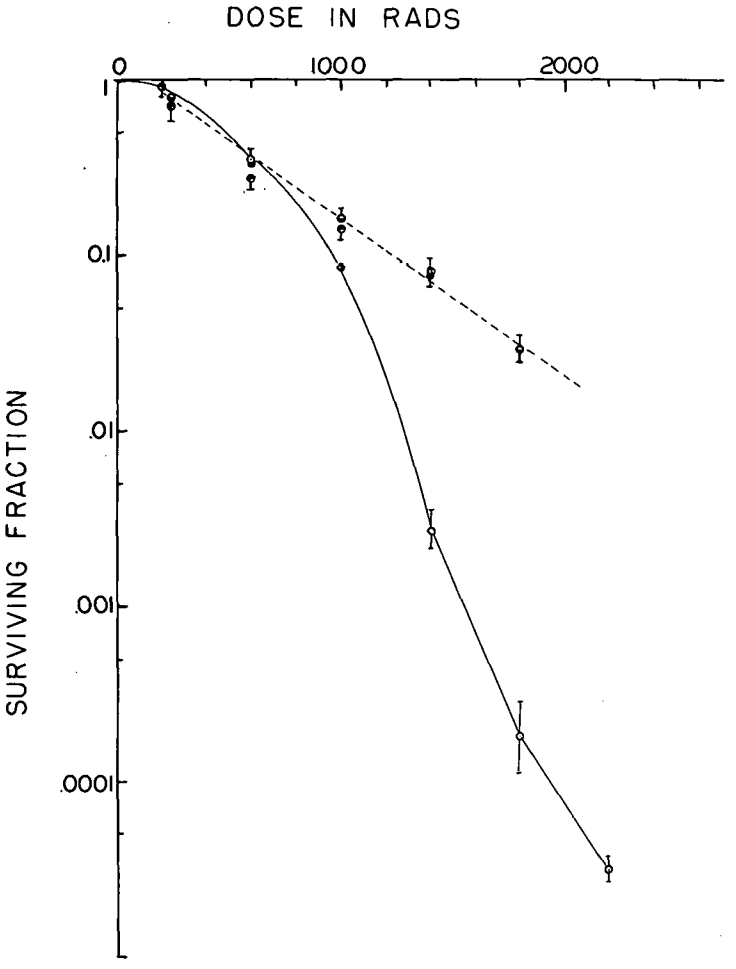

Figure 2. Survival curve for Chinese hamster cells as a function of dose. Solid line represents cell survival for sixty pulses per second. Broken line represents survival for six pulses per second.

using six, 1-microsecond pulses of radiation per second. The vertical bars represent the standard deviation. Three culture plates were exposed for each determination. Because of contamination with mold, two culture plates at 1000 rads were discarded and no standard deviation is given for this point. The solid line shows a curve with a shoulder and a straight portion and resembles the curves obtained with experiments using 250 keV radiation. The dotted line shows a more or less linear response to increasing exposures of radiation at a tenfold increase in dose rate.

At this point we can only estimate the dose rate at which radiation is delivered to the cell, since an object the size of a single cell approximately 10 microns in diameter receives approxi-

mately twenty-seven pulses of 1 microsecond's duration when the pulse frequency is sixty per second. If the dose received by the cell is 600 rads, each pulse would contain approximately 22 rads. The dose rate averaged over the 1-microsecond pulse is then 22 x 10^6 rads per second. In addition, the pulse is further modulated by the accelerated radiofrequency, so that 2856 bunches or groups of electrons arrive during each microsecond pulse. The duration of each bunch of electrons is not known accurately, but with the sharp energy collimation used, it cannot be appreciably greater than 1/20 of the inter-bunch interval and may easily be as short as 1/50 of that interval. Thus when the surface dose is 600 rads and the pulse frequency is sixty per second the modulated pulse could have dose rates of 400 to 1000 x 10^6 rads per second. When the pulse frequency is six pulses per second, and the average surface dose is 600 rads, the dose rate would be increased to 4 x 10^9 rads per second or might be as high as 10^{10} rads per second. An explanation of the curves presented in Figure 2 may be that these high dose rates deplete cellular oxygen. Our observations may be similar to those reported by Dewey and Boag[8] and Epp and co-workers,[9] and the unpublished observations of Hall and Berry.[10] In the experiments by Epp the instantaneous rate of dose delivery was of the order of 10^{12} rads per second in studies conducted on bacterial cells of the strain Escherichia coli, B/r.

These reports as well as our own may represent a phenomenon of depletion of intracellular oxygen. Most of the oxygen may be consumed during the first portion of the pulse of radiation, the remainder of the dose being delivered during relative cellular anoxia.

LITERATURE CITED

1. Carpender, J. W. J., L. S. Skaggs, L. H. Lanzl, and M. L. Griem. Am. J. Roent., Rad. Ther. & Nuc. Med., 90:221, 1963.
2. Griem, M. L., F. D. Malkinson, and P. H. Morse. Radiology, 77:486, 1961.
3. Griem, M. L., and R. J. M. Fry. Abstract #109 in First International Conference on Medical Physics. Abstracts of Papers. Yorkshire, England: Harrogate, 1965, p. 102.
4. Malkinson, F. D., and M. L. Griem. Abstract #584 in Third International Congress of Radiation Research. Book of Abstracts. Cortina D'Ampezzo, Spain: 1966, p. 147.
5. Malkinson, F. D., and M. L. Griem. Biology of the Skin and Hair Growth. Proceedings of a Symposium held at Canberra, Australia, August, 1964.
6. Schöniger, W. Microchim. Acta., 123, 1955.
7. Lanzl, L. H., F. D. Malkinson, and T. J. Ahrens. Presented at the 13th International Congress of Dermatology, Munich, July-August, 1967.
8. Dewey, D. L., and J. W. Boag. Nature, 183:1450, 1959.
9. Epp, E. R., H. Weiss, and A. Fenlon. Abstract #Fd-8 in Abstracts of Papers for the 15th Annual Meeting of the Radiation Research Society. San Juan, Puerto Rico: 1967, p. 118.
10. Hall, E., and R. Berry. Personal communication from Eric Hall, 1967.

RELATIONSHIP BETWEEN ORGAN DOSE FROM HIGH-ENERGY* ELECTRONS AND FILM BADGE READINGS

By

L. H. Lanzl and M. L. Rosenfeld

The correlation between the organ dose on or within the human body and the exposure† determination as recorded by a personnel film badge monitor is of great importance when these readings are used in an attempt to establish dose to the various organs of the body. In the case of small-beam irradiations, as distinguished from whole-body irradiations with large beams or generalized sources, this correlation can be large, small, or even nonexistent. This observation has validity for many types of radiations, including high-energy electrons.

This paper reports some observations made in connection with a serious radiation accident involving high-energy electrons (10 MeV), and resulting in amputation of an arm and a leg of a radiation worker.[1]

MEASUREMENTS

In the course of this study it was found that not all film badge concerns have the capability to calibrate, and thus interpret, films exposed to high-energy electrons.

In order to understand both the film badge response and the distribution of biological damage for electron beams, the central axis depth dose distribution in a rectangular water-equivalent phantom was measured with film‡ techniques. Film data were cross-checked with Sievert ionization chambers.§

An example of the results for a 10 MeV monoenergetic electron beam with a 10 cm by 10 cm field is shown in Figure 1. The depth dose curve shows a high surface dose, namely, 87 per cent of the peak, with a dose plateau occurring from two to two and one-half centimeters deep. The initial rise of the depth dose curve is due to a build-up of dose from secondary electrons, which can be accounted for on theoretical grounds.[2,3] Unlike x- or gamma ray beams, a sharp fall-off occurs from three to five centimeters depth. The dose beyond six centimeters is a few per cent of the peak dose, and is due to the absorption of bremsstrahlung which were produced by the electrons in the first five centimeters of the phantom.

A typical commercial film badge was exposed to the same 10 MeV monoenergetic electron beam (see Figure 2). The film used to obtain the results in this figure was the sensitive emul-

---

*This paper was presented at the Topical Symposium on Personnel Radiation Dosimetry of the Health Physics Society, Chicago, Illinois, January 30, 31, and February 1, 1967, and is published in the Proceedings thereof.

†The term "exposure" is used in this paper in its conventional sense and not in the sense of the ICRU definition, which applies to x- and gamma rays only.

‡Adlux film, Photo Products Department, E. I. Du Pont de Nemours and Company, Wilmington 98, Delaware, and Kodak Industrial AA x-ray films, Eastman Kodak Company, Rochester, New York, were used.

§The Alderson Research Laboratories, 729 Canal Street, Stamford, Connecticut, are licensed to manufacture the Sievert chambers in the United States.

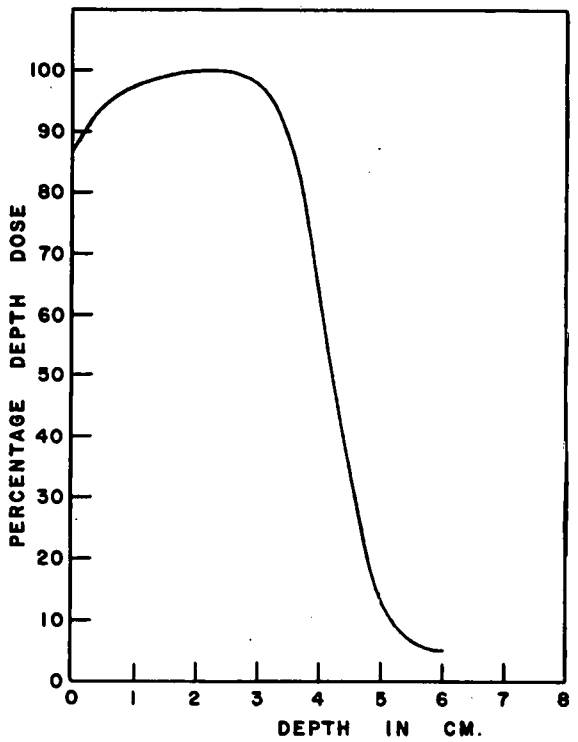

Figure 1

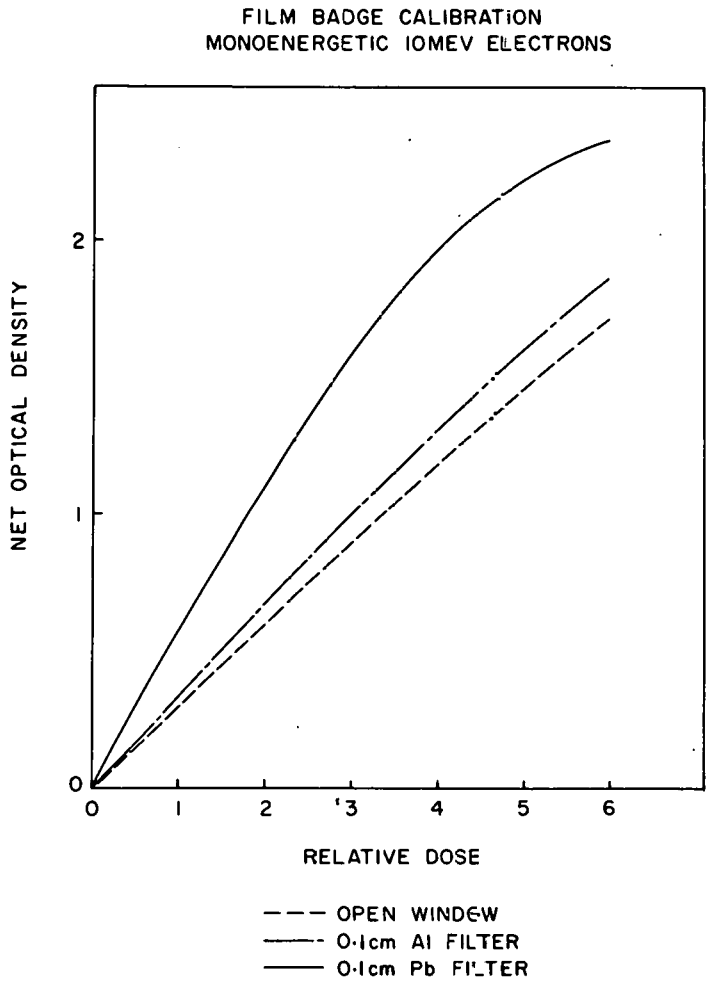

Figure 2

Figure 1. Central axis depth dose distribution for a 10 MeV monoenergetic electron beam for a 10 cm by 10 cm field. The phantom material used was of unit density.

Figure 2. Net optical density of Kodak Type 2 Film vs relative electron dose within a typical commercial film badge.

sion of Eastman Kodak personal Monitoring Film, Type 2. The water-equivalent thickness of the medium filter (0.1 aluminum) is 0.27 cm, and of the heavy filter (0.1 cm lead) 1.11 cm. Superposition of these particular filter thicknesses on the depth dose curve would show them to be on the ascending part of the curve. Thus, one would expect greater film blackening with the aluminum filter and still more with the lead filter than with the open-window part of the badge. As shown in Figure 2, this is indeed the case. For any given dose, then, the degree of blackening increases as the mass per unit area of the filter (provided, of course, that the film is not overexposed, so as to cause film reversal). On a qualitative basis, it appears that the blackening is greater under the lead filter, as would be expected solely on the basis of depth dose argument presented above. This is due most likely to an increased number of secondary electrons coming from the lead.

The situation is entirely different for scattered electrons from a beam of 10.8 MeV primary electrons. In order to obtain information concerning the directionality of the scattered electrons, a circular unit density phantom was used to measure the depth dose in this case. Examples of the results are shown in Figures 3, 4, and 5. The phantom used in these studies consisted of a stack of 8 cm diameter Masonite disks with circular pieces of film placed between them. The crescentic shape of the blackened areas on all the films indicates a high order of unidirectionality of the scattered electrons. The phantom was exposed to these electrons at various distances normal to the beam, and at various distances from the main structure at which the primary beam was directed, namely, a conveyor belt. The depth dose for these scattered electrons as measured along the radius through the center of the crescent differs from that for the primary monoenergetic electrons. The penetration is reduced, indicating a lower energy, and the build-up region has disappeared pointing up the predominance of very low energy component in the spectrum of the degraded electrons.

Figure 6 shows a typical film response curve for a film badge exposed to scattered electrons. The filters in this badge differ from those discussed above, although the range of thicknesses in mass per unit area is approximately the same. The greatest degree of blackening is now exhibited under the open window, while the least blackening occurs under the filter having the greatest mass per unit area. This situation is a complete reversal of the previous case and is due to the vastly different energy spectrum of the scattered electrons. The film used here is the insensitive emulsion of Eastman Kodak Type 2, Personal Monitoring Film. The calibration of the film is described elsewhere.[1] The short horizontal lines in Figure 7 are the density readings from the film badge worn by the worker involved in the radiation accident. These readings fit on the calibration curve for the scattered beam and not on the curve for the monoenergetic electrons. This fit gave added confidence that the reconstruction faithfully duplicated the accident.

If the film badge is worn on the trunk of the body where only scattered electrons strike, a high correlation between the film badge reading and the dose to the skin and internal organs can be expected. In this situation the dose to the skin, from the surface down to a depth depending on the energy of the scattered electrons, is comparable to the badge exposure, whereas the internal organs such as the lungs, the blood-forming organs (spleen and bone marrow), liver, kidneys, ovaries, etc. receive doses only about one per cent of the skin dose. This observation is based on the use of a body phantom (4) and agrees with what is expected on theoretical grounds. The dose to the internal organs is due to bremsstrahlung produced in the skin and tissues im-

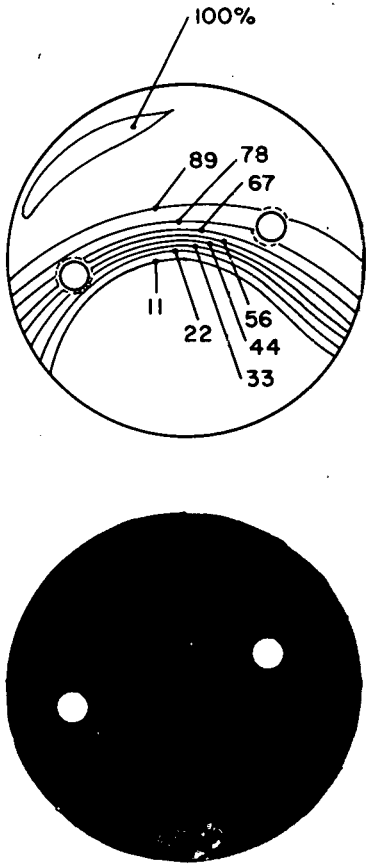

POSITION No. 5

Figure 3.

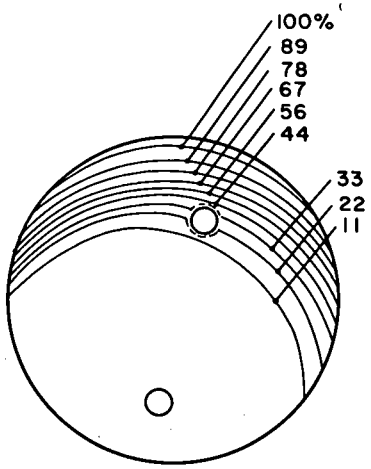

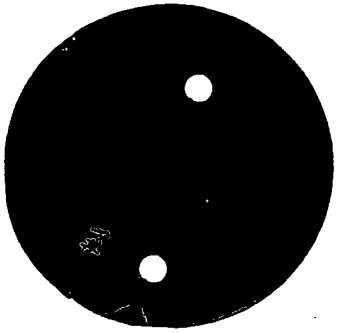

POSITION No. 9

Figure 4.

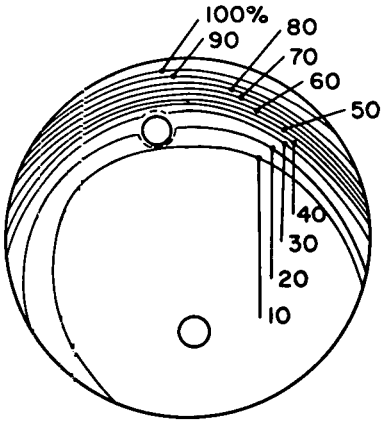

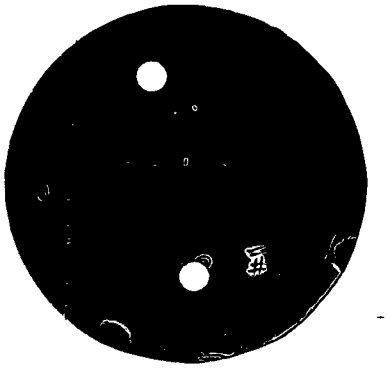

POSITION No. 11

Figure 5.

Figure 3. Irradiation of a film in a circular phantom by scattered electrons (below). Graph of isodose distribution of the film (above). The primary beam of 10.8 MeV was directed downward leaving the accelerator 83 cm above the floor. Location of phantom is 52 cm from the beam and at the floor level (Position No. 5).

Figure 4. Location of phantom is 40 cm from the beam and 52 cm above the floor level (Position No. 9.)

Figure 5. Location of phantom is 26 cm from the beam and 100 cm above the floor level (Position No. 11).

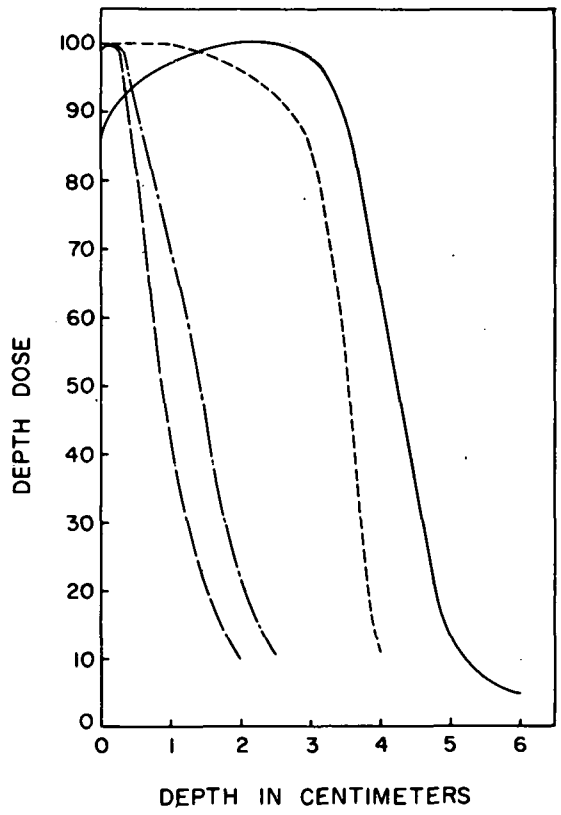

Figure 6. Plot of depth dose of scattered electrons from a 10.8 MeV beam along the diameter of the circular phantom through the beam maximum for the three locations represented by Figures 3 (- - - - -), 4 (— — — —), 5 (— · — · —), together with the central axis depth dose, in a rectangular phantom for a 10 MeV beam (———).

mediately below the skin surface by the electrons. If the scattered electron beam is contaminated with high-energy x-rays, the internal organs would receive higher doses. This observation is of use in predicting survival even if the skin dose exceeds the total body LD_{50} of a human being. Little correlation between film badge reading and the dose to the testes and extremities is expected when the badge is worn on the chest. It is our experience that, when a primary beam strikes one extremity while the scattered electrons strike the trunk of the body where the badge is worn, this extremity may receive a dose that is a thousand times that indicated by the badge, although at the same time other parts of the body may receive a small fraction of the indicated dose. Examples of the estimated dose received by various parts of the body of a worker involved in a serious radiation accident are given in Table 1.

The complete investigation of this accident required extensive measurements with heterogeneous phantoms to determine the dose to most of the body. The exposure of the worker's film badge enabled the early estimation of the skin and trunk dose only.

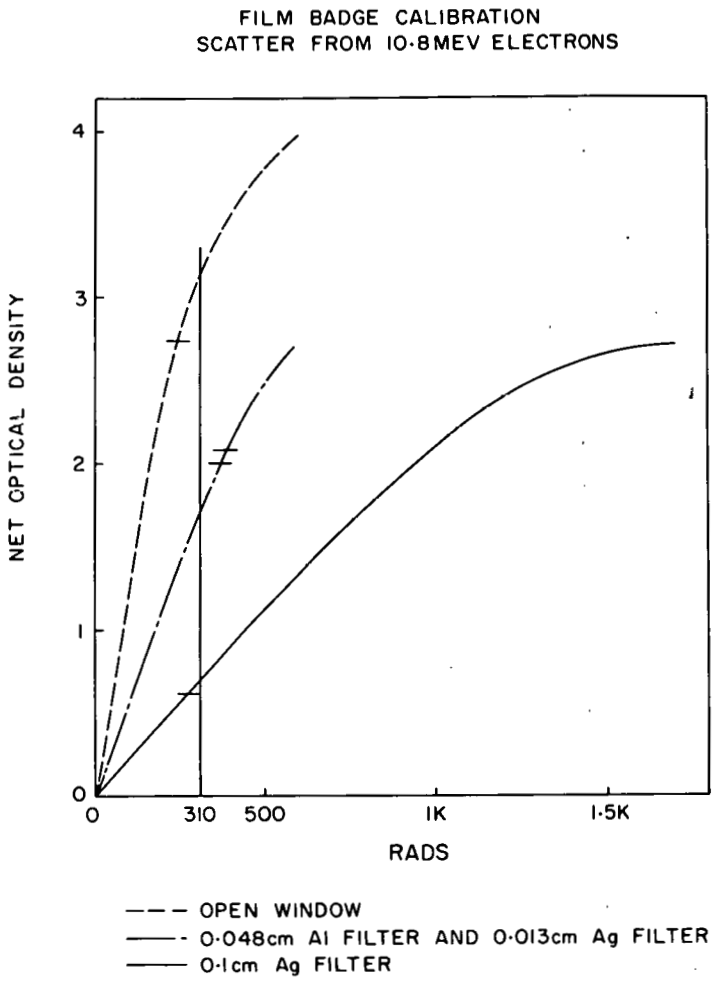

Figure 7. Film badge calibration for scattered electrons from 10.8 MeV electrons.

Table 1

DOSE TO ACCIDENT VICTIM'S BODY AND FILM BADGE

Location	Dose in rads
Film badge	310
Thumb of right hand	240,000
Ankle of right foot	29,000
Anterior surface of trunk	240-325*
Posterior surface of trunk	1.4 - 6
Interior of trunk	0.22 - 4.9

*Where two doses are given, these values give the range found in that location.

CONCLUDING REMARKS

1. In the rare case of a serious radiation accident, it is of great value to have a system for personal radiation dosimetry which not only presents information about skin dose, but also enables evaluation of the spectral quality of the radiation in some fashion. If the spectral quality can be reproduced in a reenactment of an accident, the internal organ dose can often be evaluated.

2. The traditional film badge with its series of filters and the typical spectral sensitivity of film should not be abandoned unless consideration is given to a replacement which can be used to evaluate the spectral quality of the radiation involved.

3. Curves are given which show film badge response to both monoenergetic electrons (10 MeV) and scattered electrons from a primary 10.8 MeV beam.

LITERATURE CITED

1. Lanzl, L. H., M. L. Rosenfeld, and A. R. Tarlov. Health Physics (in press), 1967.
2. Lanzl, L. H., L. S. Skaggs, and M. L. Rosenfeld. Argonne Cancer Research Hospital Semi-annual Report to the Atomic Energy Commission, ACRH-25, 15, 1966.
3. Kessaris, N. D. Physical Review, 145:164, 1966.
4. Alderson, S. W., L. H. Lanzl, M. Rollins, and J. Spira. Am. J. Roentgenol., Radium Therapy Nucl. Med., 87:185, 1962.

PRELIMINARY EXPERIENCE WITH PERMANENT INTERSTITIAL IMPLANTS USING CHROMIUM 51 SOURCES*

By

M. L. Griem,† P. Lazarovits, and P. V. Harper

At the 1958 meeting of the American Radium Society, Myers described the possible use of radioactive chromium 51 gamma ray sources for interstitial radiation therapy and compared the properties of these sources with the physical properties of several other isotopes.[1,2] Recently Henschke, et al have reviewed the experience using permanent interstitial implants of several long-lived isotopes.[3,4] Chromium 51 has a physical half life of 27 days and the decay scheme shown in Figure 1. It decays to vanadium 51 with the emission of a 323 keV gamma ray

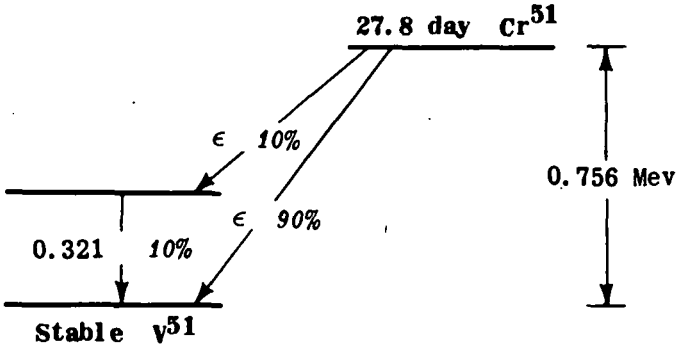

Figure 1. Decay scheme of radioactive chromium 51.[5]

in approximately 10 per cent of that time, and with the emission of soft x-rays of less than 10 kilovolts. These soft x-rays are almost completely absorbed by the chromium source itself. The decay scheme shows that no beta particles are emitted, thus this isotope is a desirable subject for interstitial implantation. The I_γ is 0.18 R per hour at 1 centimeter from a 1-millicurie source.[5] Myers described the fabrication of several sources of different sizes:[2] Our method is slightly different and was suggested by Mr. Gene Asai of the United States Bureau of Mines.

Highly pure chromium wire is drawn to proper diameter by passing it through a heated die brought to a temperature of 350°. At this temperature, chromium may be drawn to proper sizes quite easily and may also be sheared and cut very accurately to proper length. The highly pure, non-radioactive chromium wire was drawn to the diameter of 0.031 inches by the United States Bureau of Mines. In our laboratory we use a special jig and shearing device in a heated oven to cut cylinders 2.5 mm long from this wire. These sources are then loaded into aluminum cartridges supplied with the implantation gun, which is a modification of the gun described by Hodt,

*This report is taken from a paper that was presented at the 49th Annual Meeting of the American Radium Society, Toronto, Canada, May 29-31, 1967, and appears in Am. J. Roentgenol., Rad. Therapy, and Nucl. Med., 102:657, 1968.

†Career Research Development Award Number 5K3CA 19415.

Sinclair, and Smithers.[6] This gun, shown in Figure 2, is commercially available. Also shown is the stainless steel sterilization container. Activation of the sources was carried out by the Argonne National Laboratory in the research reactor CP-5.

Figure 2. Implantation gun showing aluminum cartridge, straight and curved needles and stainless steel sterilizing container.

The source strength that proved most useful was between 4 and 6 millicuries per seed, activation of which took two or three days. Following activation, these seeds were calibrated by means of Laurtisen quartz-fiber electroscope and compared with a radium standard. A second source was dissolved in strong acid and an aliquot of chromium solution counted for activity and compared with a liquid standard. The two methods of calibration of the sources compared favorably, with differences of less than 10 per cent between them.

Our first permanent chromium implant was made in a patient with metastases to the presacral area following an abdominal perineal resection for squamous cell carcinoma of the anus. The carcinoma was 6 cm in diameter and the chromium sources were implanted percutaneously through the perineum. Long spinal 18 gauge needles were positioned throughout the tumor and their positions were radiographed. Following adjustment of the position of the needles, the lesion was implanted sequentially by removing the spinal needles and implanting the needle track with chromium seeds using the implantation gun. One chromium source or seed was placed in each cubic centimeter of the tumor. Sixty seeds, each 3.55 mc, were implanted in the tumor giving an estimated tumor dose of 5500 rads. Because certain authorities at that time expressed concern over the possible radiation hazard from chromium-51, no further implants were carried out for several years. Although the patient had initially 213 mc of chromium in a permanent implant, only 10 per cent of the isotope decays with a sufficiently energetic gamma ray to be de-

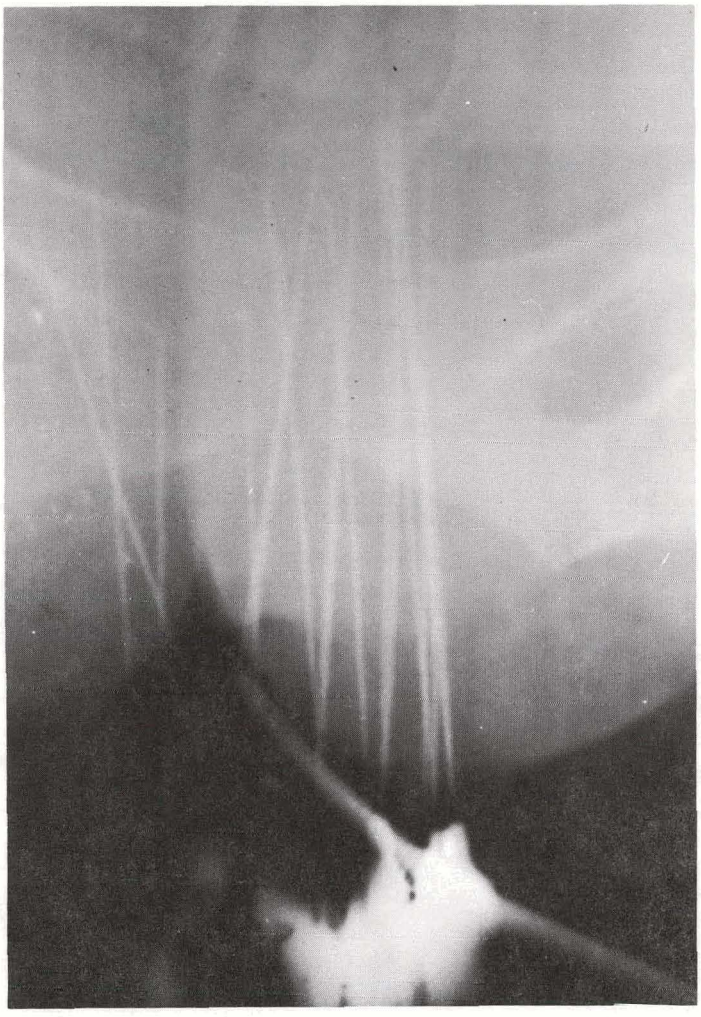

Figure 3. Radiograph showing the placement of the seeds.

tected. The chromium is extremely inert and no radioactivity was found in either the stool, urine, or expired air.

This patient has remained asymptomatic. Pelvic examination shows an indurated area in the region of the previously described mass, but there has been no progression in this area, nor have metastases been observed in over seven and a half years.

Two years ago we received permission to continue clinical investigation of these sources provided that patients with such implants were correctly identified by an arm band and a wallet card. Since then 24 patients have received 30 implants. Most of these patients had already received maximum therapy from external beam radiation and from radium. Some of them have had radical surgery and chemotherapy, including perfusion. Tables 1, 2, and 3 outline the experience in these patients. We have seen necrosis and hemorrhage in three instances. This has occurred in patients who had been heavily irradiated before implantation of the chromium. Four patients have had two implants and one patient has had three implants. Where we have made repeated implants we have used seeds of 2.5 to 3 mc in activity. We have seen excellent response in nine patients. In these patients the area irradiated has shown good local control. A number of

Table 1

FAVORABLE RESPONSE

Patient	Diagnosis	Previous treatment	No. of chromium seeds and activity	Calculated dose	Comments
Q.D.	Ca anus	Surgery	60 - 3.55 mc	5500 rads	7.5 years without recurrence.
C.S.	Ca cervix, recurrent	X-ray & radium	57 - 2.00 mc	3000 rads	Abdominal implant. Fistula in bladder two years after implant.
E.D.	Ca breast	X-ray	19 - 3.00 mc	4600 rads	Recurrence at edge of implant 1.5 years.
M.V.	Squamous cell ca base of tongue	X-ray	5 - 3.15 mc	3000 rads	Implant in metastatic node. Excellent response. No tumor in node at autopsy.
A.N.	Ca pyriform sinus	Surgery & x-ray	3 - 3.55 mc 3 - 2.88 mc	6000 rads	Treatment of recurrence about tracheotomy stoma. No slough.
R.K.	Squamous cell ca palate, anterior pillar, posterior tongue	X-ray	17 - 4.50 mc	6000 rads	Excellent local result, recurrence adjacent to implant.
W.Z.	Neck metastases, squamous cell ca	X-ray & electron therapy	22 - 4.00 mc 14 - 5.00 mc 21 - 4.50 mc	6000 rads to 6500 rads	All lesions responded dramatically to implants.
A.K.	Squamous cell ca of cervix with vaginal recurrence	X-ray, radium applicators & radium implants	12 - 4.00 mc 14 - 4.60 mc	5000 rads to 5600 rads	1 cm ulcer, 8 months after implant. Good local control.
M.S.	Squamous cell ca tongue	X-ray	3 - 2.70 mc	6000 rads	No recurrence at six months.

Table 2

GOOD RESPONSE

Patient	Diagnosis	Previous treatment	No. of chromium seeds and activity	Calculated dose	Comments
J.F.	Squamous cell ca posterior tongue	X-ray	14 - 4.10 mc	6000 rads	Good response in the tongue for six months. Lymph node metastases.
O.O.	Squamous cell ca larynx	X-ray & surgery	41 - 3.50 mc	5500 rads	Excellent response in neck metastases for four months.
G.P.	Ca oral pharynx	X-ray	13 - 4.80 mc	6800 rads	Autopsy revealed fibrosis and necrosis in the region of the implant. Patient died of distant metastases.
E.C.	Ca cervix with pelvic metastases	X-ray & radium	22 - 3.90 mc	5000 rads	Good response in pelvic mass four months after implant.
R.C.	Ca breast with skin metastases	Surgery & x-ray	13 - 4.50 mc	6500 rads	New lesions adjacent to implant four months following. Treated area shows no recurrence.
D.K.	Ca larynx	X-ray & surgery	14 - 2.88 mc	4000 rads	Marked decrease in size of neck metastases.
L.M.	Squamous cell ca penis with lymph node metastases	X-ray	15 - 4.20 mc 52 - 4.60 mc	5500 rads to 6000 rads	Marked shrinkage of lymph node metastases. Penile lesion showed small 1 cm ulceration.
C.D.	Squamous cell ca anus	Surgery	19 - 4.50 mc	5500 rads	No palpable recurrence five months after implant.
J.A.	Adenoca of rectum	Surgery & x-ray	27 - 3.50 mc	3400 rads	Good pain relief and decrease of the tumor size for three months.

Table 3

QUESTIONABLE OR UNFAVORABLE RESULTS AND INSUFFICIENT TIME FOR EVALUATION

Patient	Diagnosis	Previous treatment	No. of chromium seeds and activity	Calculated dose	Comments
R.T.	Transitional cell ca bladder	X-ray & surgery	28 - 2.00 mc	3000 rads	Died of pyelonephritis and septicemia. Insufficient time to evaluate.
V.M.	Squamous cell ca cheek	Surgery & x-ray	25 - 4.00 mc	4300 rads	Died of hemorrhage one month following implant.
A.S.	Ca cervix with vaginal recurrence	Radium & x-ray	51 - 4.00 mc	5500 rads	Necrosis and tumor present at autopsy one month later.
E.M.	Mucoepidermoid ca of nasopharynx	Surgery & x-ray	6 x 3.60 mc	6000 rads	Normal reaction at three weeks - insufficient follow-up.
A.K.	Squamous cell ca posteria tongue	X-ray	29 x 3.50 mc	6200 rads	Transient response of three months duration in tongue lesions.
M.R.	Ca cervix with involvement of bladder	X-ray & radium	48 - 3.00 mc	5000 rads	Necrosis of anterior vaginal wall. Marked relief of pain and decrease in infiltrates in parametrium.
O.L.	Squamous cell ca buccal mucosa	X-ray	10 - 3.50 mc	4500 rads	Only temporary decrease in size of neck metastases.

patients have had deeply seated tumors that could be exposed sufficiently to allow implantation at the time of surgery. Figure 4 shows a radiograph of an implant made one and one-half years previously. At surgery, metastatic nodes from carcinoma of the cervix were implanted. The patient's pain was relieved, and swelling of the leg decreased.

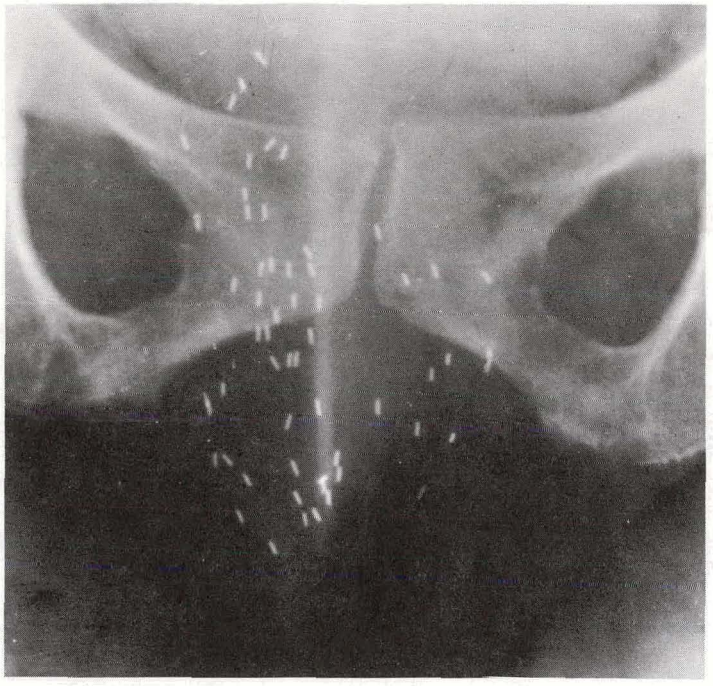

Figure 4. A radiograph of an implant in a patient with recurrent carcinoma of the cervix with metastatic tumor in iliac lymph nodes.

The relatively long half-life of chromium-51 allows us to keep a supply of radioactive chromium seeds in stock in a sterilized lead pot. Two implantation guns are available and sterilized ready for use. Sources that decay one half-life become half strength seeds for use in implantations where a tissue dose of between 2000 and 3000 rads is desired. Eight of the implants have been made under local anesthesia in the out-patient clinic.

DISCUSSION

We have found chromium-51 seeds to be very flexible and useful sources for interstitial implantation. The relatively long half-life, the absence of beta radiation, and the ease of handling have been important features. It has been possible to keep a stock of radioactive sources constantly available, sterilized and ready for operative implantation into deeply seated tumors. There has been a relatively low incidence of tissue necrosis, and in previously irradiated areas, the additional irradiation from this permanent implant has been generally well tolerated. It may be that the relatively low dose rate from these permanent implants allows the normal tissue to proliferate and repopulate the irradiated area.

We are currently using a computer program to investigate the possibilities of improving

our dosimetry in these implants. The late effects of these long lived permanent interstitial implants are also being investigated.

LITERATURE CITED

1. Myers, W. G. Radiology, 66:268, 1956.
2. Myers, W. G. Am. J. Roentgenol., Rad. Therapy & Nuclear Med., 81:99, 1959.
3. Henschke, U. K., and D. C. Lawrence. Radiology, 85:1117, 1965.
4. Lawrence, D. C., C. A. Sondhaus, B. Fader, and J. Scallon. Radiology, 86:143, 1966.
5. Slack, L., and K. Way. Radiations from Radioactive Atoms in Frequent Use. United States Atomic Energy Commission, February, 1959, p. 21.
6. Hodt, H. J., W. K. Sinclair, and D. W. Smithers. Brit. J. Radiology, 25:419, 1952.

THE EFFECT OF HYPOXIA ON COLONY FORMING UNITS IN BONE MARROW*

By

W. Fried,† M. Weisman, D. Martensen,‡ and C. W. Gurney
With technical assistance by Dolores Truss

The existence of multipotential hematopoietic stem cells in adult mammalian bone marrow is now generally accepted.[1,2] A method for studying the kinetics of these cells is based on their ability to produce discreet macroscopic colonies of hematopoietic cells on the spleens of heavily irradiated mice.[3] Each colony represents the progeny of a single cell (1), or colony forming unit (CFU), and either contains cells of the erythroid, myeloid, or megakaryocytic series; or cells that retain the potential to produce all three cell lines.[4] The nature of the stimuli that induce multipotential hematopoietic cells (CFU) to differentiate is unknown.

Erythropoietin, a hormonal substance that is produced largely in the kidneys,[5] is thought to be the physiologic regulator of erythropoiesis,[6] stimulating primitive, morphologically undifferentiated cells either to mature or to differentiate into the erythroid series.[7,8] Whether the erythropoietin responsive cell is multipotential or committed has not been definitely established. Several lines of evidence suggest that erythropoietin responsive cells are the offspring of multipotential stem cells but are able to give rise only to erythroid cells.[9-11] Bruce and McCulloch[9] have shown that prolonged exposure of mice to hypoxia does not alter the number of CFU in their bone marrow. Since CFU are thought to be multipotential stem cells, this observation lends support to the idea that erythropoietin responsive cells (ERC) are no longer multipotential. An alternative interpretation holds that erythropoietin acts directly on multipotential stem cells to induce differentiation. As a result, the rate of proliferation of multipotential cells increases, thereby maintaining the level of their numbers. Since rapidly proliferating cells are more sensitive to the destructive effects of x-radiation,[12] one would expect an increase in the radiosensitivity of CFU after exposure to hypoxia. In this paper, we shall show the effect of hypoxia and of erythropoietin on the radiosensitivity of hematopoietic stem cells (CFU).

MATERIALS AND METHODS

Eight to ten week old CF_1 mice were used.

Hypoxia was produced in a steel chamber, 3' x 4' x 2' which was evacuated to one half of normal atmospheric pressure by a vacuum pump.

X-radiation was delivered by a 250 kV Picker x-ray unit at a dose rate of 60 R per minute HVL = 1.0 mm Cu. Lead shields one-quarter inch in thickness were used for leg shielding.

---

*This report is taken from a paper that was presented in part at the Bone Marrow Conference, Atlantic City, April 1966 and appears in J. Lab. Clin. Med., 71:422, 1968. The research was supported in part by a grant from the American Cancer Society, Illinois Division and in part by Veterans Administration Research Funds.

†Present address: Veterans Administration West Side Hospital, 820 South Damen, Chicago.

‡Present address: Department of Medicine, Rutgers Medical School, New Brunswick, New Jersey.

Erythropoietin was prepared from the urine of a patient with aplastic anemia by alcohol precipitation, dialysis, and lyophilization according to the method of Lowy et al.[13] The final preparation consisted of a light tan powder which contained about 3 cobalt units of erythropoietin per mg.

Bone marrow cells were collected by dissecting a femur free of its attached tissues, and removing the femoral head. A 23-gauge needle, attached to a tuberculin syringe, was then inserted into the distal end of the femur. The proximal end was immersed in saline and saline was flushed through the marrow cavity until it appeared to be empty. After pooling marrow from the femurs of ten mice, the cell suspension was adjusted to the desired volume by dilution with normal saline.

The number of macroscopic spleen colonies was determined by the method of Till et al.[3] The mice were sacrificed and the spleens were removed and fixed in Bouin's solution. The macroscopic nodules on the spleen surfaces were then counted by one of us, without identification of the group to which the spleen belonged.

The effect of hypoxia on the endogenous colonizing potential of CFU in a leg. To measure the effect of hypoxia on the endogenous colonizing potential of CFU from a leg, groups of mice were exposed to hypoxia for 0, 1, 2, 3, or 4 days. Within three hours after removal from the hypoxic environment, they received 200 R total body x-radiation followed by 600 R with a leg shielded. Nine days later, they were sacrificed and the macroscopic spleen colonies were counted.

The ability of transplanted CFU to colonize in mice which had been exposed to hypoxia. To measure the ability of CFU to colonize in mice which had been exposed to hypoxia, groups of mice were exposed to 0, 1, 2, 3, or 4 days of hypoxia. After removal from the hypoxic environment, each received 800 R total body x-radiation. Within three hours after x-irradiation they were injected intravenously with one-half ml of a bone marrow cell suspension containing 8×10^4 nucleated cells. Nine days later the mice were sacrificed and the spleen colonies were counted.

The effect of erythropoietin on the endogenous colonizing potential of CFU in a leg. To measure the effect of erythropoietin on the endogenous colonizing potential of cells from a leg, mice were divided into two groups. Group E received 3 cobalt units of erythropoietin twice a day for four days and Group S received injections of equal volumes of saline. Six hours after the last injection of erythropoietin, the mice received 200 R total body x-radiation followed by 600 R with one leg shielded. Nine days later, the mice were sacrificed and the macroscopic spleen colonies were counted.

The effect of hypoxia on the radiosensitivity of transplantable CFU in a leg. Mice were divided into seven groups. Five groups of mice were exposed to hypoxia for periods ranging from 0 to 4 days. Immediately afterwards they received 200 R total body x-radiation and within two hours they were sacrificed. The bone marrow cells were then collected from one femur of each mouse. The cells collected from the ten mice in each group were pooled and the cell suspensions were adjusted to a concentration of 1.6×10^6 nucleated cells per ml. The remaining two groups of mice were subjected to hypoxia for 0 and 4 days respectively. They were then sacrificed and suspensions of cells from their bone marrow were prepared as described above. These were adjusted to a concentration of 1.6×10^5 nucleated cells per ml. To determine the number of CFU in each cell suspension, one-half ml was injected intravenously into each of a group of lethally

irradiated mice (800 R total body x-radiation). Nine days later, they were sacrificed and the macroscopic spleen colonies were counted.

RESULTS

The effect of hypoxia on the endogenous colonizing potential of CFU in a leg. Figure 1 shows the effect of hypoxia on the endogenous colonizing potential of CFU in a leg. The endogenous colonizing potential of cells in a leg is expressed in terms of the number of spleen colonies which develop after mice have been exposed to 200 R total body x-radiation and 600 R with a leg shielded. The amount of time which mice were exposed to hypoxia prior to x-irradiation

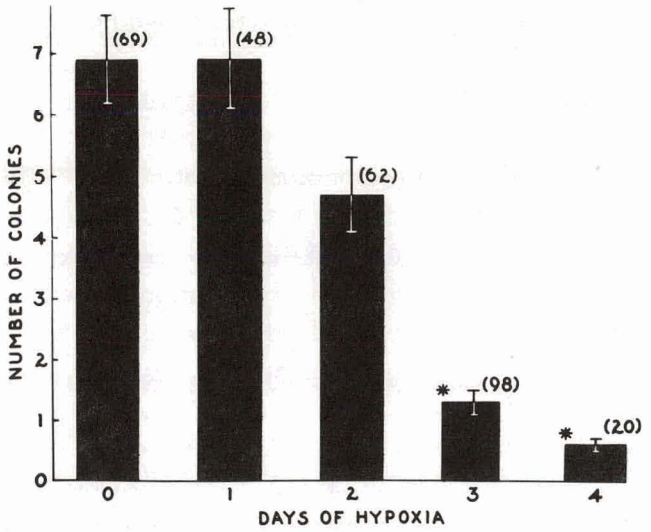

Figure 1. Effect of hypoxia on the endogenous colonizing potential of CFU in a leg. ( ) - number of mice. Brackets represent ± one standard error of the mean. * Values are significantly different from control (0 day) $p < .001$.

is recorded on the abscissa and the number of colonies that resulted is recorded on the ordinate. A significant decrease in the endogenous colonizing potential of CFU in a leg occurred in mice that had been exposed to hypoxia for three days prior to x-irradiation ($p < .001$); and decreased to even lower levels after four days of hypoxia.

The ability of transplanted CFU to colonize in mice which had been exposed to hypoxia. Figure 2 shows the ability of transplanted CFU to colonize in the spleens of irradiated hosts that had been exposed to hypoxia for varying periods of time prior to x-irradiation. The number of spleen colonies formed after transplantation of 8×10^4 nucleated bone marrow cells is recorded on the ordinate. The amount of time which host mice were exposed to hypoxia prior to x-irradiation and transplantation of cells is recorded on the abscissa. Figure 2 shows that transplanted CFU gave rise to as many spleen colonies in mice that had been exposed to four days of hypoxia as they did in mice that had not been made hypoxic.

The effect of erythropoietin on the endogenous colonizing potential of CFU in a leg. Figure 3 shows the effect of erythropoietin on the endogenous colonizing potential of CFU in a leg. Bar S represents the endogenous colonizing potential of CFU in the legs of mice that received only saline prior to x-irradiation. Bar E represents that of CFU in mice that received erythropoietin

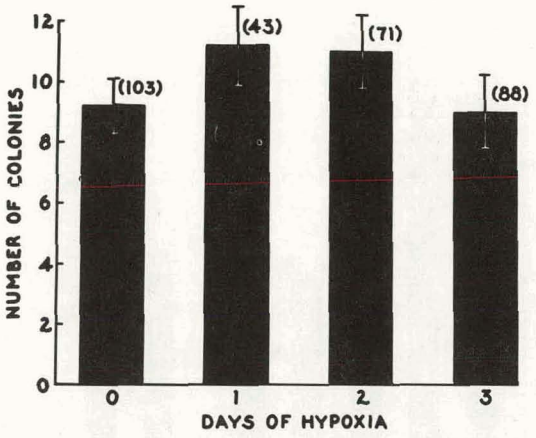

Figure 2. Ability of transplanted CFU to colonize in mice previously exposed to hypoxia. ( ) - number of mice. Brackets represent ± one standard error of the mean.

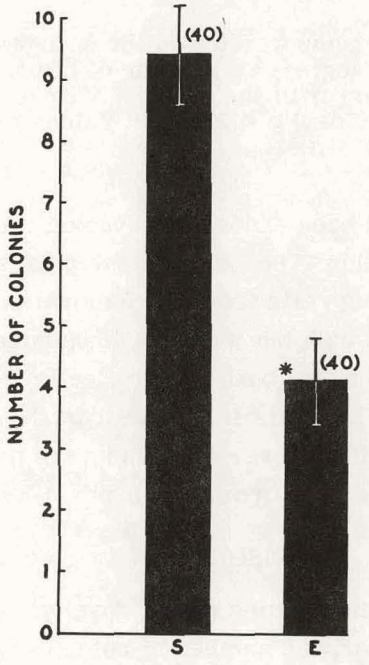

Figure 3. Effect of erythropoietin on the endogenous colonizing potential of CFU in a leg. S - mice injected with saline only. E - mice injected with 3μ erythropoietin twice daily. ( ) - number of mice. Bracket indicates ± one standard error of the mean. * Values are significantly different from group S ($p < .001$).

prior to x-irradiation. Figure 3 shows that after injecting 6 cobalt units of erythropoietin daily for 4 days there was a significant suppression of the endogenous colonizing potential of CFU in a leg ($p < .001$).

The effect of hypoxia on the radiosensitivity of transplantable CFU in a leg. The first five bars in Figure 4 represent the number of colonies formed after transplanting cells obtained from

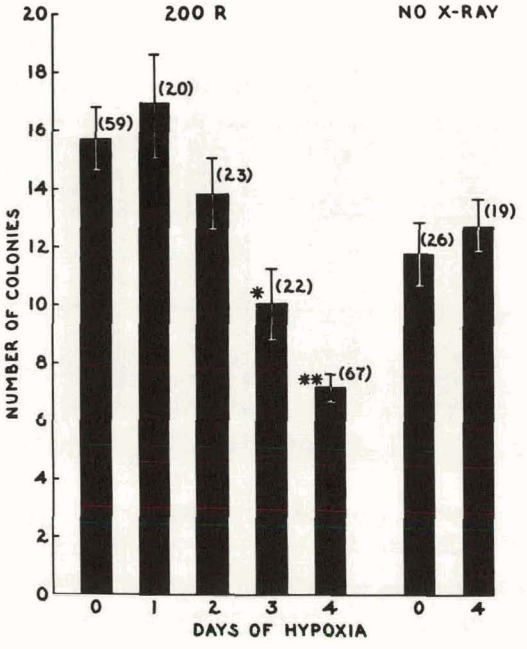

Figure 4. Effect of erythropoietin on the endogenous colonizing potential of CFU in a leg. ( ) - number of mice. Brackets represent ± one standard error of the mean. * Values significantly different from control (0 day) $p < .005$. ** Values significantly different from control $p < .001$.

the femoral marrow of mice but had been exposed to hypoxia for varying periods of time followed by 200 R total body x-irradiation. The two remaining bars represent the number of spleen colonies formed after injecting cells from the femoral marrow of mice that received either no hypoxia or four days of hypoxia but were not irradiated. Figure 4 shows that the number of colonies formed after transplanting bone marrow cells from mice exposed to hypoxia is the same as that formed after injecting cells from non-hypoxic mice. However, cells from mice that were exposed to hypoxia for at least three days and were then x-irradiated produced significantly fewer spleen colonies than did cells from non-hypoxic, irradiated mice ($p < .005$).

DISCUSSION

Endogenous hematopoietic spleen colonies do not develop in mice that have been exposed to 800 R total body x-radiation. However, the number of colonies which develop in mice exposed to 800 R with a leg shielded is so great that the spleen becomes diffusely enlarged. Therefore, to measure the endogenous colonizing potential of cells from a leg, 200 R x-radiation was directed to the leg and 800 R to the rest of the body (Figure 1). In this manner, the population of CFU in the leg was reduced to a level that resulted in a countable number of endogenously seeded spleen colonies. Using this method the endogenous colonizing potential of CFU in a leg was found to be reduced after exposure to hypoxia for three days. After injecting six units of erythropoietin daily for four days the endogenous colonizing potential of cells in a leg was also decreased, although to a lesser extent (Figure 3). Spleen colonies grew equally well where hematopoietic cells were transplanted into mice that were made hypoxic prior to lethal x-irradiation and when transplanted into non-hypoxic x-irradiated mice (Figure 4). The observation that exposure to

hypoxia decreases the endogenous colonizing ability of cells in a leg (measured after 200 R x-irradiation) without altering the number of transplantable CFU in the leg (obtained from non-irradiated donors) is consistent with the concept that hypoxia results in an increase in the radiosensitivity of CFU but does not increase their total number. This concept was further supported by the observation that the number of transplantable CFU in the legs of mice that had been exposed to hypoxia was decreased to a significantly greater extent by exposure to 200 R x-radiation than was that of CFU in the legs of mice that had not been made hypoxic. It has been shown that rapidly proliferating and actively metabolizing cells are more sensitive to the damaging effects of x-radiation than are resting cells.[14] We suggest, therefore, that the above data are in accord with the idea that the rate of proliferation of hematopoietic stem cells is increased after exposure to hypoxia or to increased erythropoietin levels for at least three days. The results reported here are compatible with the interpretation that erythropoietin acts directly on the multipotential stem cells to induce differentiation and also with the interpretation that it affects these cells only indirectly. According to the latter concept, erythropoietin stimulates a sensitive but committed cell (ERC) to mature in the erythroid series. After 72 hours of stimulation the pool of ERC begins to decrease in size as the mature erythrocytes move out of it and multipotential cells (CFU) are called on to replenish it. The latter are then stimulated to proliferate more rapidly to prevent a decrease in the size of the stem cell pool. The alternative interpretation holds that erythropoietin acts directly on multipotential hematopoietic stem cells to induce differentiation into the erythroid series. As a result of this, the stem cell compartment is decreased in size. The remaining stem cells are stimulated to proliferate more rapidly to compensate for this. After 72 hours of continuous stimulation the rate of stem cell proliferation increases to a level that results in a significant alteration in their radiosensitivity. According to this concept, one should be able to show an increase in the rate of proliferation of hematopoietic stem cells very soon after stimulating them to differentiate if more sensitive methods are used.

In conclusion we have shown that three days of exposure to hypoxia alters the hematopoietic stem cells of mice in a manner which renders them more sensitive to x-radiation. We suggest that this reflects an increased rate of proliferation of these cells in the presence of a sustained stimulus to erythroid maturation or differentiation. Although the results are consistent with the concept that erythropoietin acts directly on the multipotential hematopoietic stem cell to induce differentiation into the erythroid series, they do not exclude the possibility that erythropoietin acts on a committed cell, and only indirectly influences the multipotential hematopoietic stem cells.

ACKNOWLEDGMENTS

We with to thank Dr. Miriam Liberson and Dr. James Strubbe for their cooperation and advice in performing the x-radiation procedures. We wish to thank Mr. Vincent Yakulis for his help in preparing the erythropoietin.

LITERATURE CITED

1. Becker, A. J., E. A. McCulloch, and J. E. Till. Nature, 197:452, 1963.
2. Whang, J., E. Frei, J. H. Tjio, P. P. Carbone, and G. Brecher. Blood, 22:664, 1963.
3. Till, J. E., and E. A. McCulloch. Radiation Res., 14:213, 1961.

4. Lewis, J. P., and F. E. Trobaugh, Jr. Nature, 204:589, 1964.

5. Jacobson, L. O., E. Goldwasser, L. F. Plzak, and W. Fried. Nature, 179:633, 1957.

6. Jacobson, L. O., E. Goldwasser, C. W. Gurney, W. Fried, and L. F. Plzak. Ann. N. Y. Acad. Sci., 77:551, 1959.

7. Gurney, C. W., N. Wackman, and E. Filmanowicz. Blood, 17:531, 1961.

8. Alpen, E. L., and D. Cranmore. Kinetics of Cellular Proliferation. F. R. Stohlman, Jr., editor. New York: Grune and Stratton, 1959, p. 290.

9. Bruce, W. R., and E. A. McCulloch. Blood, 23:216, 1964.

10. Schooley, J. C., L. N. Cantor, and V. W. Havens. Exptl. Haemat., 9:55, 1966.

11. O'Grady, L. F., J. P. Lewis, and F. E. Trobaugh, Jr. Exptl. Haemat., 12:70, 1967.

12. Ellinger, F., in Medical Radiation Biology. Charles C. Thomas, ed. Springfield, Illinois, 1957, p. 69.

13. Lowy, P. H., and G. L. Keighley. Clinica Chimica Acta, 13:491, 1966.

EFFECT OF ENDOGENOUS ERYTHROPOIETIN ON REPLICATING HEMOPOIETIC STEM CELLS

By

R. L. DeGowin and S. Johnson*

Cells of most neoplastic tissues fail to differentiate normally. Although elevated levels of erythropoietin have been detected in patients with leukemia,[1] inappropriately diminished erythroid differentiation[2] of hemopoietic stem cells leads to anemia in many of them. It remains unclear how the target cell for erythropoietin has become refractory to the hormone that usually induces its differentiation.

We have examined the suggestion that replication, per se, might render hemopoietic stem cells refractory to erythropoietin.[3] Previous autorepopulation experiments in mice indicated that stem cells in the leg, shielded from a supra-lethal dose of x-rays, colonize the spleen and synthesize deoxyribonucleic acid (DNA) during the first five days after irradiation.[4] Injections of human urinary erythropoietin failed to induce erythropoiesis during this proliferative phase.[4] We wondered whether the exogenous erythropoietin had been inactivated or if the stem cell had become temporarily refractory to it.

Studies described in this paper were undertaken: (1) to demonstrate by a radiobiological method that replication of stem cells occurs within the first five days after irradiation; and (2) to see whether erythropoietin secretion produced by hypoxia would induce erythroid differentiation in the "shielded mouse" during this postulated proliferative phase.

METHODS

Mice. Carworth Farms No. 1, 10-to-12-week-old female mice were used in these studies. They were housed, 8 to a cage, on a bed of sterilized ground corn cobs, and fed Rockland complete mouse diet. Drinking water, provided ad libitum, was acidified to pH 2.5 with HCl to control Pseudomonas infections.

Irradiation. Irradiation procedures were identical to those previously described.[4] Total-body x-ray, from a General Electric Maxitron, 250 x-ray machine delivering an average output of 60 R/min, was administered to the mice, which were confined during irradiation in perforated lusteroid tubes on a lucite turntable that rotated at 3.5 rpm. Physical factors were: 250 kV, 30 ma, 0.25 mm Cu plus 1.0 mm Al filter; HVL 1.04 mm Cu: target distance 79.5 cm.

"Shielded mice" (850 R L.S.) were placed on the turntable and had their entire left hind legs restrained by a rubber band under a tunnel-shaped, 3 mm lead shield during the partial body irradiation. 850 R x-ray was delivered to these shielded mice in a single dose. Mice were not anesthetized during irradiation.

Splenic uptake of ^{59}Fe. The splenic uptake of ^{59}Fe was determined by the method of Smith.[5] Approximately 0.1 μC of ^{59}Fe chloride in 0.25 ml of isotonic saline solution was injected intraperitoneally. Six hours later, spleens were removed, fixed in Bouin's fluid, and their radioactiv-

*This report is taken from a paper that appears in Proc. Soc. Biol. Med., 126:442, 1967.

ity was measured in a well-type scintillation counter. A standard prepared at the time of injection was counted, and splenic uptake of ^{59}Fe was expressed as percentage of the injected dose.

The splenic uptake of ^{59}Fe was regarded as a valid estimate of erythropoiesis, because those conditions that suppress erythropoiesis, like plethora, decrease uptake of iron; and those that enhance erythropoiesis, like exposure to hypoxia or injection of erythropoietin, increase the splenic uptake of radioiron.[4] Moreover, after a lag of 24 hours, reticulocytosis paralleled the splenic uptake of ^{59}Fe.

Resistance to irradiation. Stem cell replication was estimated by noting increased resistance to irradiation. Shielded mice were given an initial dose of 850 R L.S. Each day thereafter, a sublethal dose of total-body x-ray (100 R, 200 R, or 300 R) was administered to a different group of previously irradiated, shielded mice. Six days after the total-body irradiation, ^{59}Fe Cl_3 was administered intraperitoneally and splenic uptake in 6 hours was measured as described above.[5] Increasing splenic uptake of ^{59}Fe, despite exposure to identical doses of x-rays, was interpreted as evidence that stem cell replication had occurred, giving rise to more daughter erythroblasts, which incorporated more radioiron.

Hypoxia. Hypoxia was produced by placing mice in a chamber evacuated to 1/2 atmosphere for 16 hours (overnight) on 3 consecutive nights. The mice were removed on the morning of the third day. Splenectomy or exsanguination for assay of plasma erythropoietin was carried out at that time.

Assay of plasma erythropoietin. Plasma from groups of 32 experimental mice was pooled and frozen immediately after bleeding. After thawing at room temperature, 1.0 ml of plasma was injected subcutaneously into a plethoric mouse prepared for assay by the methods described previously.[6,7]

RESULTS

Stem cell replication in the spleen, as shown by increasing radioresistance, increased markedly during the first four days after irradiation, an interval devoid of erythroid differentiation. Intermittent periods of hypoxia produced elevated plasma levels of endogenous erythropoietin, but did not induce erythropoiesis during the early proliferative phase of stem cell replication.

Stem cell replication. Figure 1 shows that incremental sublethal doses of total-body x-ray administered to mice one day after they had received partial body x-ray (850 R L.S.) resulted in a corresponding dose-response when the splenic uptake of ^{59}Fe was measured six days later. After day 1, radioresistance increased nearly 5 times, reaching a peak on day 4. After falling to a nadir on day 6, the dose-response disappeared, and another peak, higher than the first, was attained on day 8.

Plasma erythropoietin levels. Figure 2 shows that plasma from hypoxic mice 3, 5, and 7 days after 850 R L.S., contained levels of erythropoietic activity 5 to 8 times that of plasma from unirradiated mice after a similar exposure to intermittent hypoxia. Plasma levels in shielded mice at ambient pressure did not differ significantly from those of unirradiated mice.

Erythropoiesis. Figure 3 demonstrates that although the splenic uptake of radioiron was increased in normal mice exposed to intermittent hypoxia, there was no increase in shielded mice on days 3 and 5 after 850 R L.S., whether they had been exposed to hypoxia or not. Morever, hy-

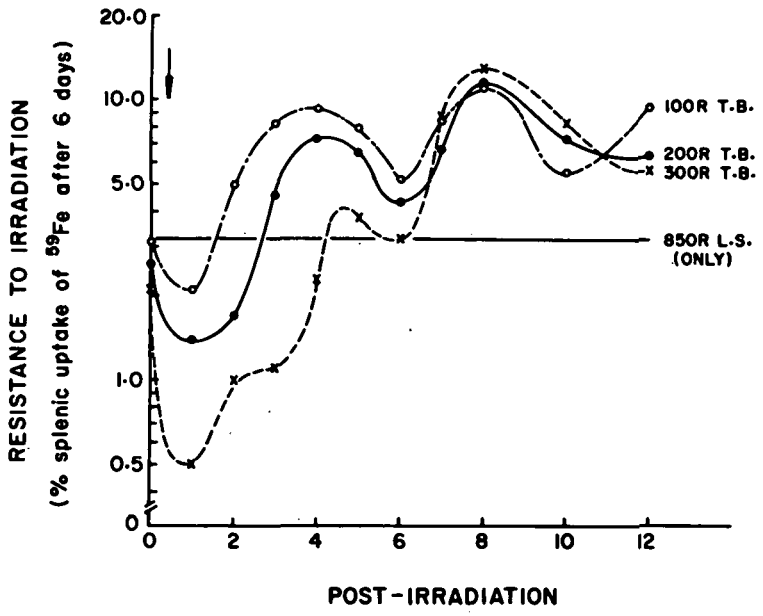

Figure 1. Resistance to irradiation, a measure of stem cell replication, was estimated by the splenic uptake of ^{59}Fe given 6 days after a sublethal dose of total-body (TB) x-ray was administered to shielded (850 R L.S.) mice. "Days post-irradiation" refers to the day after 850 R L.S. on which the sublethal dose of x-ray was administered. Each point represents the mean splenic uptake of a group of at least 12 mice. The horizontal line is the mean value for 53 mice that received no total-body x-ray. The arrow indicates the administration of 850 R L.S. The ordinate is a logarithmic scale.

poxia did not enhance erythropoiesis on day 7, when splenic uptake of ^{59}Fe had increased about 5-fold in shielded mice kept at ambient pressure.

DISCUSSION

Data reported here indicate that elevated plasma levels of endogenous erythropoietin elicited by hypoxia fail to induce erythroid differentiation during the 5 days immediately after partial body irradiation. This suggests that the erythropoietin target cell is temporarily refractory to the hormone and not that the hormone is inactivated, an alternative proposal that was made in a previous paper.[4] The radiobiological method of demonstrating cellular replication supports conclusions from earlier work which suggested that endogenous hemopoietic stem cell proliferation occurred during the first 5 days after partial body x-ray (850 R L.S.)[4]

Because of the discrepancies encountered when comparing results obtained with exogenous colony-forming cells[8] and endogenous stem cells,[9] a review of the evidence for early stem cell replication is necessary. Our initial work[4] showed that previous shielding of the left hind leg of mice subsequently exposed to supralethal doses of x-ray effected 100 per cent survival. Unlike spleens of unshielded mice, which died of bone marrow failure following total-body x-ray, spleens of shielded surviving mice developed macroscopic hemopoietic colonies 4 or 5 days after 850 R L.S. Increasing splenic uptake of ^{131}I-labeled iododeoxyuridine (^{131}I-UdR) during those first 5 days indicated accelerated DNA synthesis. There was, however, no evidence of differen-

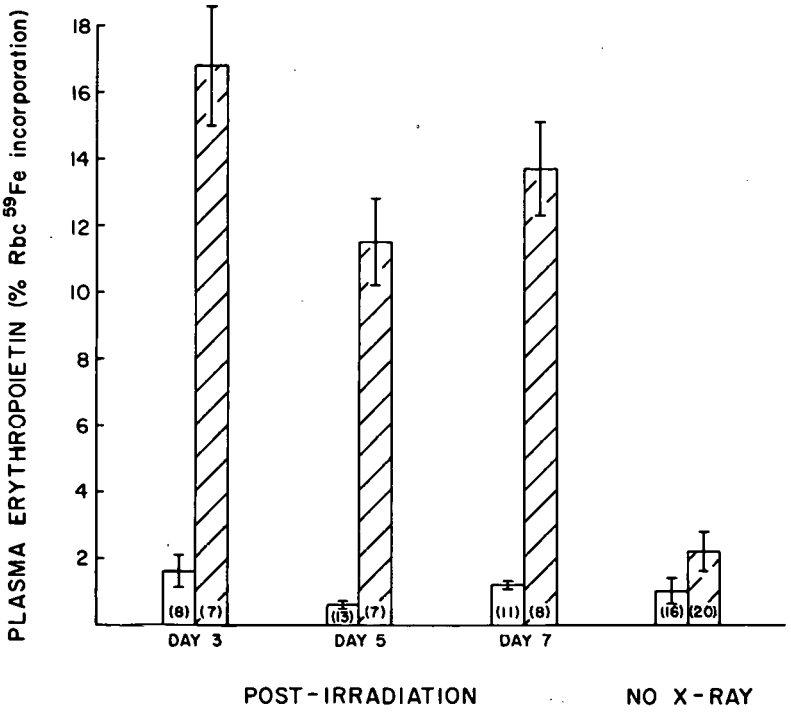

Figure 2. Plasma erythropoietin was estimated by measuring the erythrocyte (RBC) radioiron incorporation in plethoric assay mice. Time elapsed after the administration of 850 R L.S. to shielded mice is indicated by "post-irradiation." Cross-hatched bars denote mean values of pooled plasma from mice exposed to intermittent hypoxia; open bars depict plasma activity from mice at ambient pressure. Brackets enclose ± 1 standard error of the mean. Numbers in parentheses indicate the number of assay mice.

tiation until after day 5. At this time, splenic uptake of ^{59}Fe increased, and later, the reticulocyte, leukocyte, and platelet concentrations began to increase. Thus, during the first 5 days after 850 R L.S., the spleens of shielded mice contained cells that were capable of forming hemopoietic colonies and synthesizing DNA before their differentiation, in this way preventing death from radiation-induced marrow failure.[4]

Results reported in this paper confirm the idea that there is early replication of hemopoietic stem cells after irradiation. The method is based on the evidence that erythroblasts, which incorporate radioiron, arise from hemopoietic stem cells.[10,11] Other workers have considered the amount of radioiron incorporated by erythroblasts, and hence their number, to be a function of the number of stem cells available for erythroid differentiation.[12,13] The diminishing ability of incremental doses of radiation to produce a measurable lesion has been used as an estimate of cellular replication.[9] When, therefore, sublethal doses of x-ray delivered to colonized spleens of shielded mice progressively failed to suppress splenic uptake of ^{59}Fe, we concluded that more stem cells were present on each succeeding day after 850 R L.S.

The low point of the curves on day 6 in Figure 1, coincides with the onset of erythroid differentiation in the spleen indicated by splenic uptake of radioiron.[4] Thereafter the dose-response phenomenon disappears. Presumably, this is because erythroblasts are more radioresistant than

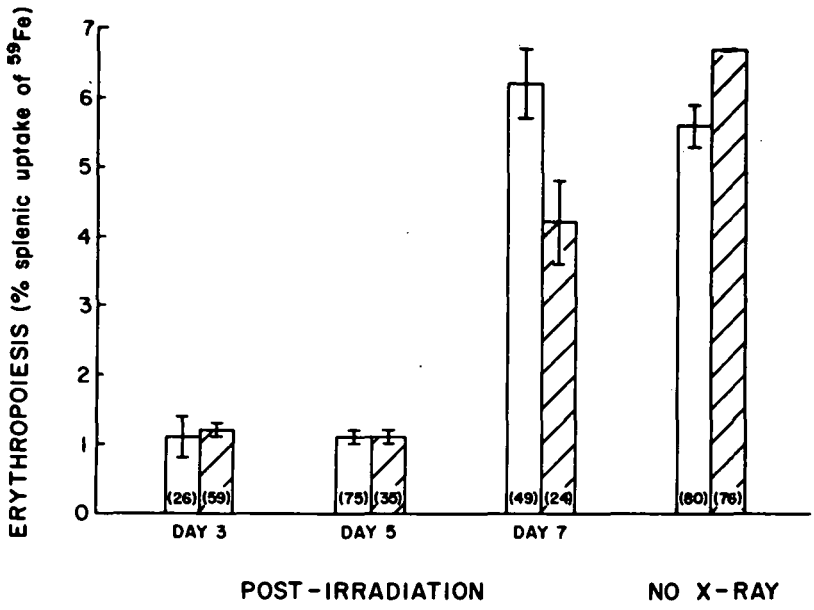

Figure 3. Erythropoiesis in mouse spleens was estimated by measuring the splenic uptake of radioiron. Numbers in parentheses indicate the number of experimental animals from which the mean values (bars) were obtained. Cross-hatching, brackets, and titles are explained in the legend for Figure 2.

stem cells.[14] After day 6, the curve closely corresponds to the splenic uptake of radioiron which precedes a reticulocytosis in the peripheral blood.[4] Thus, in the absence of splenic erythropoiesis during the first 5 days after 850 R L.S., the curves in Figure 1 must depict an increase in undifferentiated cells that will later give rise to erythroblasts. After day 5, the curves undoubtedly reflect the increase in radioiron incorporation which accompanies hemoglobin synthesis by differentiated cells.

Erythropoietic activity of plasma from shielded mice made hypoxic was markedly increased over the activity of plasma from mice maintained at ambient pressure, and greatly exceeded the activity of plasma from normal mice exposed to hypoxia. The site where erythropoietin is inactivated has not been ascertained, but some evidence suggests that it is consumed by an erythropoietically active bone marrow.[15] Immediately after irradiation, only a small fraction of active marrow cells remains in shielded mice, and therefore, decreased utilization of erythropoietin because of this depleted marrow may conceivably explain the higher levels of the hormone detected in irradiated animals. If erythropoietin derepresses the gene for hemoglobin synthesis to induce erythroid differentiation of stem cells,[16] one might predict that erythropoietin would be cleared from the blood during erythropoiesis. It seems unlikely that the irradiation alters the kidney so that hypoxia causes it to secrete more erythropoietin than normal, but this remains a possibility.

Finally, these studies on increasing radioresistance, supported by previous results with splenic colony formation and increasing splenic uptake of ^{131}I-UdR,[4] permit the observation that stem cell replication occurs during the first 5 days after irradiation. During this early proliferative phase of autorepopulation, stem cells are refractory to elevated levels of either exog-

enous or endogenous erythropoietin; erythroid differentiation, as indicated by splenic uptake of radioiron and reticulocytosis, does not occur until after the fifth day.

How does the replicating stem cell transform to the erythropoietin responsive cell? Kretchmar postulates that erythropoietin enters the cell during the G_1 phase of the cell cycle.[17] During marrow repopulation, however, most stem cells are in the S phase of the cycle, and G_1 is too short to permit the entry of the erythropoietin that would induce differentiation. His computer model relates the duration of G_1 as a function of the number of cells in the stem cell compartment. Once this is replete, G_1 lengthens, and erythroid differentiation may proceed in the presence of erythropoietin. His preductions[17] are strikingly similar to our experimental results.

ACKNOWLEDGMENTS

Mrs. Myra Swatek, Mr. James Bland, Mr. Donald Charleston, Mr. John Stupka, and Dr. Eric Simmons provided valuable technical assistance in the work.

LITERATURE CITED

1. Gurney, C. W., E. Goldwasser, and C. Pan. J. Lab. Clin. Med., 50:534, 1957.
2. Troup, S. B., S. N. Swisher, and L. E. Young. Am. J. Med., 28:751, 1960.
3. Lajtha, L. G., R. Oliver, and C. W. Gurney. Brit. J. Haematol., 8:442, 1962.
4. DeGowin, R. L. J. Lab. Clin. Med., 70:23, 1967.
5. Smith, L. H. Am. J. Physiol., 206:1244, 1964.
6. DeGowin, R. L., D. Hofstra, and C. W. Gurney. Proc. Soc. Exptl. Biol. and Med., 110:48, 1962.
7. DeGowin, R. L., D. Hofstra, and C. W. Gurney. J. Lab. Clin. Med., 60:846, 1962.
8. Lewis, J. P., and F. E. Trobaugh, Jr. Nature, 204:589, 1964.
9. Till, J. E., and E. A. McCulloch. Ann. N. Y. Acad. Sci., 114:115, 1964.
10. Alpen, E. L., and D. Cranmore. In The Kinetics of Cellular Proliferation. F. R. Stohlman, Jr., ed. New York: Grune and Stratton, 1959, p. 290.
11. Filmanowicz, E., and C. W. Gurney. J. Lab. Clin. Med., 57:65, 1961.
12. Gurney, C. W., L. G. Lajtha, and R. Oliver. Brit. J. Haematol., 8:461, 1962.
13. Hodgson, G., and I. Eskuche. Nat. Cancer Inst., Monograph 14:169, 1964.
14. Suit, H. D., L. G. Lajtha, R. Oliver, and F. Ellis. Brit. J. Haematol., 3:165, 1957.
15. Stohlman, F., Jr. Ann. N. Y. Acad. Sci., 77:710, 1959.
16. Goldwasser, E. In Current Topics in Developmental Biology. A. A. Moscona and A. Monroy, eds. New York: Academic Press, vol. 1, chap. 7, 1966, p. 203.
17. Kretchmar, A. L. Science, 152:367, 1966.

A REQUIREMENT FOR TWO CELL TYPES FOR ANTIBODY FORMATION IN VITRO*

By

D. E. Mosier†

Antibody synthesis may result from the interaction of two functionally different cell types; one that phagocytizes and "processes" the antigen to provide the stimulus for a second type, the lymphoid cells that synthesize specific antibody.[1] Unequivocal support for this suggestion has not been obtained from in vivo experiments. The following studies, however, in which mouse spleen cells are cultured in vitro with sheep erythrocytes as antigen after the method of Mishell and Dutton,[2] provide provisional support for the hypothesis that two functionally different cell types indeed are required for the induction of antibody synthesis to the antigen.

Spleen cell suspensions were prepared by gently teasing apart the spleens of unimmunized DBA/2 Jax mice in cold Hank's balanced salt solution (BSS). Cell aggregates were allowed to sediment briefly and the resulting supernatant was centrifuged 10 minutes at 600 G at 4° C. The pooled sedimented cells were resuspended to a concentration of 10^7 cells per ml in Eagle's minimum essential medium supplemented with non-essential amino acids, pyruvate, glutamine, and 10 per cent fetal bovine serum. Each culture contained 1 ml of the cell suspension in a 35 x 10 mm plastic culture dish (Falcon). Cultures were maintained on a tilt table (Bellco, Vineland, N. J.) at 13 oscillations per minute in an atmosphere of 7 per cent O_2, 10 per cent CO_2, 83 per cent N_2 as described by Mishell and Dutton.[2] To each dish were added daily 0.05 ml 2X concentrated medium and 0.05 ml fetal bovine serum.

Normal spleen cells were separated into two populations; one population that adheres to plastic during a 30 minute culture interval, and a second population that does not adhere to plastic during the same interval. Thus, separation of cells was based on a functional property; adherence or non-adherence to plastic during a short interval of culture. Ten million spleen cells per culture dish were cultured for 30 minutes and the non-adhering cells were removed by aspiration and used for the preparation of further adherent and non-adherent cell populations. About half of the cells initially plated remained in the culture dish. These remaining cells were either firmly or loosely adherent to the plastic. The loosely adherent cells were removed by three gentle washings with BSS and discarded. About one million cells remained firmly attached to the dish; most of these cells rapidly phagocytized titanium dioxide and for convenience are referred to as a "macrophage rich" (M.R.) population.[3] Culture of the non-adherent cells for two more intervals of 30 minutes removed additional cells capable of adhering to plastic. Most of the non-adherent cells had the morphological characteristics of small lymphocytes and for convenience will be termed a "lymphocyte rich" (L.R.) population. This method of cell separation is shown diagrammatically in Figure 1. Cells adhering to plastic after each of the three pe-

*This paper appeared in Science, 158:1573, 1967. The work was supported in part by USPHS Grant 2T1-GM-93, in part by Argonne Cancer Research Hospital.

†Department of Pathology, University of Chicago.

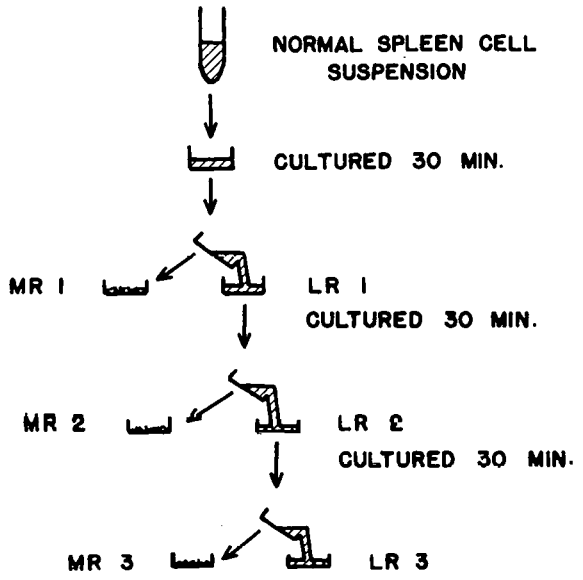

Figure 1. Method of culturing DBA mouse spleen cells to obtain adherent (M.R.) and non-adherent (L.R.) populations.

riods of culture are referred to as M.R. 1, M.R. 2, and M.R. 3 populations. Corresponding non-adherent cells are referred to as L.R. 1, L.R. 2, and L.R. 3 populations.

The number of cultured cells releasing antibody to sheep red blood cells (SRBC) was enumerated by a modification of the Jerne technique using microscope slides. Cultured cells, including cells free in the culture medium and cells adherent to plastic, were harvested by scraping the dishes with a plastic policeman. The harvested cells were washed, dispersed by agitation with a vortex mixer, and added to agarose containing SRBC.[4] Results are expressed as plaque forming cells per 10^6 cells initially cultured. In repeated experiments the optimal dose of antigen was 10^7 SRBC per culture dish; increasing the dose of antigen tenfold did not enhance the response further, and decreasing the dose to 10^6 SRBC produced significantly fewer plaque forming cells. An exponential increase in the number of antibody releasing cells occurred between day 2 and day 4 when 10^7 normal spleen cells were cultured with 10^7 SRBC, as indicated by the solid line in Figure 2. An identical response was obtained when L.R. 3 cells were added to M.R. 1 cells (see Figure 1) and the recombined cell populations were cultured with 10^7 SRBC. Thus, the procedure for separating the two cell populations had not impaired the capacity of the recombined cells to respond to antigen. No plaque forming cell response occurred if either M.R. 1 (1×10^6 cells per dish) or L.R. 3 (adjusted to 10^7 cells per dish) cells were cultured with 10^7 SRBC, indicating that both cell types were essential for the response.

The following experiment demonstrated that antigen rapidly phagocytized by M.R. cells could stimulate the response of the L.R. cells. Macrophage rich cells were cultured with 10^7 SRBC for 30 minutes. The culture fluid was aspirated and each culture dish was washed three times with BSS to remove erythrocytes not phagocytized. Examination of the dishes by phase microscopy showed SRBC present within some macrophages but no free SRBC. An estimated 5 per cent or less of the antigen dose had been phagocytized in 30 minutes.[5] Lymphocyte rich cells (10^7) were added to each culture dish containing 10^6 M.R. cells and phagocytized SRBC.

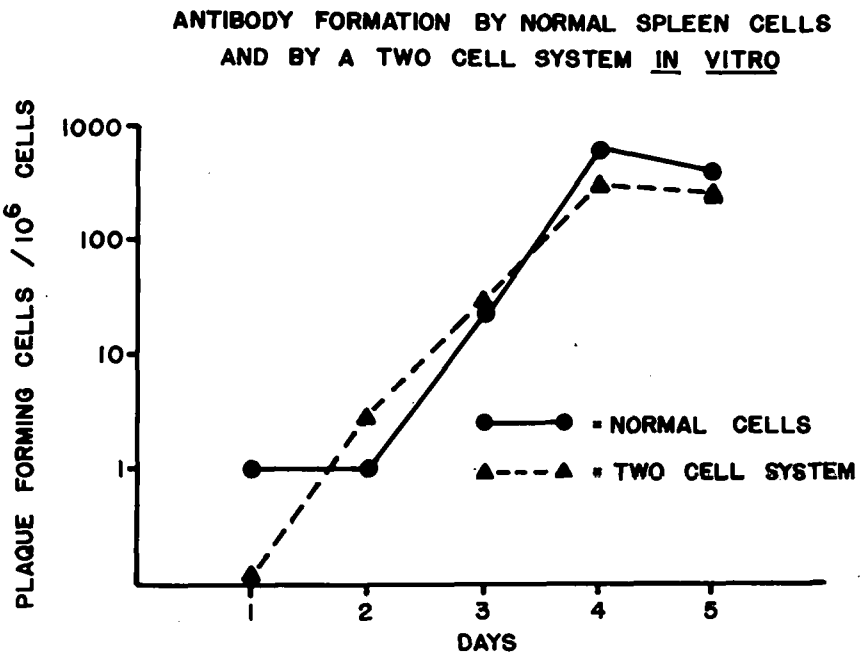

Figure 2. Plaque forming cell response of normal DBA mouse spleen cells and M.R./L.R. cells cultured with 10^7 sheep red blood cells. Antigen was given only to the M.R. cells in the two cell system (see text).

The plaque forming cell response was equivalent to that of normal spleen cells with 10^7 SRBC present throughout culture, and is indicated by the broken line in Figure 2. These results were confirmed in subsequent experiments. A single pool of normal spleen cells was divided into various populations as listed in Table 1. A M.R. population (M.R. 1, 10^6 cells per dish; M.R. 2, 5×10^5 cells per dish; M.R. 3, 2.5×10^5 cells per dish) was incubated with 10^7 SRBC per culture dish for 30 minutes. The dishes were washed carefully, and either 10^7 normal spleen cells or 10^7 L.R. 3 cells were added to each culture dish. Both methods of culture produced a significant plaque forming cell response, comparable in magnitude to that produced by normal spleen cells continuously exposed to antigen. Little or no response occurred if either M.R. cells or L.R. cells alone were cultured with 10^7 SRBC; the very small response of the L.R. 1 cells can be attributed to a few macrophages remaining in this cell population. Similar results were obtained in two additional experiments of identical design presented in Table 1.

Thus, both adherent and non-adherent mouse spleen cells are essential for development of plaque forming cells in vitro. Moreover, an amount of phagocytized antigen estimated to account for less than 5 per cent of the total antigen dose, is sufficient to produce a maximum in vitro immune response. That more antigen is not required for immune induction is consistent with the studies of several workers.[6]

It appears that in the mouse spleen production of antibody to sheep erythrocytes involves both antigen phagocytosis by macrophages and macrophage lymphocyte interaction, both processes being essential for development of lymphoid cells releasing hemolytic antibody. It has been suggested that transfer of information between two cell types involves RNA or RNA-antigen complexes.[7] It may now be possible to determine the nature of "information transfer" between two cell types using in vitro induction of antibody synthesis.

Table 1

CONTRIBUTION OF CELL POPULATIONS TO ANTIBODY FORMATION IN VITRO

(Three separate experiments illustrating the plaque forming cell response of various cell populations. In each experiment the populations were derived from a pool of DBA mouse spleen cells, and exposed to SRBC in vitro.)

Cell population (S)	Day 4 response*		
	Exp. 1	Exp. 2	Exp. 3
Normal spleen cells	1	2	1
Normal spleen cells + SRBC†	170	60	342
(MR 1 + SRBC) + normal cells	215	96	280
(MR 2 + SRBC) + normal cells	115	45	172
(MR 3 + SRBC) + normal cells	90	36	96
(MR 1 + SRBC) + LR 3	50	20	110
(MR 2 + SRBC) + LR 3	125	30	105
(MR 3 + SRBC) + LR 3	50	50	70
MR 1 + SRBC‡	1	0	0
MR 2 + SRBC‡	0	0	0
MR 3 + SRBC‡	0	0	0
LR 1 + SRBC	6	2	4
LR 2 + SRBC	0	0	0
LR 3 + SRBC	0	0	0

*Plaque forming cells per 10^6 cells at initiation of culture.

†10^7 sheep red blood cells.

‡Exposure to antigen either 30 minutes or throughout culture gave the same results.

ACKNOWLEDGMENTS

The advice of Drs. D. A. Rowley and F. W. Fitch is gratefully acknowledged.

LITERATURE CITED AND NOTES

1. Fishman, M. Nature, 183:1200, 1959. Fishman, M., and F. L. Adler. J. Exptl. Med., 117: 595, 1963. Schoenberg, M. D., V. R. Mumaw, R. D. Moore, and A. S. Weisberger. Science, 143:964, 1964. Harris, G. J. Immunol., 9:529, 1965. Gallily, R., and M. Feldman. Israel J. Med. Sci., 2:358, 1966.

2. Mishell, R. I., and R. W. Dutton. Science, 153:1004, 1966. Mishell, R. I., and R. W. Dutton. J. Exptl. Med., 126:423, 1967.

3. Macrophage rich cells were not enumerated in each experiment reported, but in a separate set of experiments the adherent cells were eluted by culturing for 30 minutes in medium supplemented with 30 mM EDTA. The M.R. 1 population was found to contain 1 x 10^6 cells per culture dish, the M.R. 2 population 5 x 10^5 cells per dish, and the M.R. 3 population 2.5 x 10^5 cells per dish. Approximately 95% of adherent cells actively phagocytized sufficient titanium dioxide (0.01%, weight/volume) during 30 minutes of culture to contain many refractile granules visible by phase microscopy.

4. Jerne, N. K., and A. A. Nordin. Science, 140:405, 1963. The assay procedure was modified as follows: spleen cell populations were collected after 4 or 5 days of culture, centrifuged at 600 G for 10 minutes at 4° C, and resuspended in an appropriate volume of BSS. A 0.1 ml aliquot of the cell suspension was added to a test tube containing 0.4 ml 0.5% agarose and 0.05 ml 5% SRBC at 43° C. The mixture was immediately poured onto a microscope slide which had previously been coated with 0.1% agarose. The slides were inverted on a Plexiglas trough containing fresh guinea pig serum diluted 1:10 and incubated 2 hours at 37° C and overnight at 4° C.

5. Ten replicate hemacytometer counts were made on: the suspension of SRBC used to inoculate the culture dishes, and the suspension of SRBC obtained by combining the recovered culture fluid and the repeated washings after the 30 minute culture interval. By this method of enumeration, as many SRBC were recovered as were inoculated. Considering the error of replicate counts to be 5% or less with the dilution method employed, 5×10^5 or fewer SRBC are estimated to have been phagocytized by the macrophages.

6. Roberts, A. N., and F. Haurowitz. J. Exptl. Med., 116:407, 1962. Askonas, B. A., and J. M. Rhoades. Nature, 205:470, 1965. Franzl, R. E. Nature, 195:457, 1962.

7. Fishman, M., R. A. Hammerstrom, and V. P. Bond. Nature, 198:549, 1963. Cohen, E. P., and J. J. Parker. Science, 144:1012, 1964. Friedman, H. P., A. B. Stavitsky, and J. M. Solomon. Science, 149:1106, 1965. Askonas, B. A., and J. M. Rhoades. Nature, 205:470, 1965.

EFFECT OF BACTERIOPHAGE INFECTION ON THE SULFUR-LABELING OF sRNA

By

W-T Hsu, J. W. Foft, and S. B. Weiss*

Several examples of viral-induced modifications of cellular ribonucleic acids have been reported. After infection of Escherichia coli with T-even bacteriophage, Sueoka and Kano-Sueoka[1,2] found quantitative as well as qualitative changes in leucyl-tRNAs, when compared to uninfected cells by chromatography on methylated albumin-kieselguhr (MAK). More recently, Waters and Novelli,[3] using reverse phase chromatography, were able to confirm the early changes in leucyl-tRNA after T2 infection of E. coli, and in addition, observed two new leucyl-tRNA peaks which appeared very late after infection. Wainfan, et al.[4] have reported on the alteration in the relative activities of the base-specific methylases after T2 infection.

The presence of thiolated bases in sRNA and the demonstration that cell-free extracts catalyze the transfer of cysteine-sulfur to sRNA,[5,6] prompted an inquiry as to whether any changes occurred in sulfur-containing RNAs after viral infection. The present communication describes changes in the MAK chromatographic profiles of ^{35}S-labeled sRNA after E. coli infection with T-even bacteriophages. Evidence is offered which indicates that these changes are viral-induced, and that they require protein synthesis to be manifest.

EXPERIMENTAL

Growth of cells and viral infection. E. coli B cells were grown in a medium that contained the following constituents per liter: 2 g of NH_4Cl, 6 g of NaCl, 0.01 g of $MgCl_2$, 6 g of Na_2HPO_4, 3 g of KH_2PO_4, 0.026 g of Na_2SO_4, 2 g of glucose, and 10 mM Tris · HCl of pH 7.5. This medium was further supplemented with 0.04 volumes of 3 XD medium.[7] The cell suspension (2 per cent inoculum of an overnight culture) was vigorously shaken in a gyratory apparatus at 37° (generation time approximately 50 minutes) until a density of 7×10^8 cells/ml was reached, at which time L-tryptophan was added to a concentration of 100 μg/ml, and then T4 phage at a ratio of 13 plaque-forming units per cell. Under these conditions, cell death was found to be greater than 99 per cent after 2.5 minutes, and the number of infective centers was 95 per cent or more of the bacterial cell count. The infected cell suspension was shaken at 37°, and after a given time infection was stopped by the rapid addition of 0.5 M NaN_3 (2 ml per 100 ml of culture), crushed ice, and rapid cooling in an ice-salt water bath to 4°. The cells were collected by centrifugation and either handled immediately for RNA extraction or stored frozen at -20°. Infection with the coliphages T2, T7, MS2, and ϕX174ρ^- was carried out in a similar manner except that the infecting ratio of phage/cell was 10, and E. coli K12W1485 and E. coli C were used as the respective hosts for MS2 and ϕX174ρ^- phage.

^{35}S-labeling of cells. E. coli cells (either infected or uninfected) were labeled with ^{35}S by the addition of radioactive Na_2SO_4 (New England Nuclear Corporation) to the culture medium.

*This report is taken from a paper that appeared in Proc. Nat. Acad. Sci., U.S., 58:2028, 1967. The work was supported in part by the Joseph and Helen Regenstein Foundation.

Cells were collected as described above except that nonradioactive 0.5 M Na_2SO_4 (2 ml per 100 ml of culture) was added to the suspension at the same time as the azide. "Prelabeled-chased" cells were grown in a 300 ml culture which contained 20 mc of $Na_2S^{35}O_4$. At a density of 5 x 10^8 cells/ml, the cells were centrifuged, washed with cold medium several times, and resuspended in 300 ml of fresh medium containing nonradioactive Na_2SO_4. The cells were grown to 1 x 10^9/ml and then divided into two portions; one served as the uninfected control and the other was infected with T4 phage.

Extraction of RNA. The pelleted cells were suspended in 2 ml of 10 mM $MgCl_2$ - 1 mM Tris · HCl, pH 7.5 (sodium dodecyl sulfate [SDS] was sometimes included), and extracted 3 times with an equal volume of phenol.[8] The nucleic acid was precipitated from the aqueous phase by the addition of 0.10 volumes of potassium acetate, pH 5.4, and 2 volumes of ethanol. Subsequently, the RNA preparation was treated with DNase (RNase free, Worthington Biochemical Corporation), then with phenol, and then deacylated by incubation for 45 minutes at 37° in 1 M Tris · HCl, pH 9. The RNA was precipitated and redissolved in the appropriate salt solution for MAK loading.

Chromatography. MAK chromatography was carried out essentially as described by Sueoka and Yamane.[9] In most experiments, 2-3 mg of nucleic acid was added to a 30 ml MAK column (approximately 3 cm in height) in 0.3 M NaCl - 0.05 M Na_2HPO_4, pH 6.7, at a concentration of 20 μg per ml, washed with 300 ml of the same solution, and then eluted with a 240 ml linear salt-gradient from 0.3 M NaCl to 1.2 M NaCl containing the same phosphate buffer concentration as above. Prior to column loading and when necessary, the labeled sample was adjusted to contain approximately 2 mg of total nucleic acid with commercial E. coli B sRNA. The column was run at room temperature, and 2 ml fractions were collected. The fractions were examined for 260 mμ absorbing material and radioactivity by liquid scintillation counting. The samples were counted either directly, or by acid-precipitation and collection on millipore discs (0.45 μ pore size); similar radioactivity profiles were obtained by both methods. In several experiments, the MAK fractions were treated with ribonuclease (10 μg/ml of pancreatic RNase and 1 μg/ml of T1 RNase) prior to radioactivity determinations. In these instances, acid-precipitable radioactivity was measured. Recovery of the ^{35}S-RNA applied to MAK columns ranged between 80-95 per cent.

Thiol-transferase activity measurements. Cells were grown as described above. Infected cells were harvested 20 minutes after T4 infection, 105,000 x g supernatants were prepared from infected and uninfected E. coli B extracts as previously described except that cell washing was omitted.[5] The soluble extracts were dialyzed for several hours against 0.01 M 2-mercaptoethanol - 0.01 M Tris · HCl, pH 7.5, and the protein content was determined by the method of Lowry.[10] Thiol-transferase activity was measured by determining the amount of radioactivity incorporated into the RNA fraction from ^{35}S-cysteine catalyzed by the above extract. Assay conditions were as previously reported.[5]

RESULTS

When E. coli is grown on a medium containing radioactive sulfate for several generations, the cellular RNA becomes readily labeled.[11-13] This radioactivity is associated only with the low molecular weight RNA species. When RNA extracts are prepared from sulfur-labeled E. coli cells and subjected to chromatography on MAK, several radioactive peaks are usually observed in the region where sRNA is eluted (Figure 1). The ^{35}S-labeled material is acid-insoluble but is

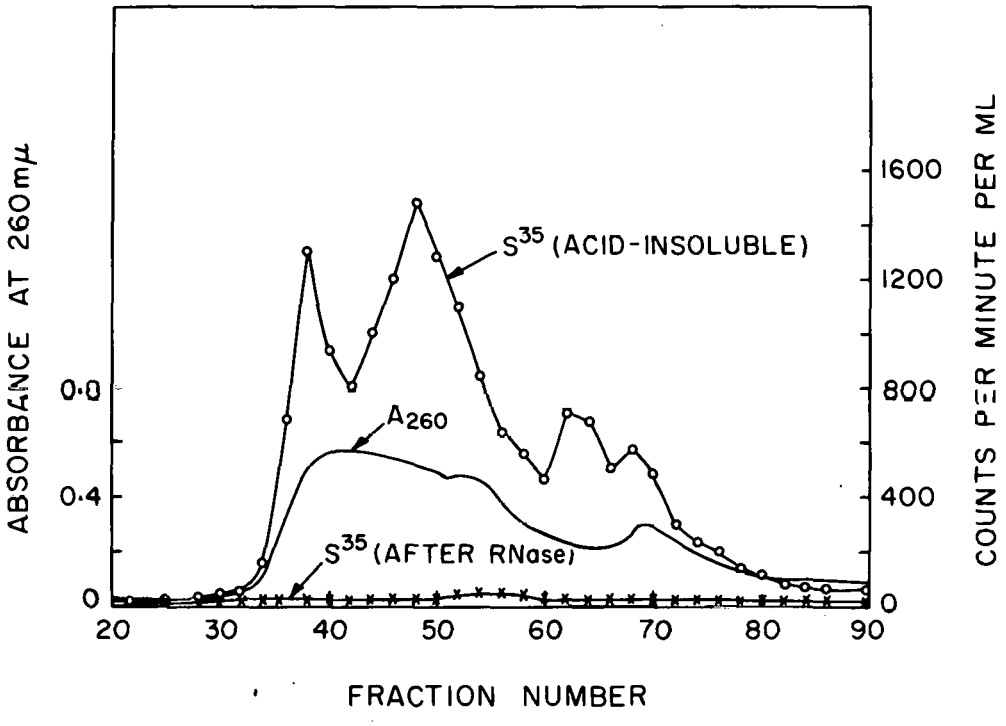

Figure 1. Chromatography of E. coli ^{35}S-RNA on MAK. E. coli B was grown in 100 ml of medium containing 50 mc of $Na_2{}^{35}SO_4$, and labeled RNA was prepared from these cells as described under "Experimental." Thirty-six μg of ^{35}S-RNA (80,000 cpm) was mixed with 2 mg of carrier E. coli B sRNA and chromatographed on MAK.

readily converted to an acid-soluble form by treatment with RNase, but not with DNase.

RNA extracts prepared from T4 infected and uninfected cells, pulse-labeled for 17.5 minutes with ^{35}S-Na_2SO_4, give similar radioactive profiles after centrifugation in a sucrose gradient (Figure 2). In both cases, all of the label is found with the slowly sedimenting RNA species. When these same RNA extracts are subjected to chromatography on MAK, a striking difference is observed in the radioactive elution pattern (Figure 3). The RNA extract from uninfected cells shows two predominant radioactive peaks in the early part of the sRNA elution profile and a minor third radioactive region following, whereas the T4 infected profile appears to be reversed, the first and second ^{35}S-peaks are sequestered and the third peak is now predominant. As is the case for the labeled material from uninfected cells, the T4 ^{35}S-labeled fractions are nondialyzable, acid and alcohol precipitable, and rendered soluble to these reagents by treatment with RNase.

Experiments were carried out to test the dependence of the observed chromatographic changes of ^{35}S-RNA on viral infection. Pulse-labeling of T4 infected E. coli revealed that the first observable changes in the labeled RNA profiles occurred between 4.5 and 7.5 minutes after infection (Figure 4). As compared with noninfected cells, infected E. coli showed a diminished rate of ^{35}S-incorporation into the first two peaks and a marked increase in the rate of labeling of the peak 3 region.

The transition of the ^{35}S-RNA labeling pattern from the "uninfected" to the "infected" profile is prevented by the addition of chloramphenicol to the medium just prior to, or at the same

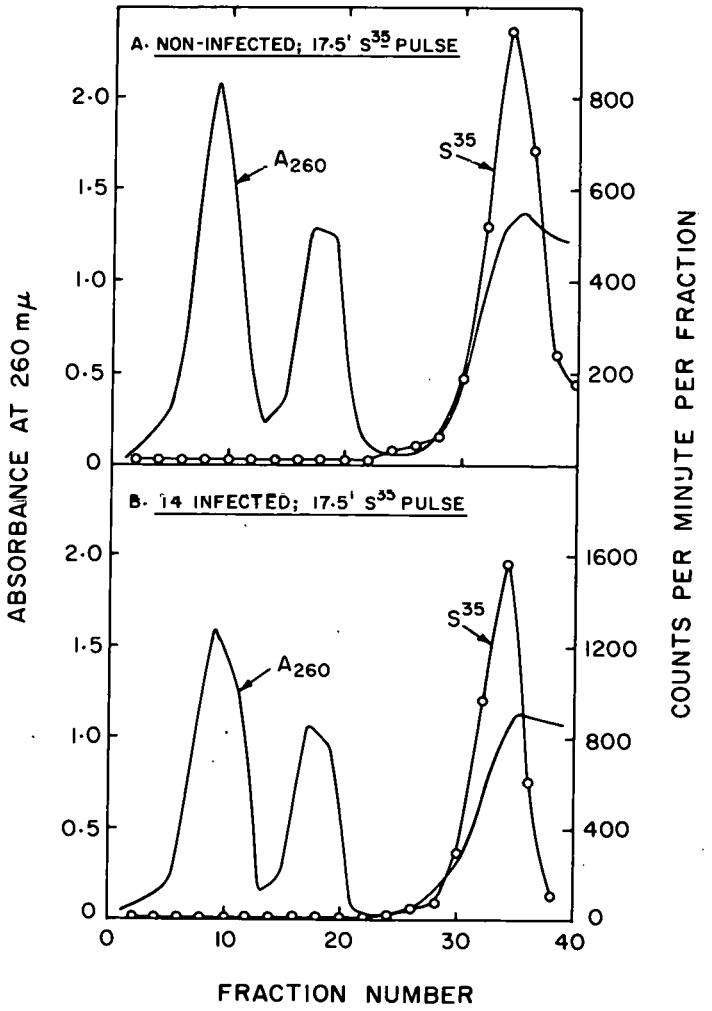

Figure 2. Sucrose-gradient centrifugation of ^{35}S-RNA from noninfected T4 infected E. coli. E. coli B (400 ml culture) was pulsed for 17.5 minutes with 15 mc of $Na_2{}^{35}SO_4$. A second 400 ml culture was infected with T4 phage, 15 mc of $Na_2{}^{35}SO_4$ was added 2.5 minutes later and incubation proceeded for 17.5 minutes more. RNA was extracted from the collected cells as described under "Experimental" (1% SDS was included in the phenol extraction procedure). Uninfected (840 μg) and infected (670 μg) ^{35}S-RNA were subjected to sucrose-gradient centrifugation at 24,000 rpm for 19 hours at 4° in a Spinco SW-25 rotor, and fractions were collected from the bottom of the tube. The sucrose-gradient was from 3-20% in 0.1 M NaCl-0.01 M Tris· HCl, pH 7.5, and the radioactivity shown represents acid-precipitable counts.

time as initiation of infection (Figure 5). Chloramphenicol by itself does not alter the ^{35}S-RNA profile in normal cells. If chloramphenicol is added 5 minutes after infection, or later, the viral-induced transition is observed once more. Under the conditions employed here, chloramphenicol inhibits ^{14}C-leucine incorporation into acid-insoluble material by 98 per cent, indicating an almost complete shut off of cellular protein synthesis.

An analysis of the sulfur-containing nucleotides in the early and late RNA fractions (alkaline hydrolysis and chromatography on DEAE cellulose[5]) revealed no great differences between uninfected peaks 1 and 2 and infected peak 3. In each RNA peak approximately 70-80 per cent of

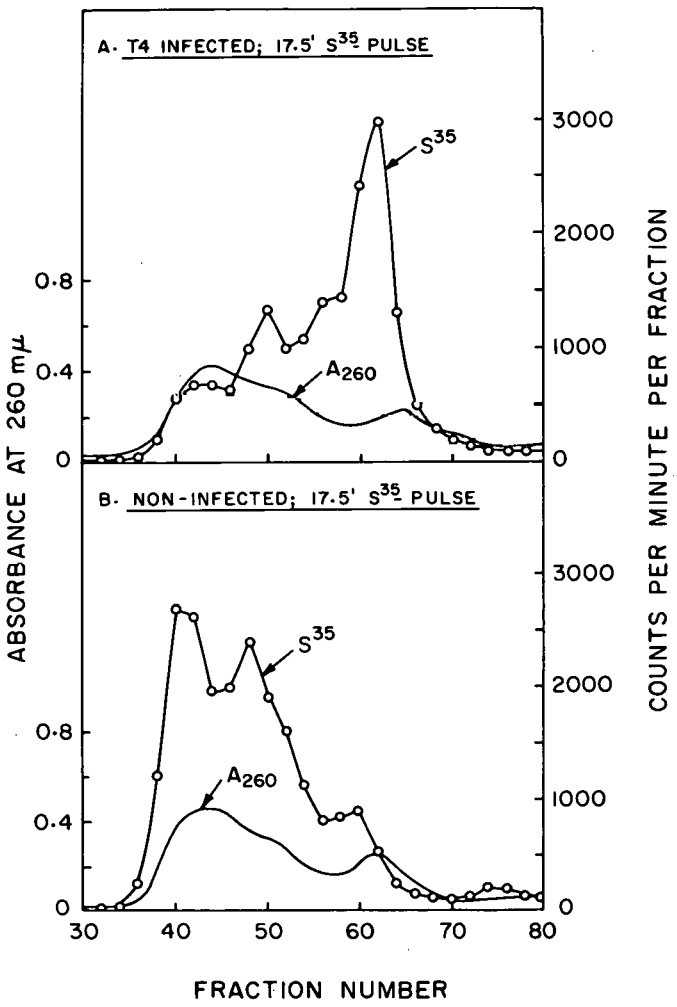

Figure 3

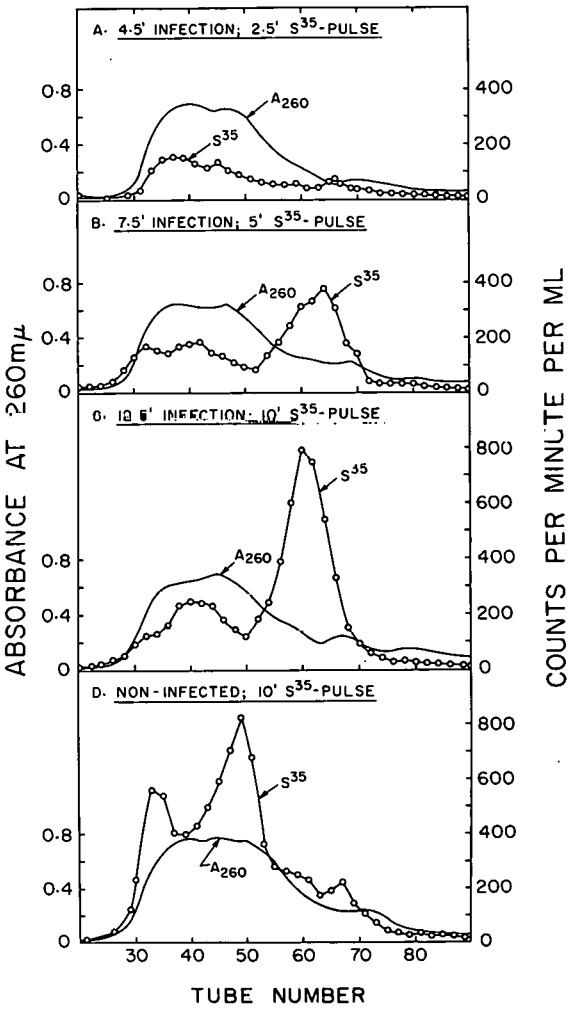

Figure 4

Figure 3. Comparison of MAK ^{35}S-RNA profiles from T4 infected and uninfected pulse-labeled cells. Pulse-labeled ^{35}S-RNA from T4 infected (A) and uninfected (B) E. coli B was prepared as described for Figure 2. The extracted RNAs were subjected to MAK chromatography as described under "Experimental."

Figure 4. MAK profiles of ^{35}S-sRNA extracted from E. coli cells exposed to T4 infection for various periods. E. coli B were infected with T4 phage, $Na_2{}^{35}SO_4$ was then added several minutes later (5 mc/100 ml of culture) and infection stopped at various times after the isotope addition. The RNA was extracted from the infected cells and subjected to chromatography on MAK. (A) Isotope added 2.0 minutes after infection; infection stopped after 4.5 minutes. (B) Isotope added 2.5 minutes after infection; infection stopped after 7.5 minutes. (C) Isotope added 2.5 minutes after infection; infection stopped after 12.5 minutes. (D) E. coli B cells pulsed for 10 mintues with isotope (no infection). The amount of ^{35}S-RNA used for chromatography was 1.8 mg, 0.8 mg, 0.4 mg, and 0.48 mg for A, B, C, and D respectively. Carrier E. coli sRNA was added to each of these prior to loading onto MAK, so that a total of 2 mg of sRNA was chromatographed.

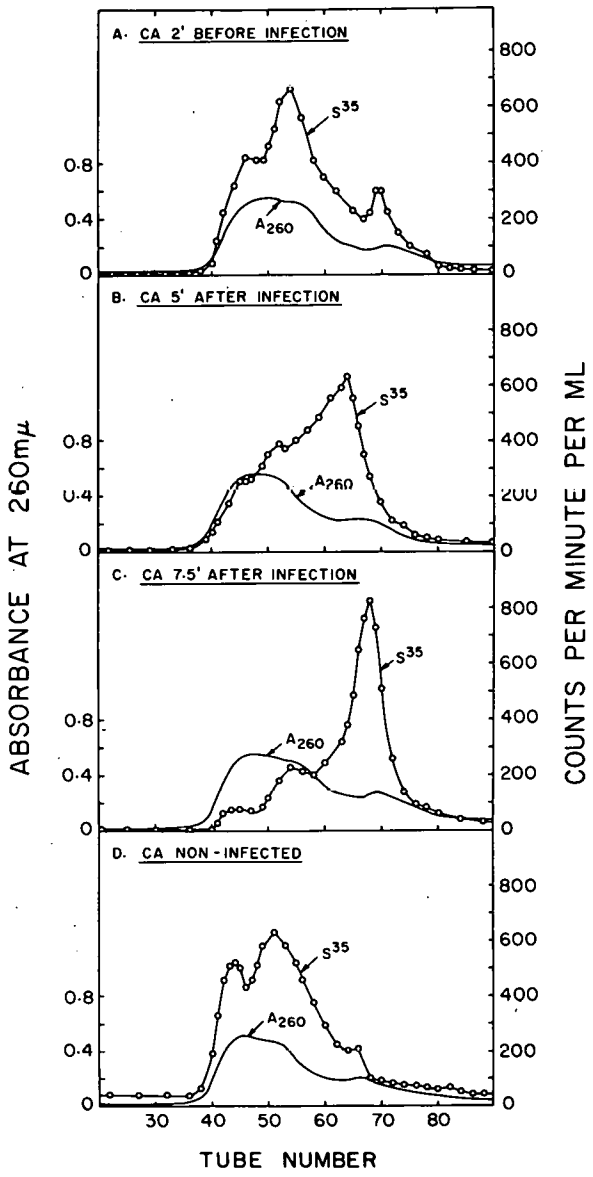

Figure 5. Effect of chloramphenicol on ^{35}S-labeling of RNA in T4 infected cells. One hundred ml cultures were employed for A, B, and C, and a 200 ml culture for D. In each case, 10 mc of $Na_2{}^{35}SO_4$ was added to the cultures and chloramphenicol (CA) was present at a concentration to 50 μg/ml. At the end of the incubation, cells were collected, RNA extracted, and subjected to chromatography on MAK. (A) CA added 2 minutes before T4, and $Na_2{}^{35}SO_4$ added 2.5 minutes after infection. (B) CA added 5 minutes after T4, and $Na_2{}^{35}SO_4$ added 30 seconds later. (C) CA added 7.5 minutes after T4, and $Na_2{}^{35}SO_4$ added 30 seconds later. Infection was stopped 20 minutes after T4 addition in each of the above runs. (D) $Na_2{}^{35}SO_4$ added 2 minutes after CA, and cells collected after 17.5 minutes.

the ^{35}S-label was found in 4-thioUMP and the remainder distributed in unidentified nucleotides. It seems unlikely, therefore, that the T4-induced transition in ^{35}S-RNA is due to any large alteration in the ratio of the different thionucleotides in the various RNA peaks obtained by MAK

chromatography. For this reason, it was thought possible that the sulfur-containing RNA of peak 3 might be derived from peaks 1 and 2 by specific chemical or structural modifications induced by viral infection. If this were so, the increase of peak 3 ^{35}S-radioactivity after infection could be accounted for by the observed reduction in the labeling of peaks 1 and 2.

To test this hypothesis, E. coli cells were grown on ^{35}S-Na_2SO_4 for several generations, collected, washed, and resuspended in a medium containing cold Na_2SO_4. After "chasing" for approximately one generation, the cells were divided into two portions; one was infected with T4 phage and the other served as an uninfected control. As shown in Figure 6, the sRNA extracted

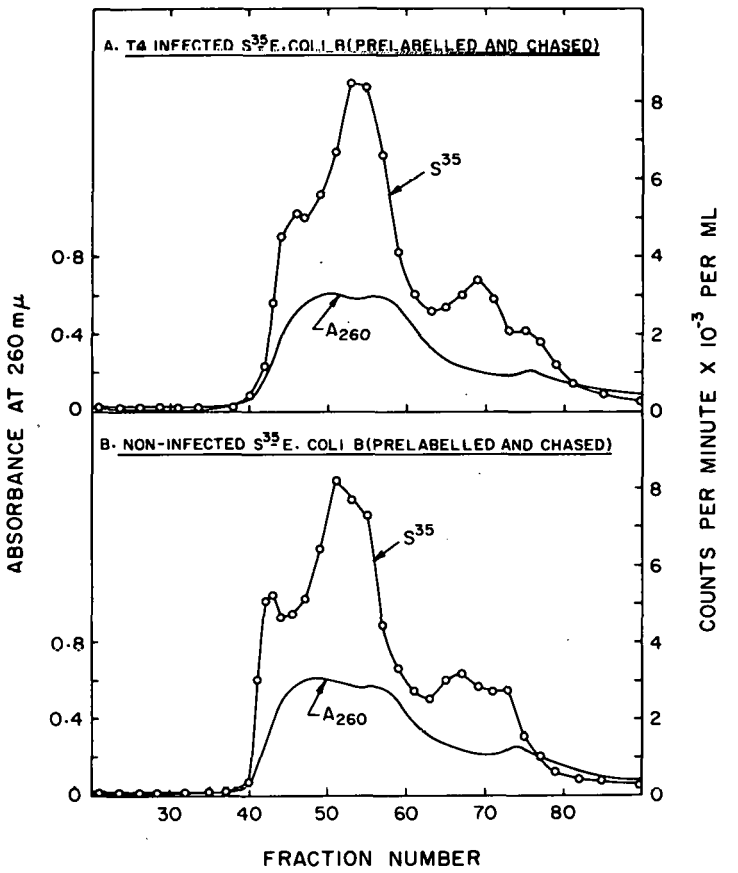

Figure 6. MAK chromatography of ^{35}S-RNA from T4 infected and uninfected "pre-labeled and chased" E. coli cells. E. coli B cells prelabeled with ^{35}S and chased for 1 generation were prepared as described under "Experimental." (A) One portion of cells was infected with T4 phage and infection was stopped after 20 minutes. (B) Another portion was treated the same way but infection was omitted. ^{35}S-RNA was extracted from the collected cells and equivalent samples were subjected to MAK chromatography.

from the uninfected and infected "prelabeled-chased" cells had a similar ^{35}S-radioactive profile, suggesting that the enhancement of peak 3 labeling and sequestration of peaks 1 and 2 labeling, normally seen after infection, are not due to an interconversion of the radioactivity from these fractions. So far, the changes described above in sulfur-labeling of RNA have only been observed with T4 and T2 bacteriophages; pulse-labeled RNA extracts prepared from E. coli in-

fected with T7, ϕX174ρ^-, and MS 2 viruses show ^{35}S-RNA profiles similar to uninfected extracts when subjected to chromatography on MAK (Figure 7).

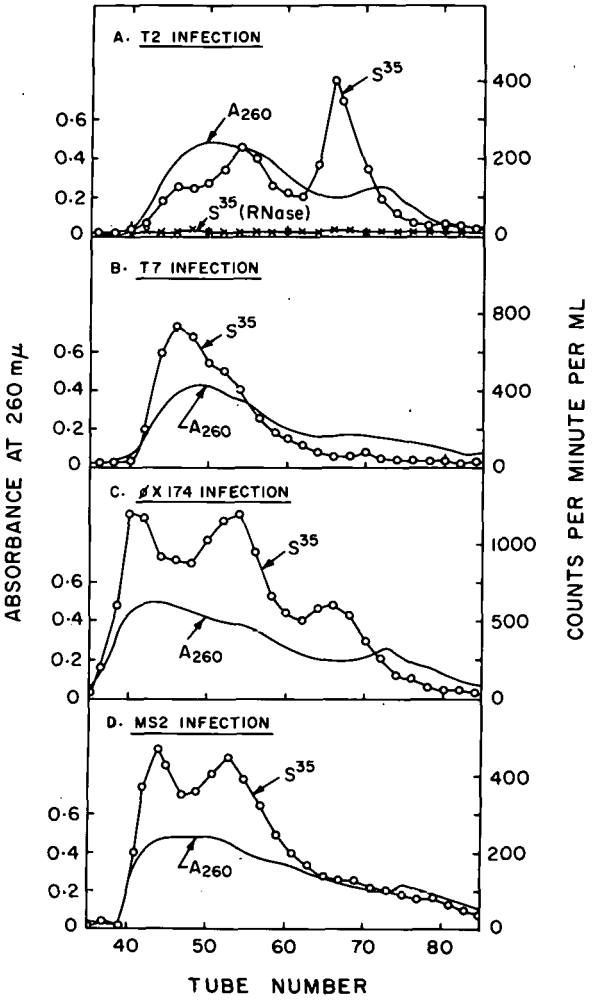

Figure 7. MAK chromatography of pulse-labeled ^{35}S-RNA extracted from T2, T7, MS2, and ϕX174ρ^- infected E. coli. Fifty ml cultures of E. coli were infected with coliphage, and 2.5 minutes later 5 mc of $Na_2{}^{35}SO_4$ was added to the medium. Incubation was continued for 12.5 minutes before the infection was stopped and the cells were collected. The labeled RNA was prepared as described under "Experimental" and then subjected to MAK chromatography. The ^{35}S-RNA chromatographic profiles from the various phage-infected cells are indicated above. The different infected cultures were identical in all respects except that the strain of E. coli host used was as indicated in "Experimental." RNA extracted from control E. coli B pulse-labeled cells was also chromatographed on MAK; no difference from the usual uninfected ^{35}S-RNA profile was observed (not shown here).

An examination of the thiol-transferase activity in the 105,000 X g soluble extract indicates that whereas the initial rates of thiolation are similar for both the uninfected and infected enzyme preparations, the T4 reaction quickly deviates from linear kinetics and levels off early (Figure 8). This phenomenon is found either with or without added acceptor sRNA (yeast); the

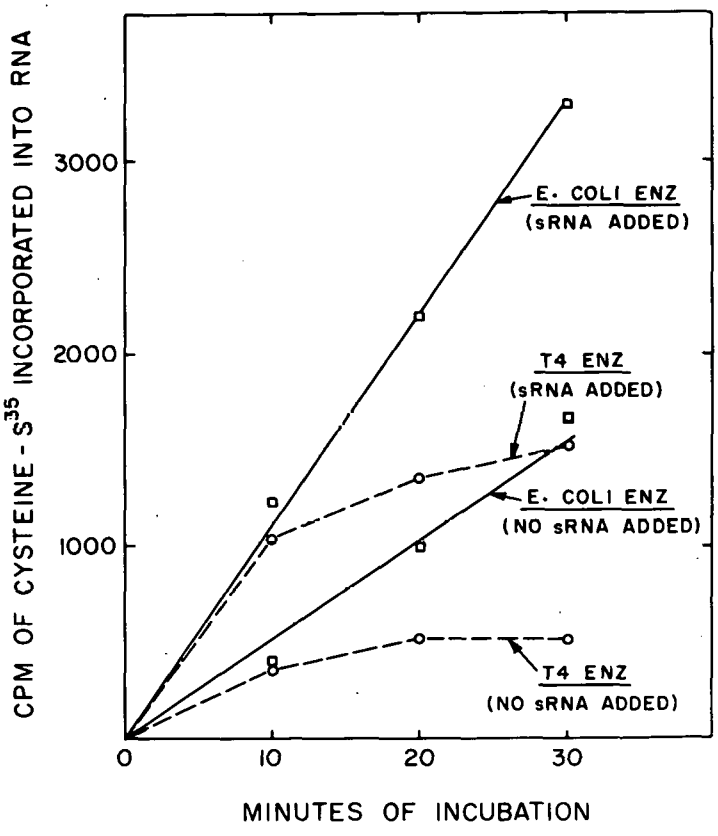

Figure 8. Thiol-transferase activity in uninfected and T4 infected E. coli extracts. The complete system, 0.50 ml, contained 50 μmoles of Tris · HCl (pH 8.2), 1.5 μmoles of ATP, 5 μmoles of 2-mercaptoethanol, 5 μmoles of $MgCl_2$, 0.1 μmole of ^{35}S-cysteine (22 x 10^6 cpm/μmole) and 1.6 mg of protein from either uninfected or infected 105,000 x g extract. Where indicated, 500 μg of acceptor yeast sRNA was included in the reaction mixture. The reaction was incubated at 37° for the times shown above, and the RNA fraction assayed for ^{35}S as described under "Experimental."

overall result is that the extent of thiolation catalyzed by the T4 extract is significantly less than for extracts prepared from uninfected cells.

DISCUSSION

Previous reports from several laboratories indicate that the replication mechanism for certain coliphages involves some modification of the host's translating machinery; phage-induced changes for certain tRNAs[1-3] as well as the appearance of a new tRNA synthetase,[14] have been observed. As described in this report, chromatography on MAK reveals a striking alteration in the sulfur-labeled profiles of soluble RNA after T4 phage infection of E. coli. This phenomenon occurs within 7.5 minutes after infection and may therefore be considered as one of the early events in the viral replicative process. The changes described here appear to be viral-induced since (1) infection with only certain coliphages, T2 and T4, shows this response, and (2) the transition in sulfur-labeling can be prevented by the presence of chloramphenicol just prior to, but not 5 minutes after, infection, suggesting that some phage-induced protein synthesis is necessary.

The possibility that the changes observed in the ^{35}S-RNA profiles by T4 infection might arise from ^{35}S-exchange between different sRNA molecules seems unlikely, since RNA extracts prepared from infected and uninfected cells, pre-labeled with ^{35}S and "chased," show the same type of "uninfected" ^{35}S-RNA distribution pattern on chromatography. Moreover, when the individual peaks are rechromatographed on MAK with the addition of cold carrier sRNA, the radioactivity elutes in the same relative position. The experiment using relabeled ^{35}S-E. coli cells also indicates that the altered T4 ^{35}S-RNA profile is not due to viral-induced alterations of pre-existing host sRNA (e.g., methylation) and that the thiolation of sRNA molecules after infection must represent the de novo addition of sulfur.

The questions that remain unanswered are: whether de novo sRNA synthesis occurs after T-even coliphage infection and if so, whether it is host- or viral-directed. Earlier studies[15-17] have clearly shown that infection of E. coli with T-even phage results in a shutdown of host nucleic acid synthesis, although the extent of this shutdown has not been exactly established. Nomura, et al.[16] found newly synthesized RNA in both the soluble and ribosomal fractions after pulse-labeling T2 infected cells with ^{32}Pi; both labeled RNA fractions were identified as being T2-specific since base analysis indicated a composition similar to T2 DNA. It therefore appeared that very little, if any, host sRNA was being made. On the other hand, the method of analysis might not have permitted the detection of host sRNA synthesis at the level of a few per cent. At the same time, it has never been established whether or not the T-even phage genome codes for any viral-specific RNA other than phage messenger RNA. Preliminary hybridization experiments with highly labeled T4 ^{35}S-RNA obtained from the peak 3 region after MAK chromatography indicates that a significant degree of ribonuclease-resistance is imparted to the ^{35}S-RNA after annealing to T4 DNA; E. coli DNA is far less effective.

The in vitro assays for thiol-transferase activity indicate that viral-infected extracts thiolate sRNA at a slower overall rate and to a lesser extent than extracts from normal cells. Furthermore, the level of endogenous acceptor sRNA for the transfer of cysteine-sulfur also appears to be lower in the infected extracts. These findings could explain the reduced sulfur incorporation in the early MAK-RNA fractions from infected cells, but not the increased sulfur incorporation into the peak 3 region. Several explanations are possible: (1) T4 infection induces the formation of an inhibitor that specifically prevents the thiolation of certain sRNA molecules but not others; (2) Viral infection initiates the synthesis of a specific thiol-transferase and/or viral-specific sRNA acceptors; (3) Infection induces enzymes that specifically degrade or dethiolate certain sulfur-containing sRNAs. This last possibility seems unlikely since infected extracts show no greater rate of ^{35}S-RNA degradation than uninfected extracts. No firm information has been obtained to support or deny the other two possibilities.

Finally, the use of radioactive sulfur as a tool for studying special aspects of RNA metabolism might offer certain advantages over other isotopes. Its primary uniqueness is that so far only the low molecular weight cellular RNA species appear to contain thiolated nucleotides;[9-11] therefore, it may serve as a specific labeling device for following the metabolism of sulfur-containing sRNA molecules. If sulfur-containing nucleotides are indeed absent in the higher molecular weight RNA species, as shown here, then the present results cannot be attributed to the degradation of other cellular RNAs, as might be the case if other isotopes were employed.

The labeled RNA preparations have been examined by chromatography on columns of G-100 Sephadex which clearly resolves mixtures of 4S and 5S RNA into two separate and distinct peaks.[18]

The ^{35}S-RNA behaves like 4S RNA from both control and T4-infected cells; no radioactivity is found in the region where carrier 5S RNA is located.

LITERATURE CITED

1. Sueoka, N., and T. Kano-Sueoka. Proc. Nat. Acad. Sci., U.S., 52:1535, 1964.
2. Kano-Sueoka, T., and N. Sueoka. J. Mol. Biol., 20:183, 1966.
3. Waters, L. C., and G. D. Novelli. Proc. Nat. Acad. Sci., U.S., 57, 979, 1967.
4. Wainfan, E., P. R. Srinivasan, and E. Borek. Biochemistry, 4:2845, 1965.
5. Hayward, R. S., and S. B. Weiss. Proc. Nat. Acad. Sci., U.S., 55:1161, 1966.
6. Lipsett, M. N., and A. Peterkofsky. Proc. Nat. Acad. Sci., U.S., 55:1169, 1966.
7. Fraser, O., and E. A. Jerrel. J. Biol. Chem., 205:291, 1953.
8. von Ehrenstein, G., and F. Lipmann. Proc. Nat. Acad. Sci., U.S., 47:941, 1961.
9. Sueoka, N., and T. Yamane. Proc. Nat. Acad. Sci., U.S., 48:1454, 1962.
10. Lowry, O. H., N. J. Rosebrough, A. L. Farr, and R. J. Randall. J. Biol. Chem., 193:265, 1951.
11. Peterkofsky, A., and M. N. Lipsett. Biochem. Biophys. Res. Commun., 20:780, 1965.
12. Carbon, J. A., L. Hung, and D. Jones. Proc. Nat. Acad. Sci., U.S., 53:979, 1965.
13. Schleich, T., and J. Goldstein. Science, 150:1168, 1965.
14. Neidhardt, F. D., and C. F. Earhart. Cold Spring Harbor Symposia on Quantitative Biology, 31:557, 1966.
15. Volkin, E., and L. Astrachan. Virology, 2:149, 1956.
16. Nomura, M., B. D. Hall, and S. Spiegelman. J. Mol. Biol., 2:306, 1960.
17. Brenner, S., F. Jacob, and M. Meselson. Nature, 190:576, 1961.
18. Galibert, F., C. J. Larsen, J. C. Delong, and M. Boiron. Nature, 207:1039, 1965.

THE CONSTANT SIZE OF CIRCULAR MITOCHONDRIAL DNA IN SEVERAL ORGANISMS AND DIFFERENT ORGANS*

By

J. H. Sinclair,† B. J. Stevens,‡ N. Gross, and M. Rabinowitz

There can be little doubt that DNA is present in mitochondria of all organisms. It has been localized to mitochondria by autoradiography[1] and electron microscopy,[2] and a unique species of DNA has been extracted from purified mitochondrial preparations.[3,4] Mitochondrial DNA from birds and mammals has been shown to be circular,[5-7] a configuration heretofore not observed in DNA of animals or plants. This circular form has been useful for obtaining accurate measurements of the length of the molecule. The sizes of mitochondrial DNA from different organisms and from different tissues of a single organism can be compared by electron microscopy. The preliminary data presented in this communication describe such a comparison.

Mitochondria of mouse and chick liver were purified by previously described methods.[4] Mitochondria were isolated from beef heart and from rat and guinea-pig liver by homogenizing the minced tissues in 0.25 M sucrose with a Potter-Elvehjem tissue grinder. Nuclei and large cell fragments were removed by centrifugation at 600 g for 10 min; the mitochondria were purified by centrifuging them 3-4 times for 10 min in 0.25 M sucrose at 600 g and 7500 g. The DNA from chick, beef, and mouse mitochondria and from mouse whole cells was extracted with phenol. Rat and guinea pig mitochondria were extracted with chloroform/isoamyl alcohol and the DNA was further purified by passage through a methylated albumin kieselguhr column. A modification of the Kleinschmidt technique was used in preparation of DNA for observation in a Siemens-Elmiskop I.[6] The microscope was frequently calibrated with replicas of diffraction gratings (54,800 and 28,800 L/in).

Mitochondrial DNA of chick, rat, and beef exists as circular filaments about 5μ in length, which is about the same as that of the circles previously observed in mouse liver.[6] Figure 1 presents an electron micrograph of a representative field of DNA from rat liver mitochondria. Histograms comparing the length of circular mitochondrial DNA are shown in Figure 2. An asymmetry in distribution may be present in both rat and beef. This observation suggests the possibility that there is a minor class at 5.4 μ, but too few molecules have been measured to permit a statistical analysis. Guinea pig mitochondrial DNA is also circular; the average length is about 5.6 μ, i.e., somewhat longer than the DNA of the other organisms. The distributions observed here are similar to those recently reported for mouse, ox, sheep, chicken, and duck,[8] L cells,[7] Xenopus laevis,[9] and sea urchins.[10]

The considerable variation in the morphological appearance of mitochondria in different

*This report is taken from a paper that appeared in B.B.A., 145:528, 1967. The work was supported in part by NIH and NSF grants to Dr. H. Swift andM.R.; USPHS Career Development award to M.R.; NASA Traineeship to J.H.S.; USPHS Training Grant to B.J.S. and to N.G.

†Present address: Department of Embryology, The Carnegie Institute of Washington, Baltimore, Maryland.

‡Present address: Biologie Cellulaire 4, Bâtiment 400, Faculté des Sciences, 91 Orsay, France.

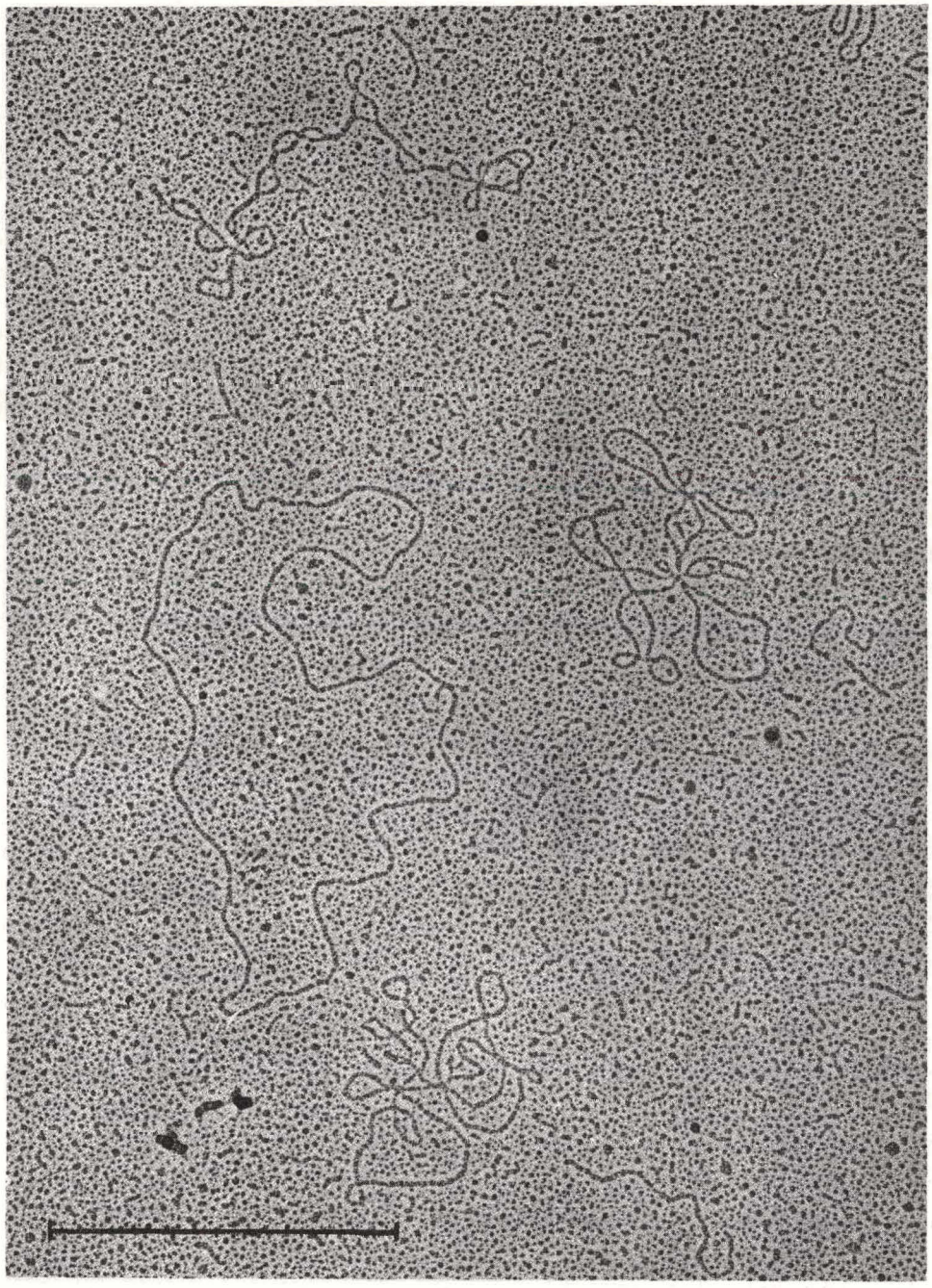

Figure 1. Rat liver mitochondrial DNA prepared by the Kleinschmidt technique (3-6 μg/ml DNA; 1 mg/ml cytochrome c; 1 M ammonium acetate; rotary shadowing with 10-12 mg uranium oxide at an angle of 6° and a distance of 11 cm). x 48,000.

organs such as liver, heart, pancreas, and kidney makes it of interest to determine whether mitochondrial DNA also differs. It has previously been shown that the buoyant densities of mitochondrial DNA from chick liver and chick heart are the same.[4] Since circular mitochondrial DNA is readily distinguishable from nuclear DNA, it is possible to measure the molecular size of mitochondrial DNA from different sources in whole cell DNA extracts. DNA was extracted

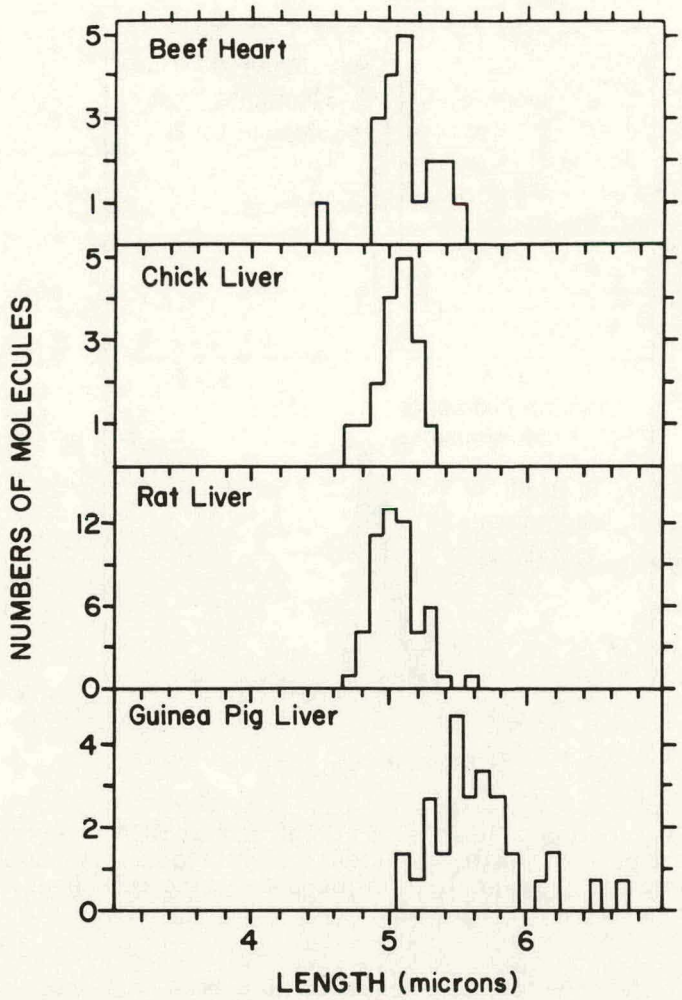

Figure 2. Distribution of lengths of mitochondrial DNA circular filaments extracted from beef, chick, rat, and guinea pig tissues.

from mouse brain, pancreas, and kidney and prepared for electron microscopic observation by the method used to extract mitochondrial DNA from mouse liver.[6] Circular filaments are present in each organ. In Figure 3, the sizes of the mitochondrial DNA filaments have been plotted as a histogram. Although relatively few molecules were measured, there is no evidence that the molecular size is different in these four tissues.

These data show that mitochondrial DNA molecules from several different organisms and from several different tissues of a single organism are very similar in size. Mitochondrial DNA that exists as open ended filaments in Neurospora[3] and yeast[9] is also similar in size to that observed here. It is not clear what the relatively constant size of mitochondrial DNA from different organisms means. This finding may be related to a limited but similar informational content of heterologous mitochondrial DNA. It would be of value to measure the size of mitochondrial DNA in a wider variety of organs and organisms. Assuming that all mitochondrial DNA molecules in an organism are identical, the size of 5 μ, which corresponds to about 10^7 daltons, limits the informational content of mitochondrial DNA. This assumption is not firmly established

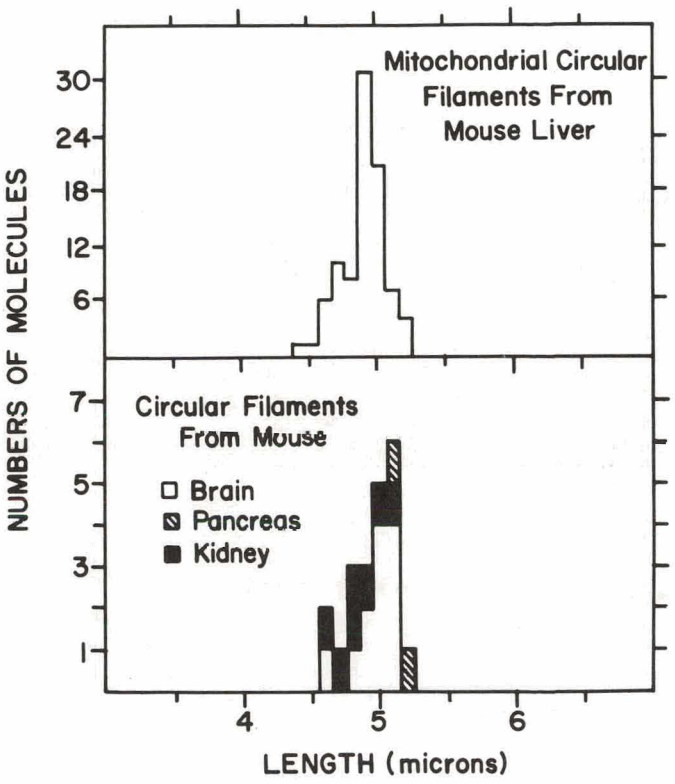

Figure 3. Distribution of lengths of mitochondrial DNA circular filaments present in liver, brain, and kidney of the mouse. The DNA from liver was extracted from purified mitochondria; the DNA from brain and kidney was extracted from whole cells.

since it is possible that differences in base sequence may exist even though measurements of buoyant density and molecular length fall within a single narrow distribution. The observation that the length of mitochondrial DNA from different organs is similar does not eliminate the possibility that genomic difference may be a factor in mitochondrial differentiation.

ACKNOWLEDGMENTS

We thank Professor H. Swift of the Department of Zoology, University of Chicago, for many helpful suggestions and use of his facilities.

LITERATURE CITED

1. Stone, G. E., and O. L. Miller. J. Exptl. Zool., 159:33, 1965.
2. Nass, M. M. K., and S. Nass. J. Cell Biol., 19:593, 1963.
3. Luck, D. J. L., and E. Reich. Proc. Nat. Acad. Sci., U.S., 52:930, 1964.
4. Rabinowitz, M., J. H. Sinclair, L. DeSalle, R. Haselkorn, and H. Swift. Proc. Nat. Acad. Sci., U.S., 53:1126, 1965.
5. Van Bruggen, E. F. J., P. Borst, G. J. C. M. Ruttenberg, M. Gruber, and A. M. Kroon. Biochim. Biophys. Acta, 119:437, 1966.
6. Sinclair, J. H., and B. J. Stevens. Proc. Nat. Acad. Sci., U.S., 56:508, 1966.

7. Nass, M. M. K. Proc. Nat. Acad. Sci., U.S., 56:1215, 1966.

8. Kroon, A. M., P. Borst, E. F. J. Van Bruggen, and G. J. C. M. Ruttenberg. Proc. Nat. Acad. Sci., U.S., 56:1836, 1966.

9. Wolstenholme, D. R., and I. B. David. Chromosoma, 20:445, 1967.

10. Piko, L., A. Tyler, and J. Vinagrad. Biol. Bull., 13:68, 1967.

11. Sinclair, J. H., B. J. Stevens, P. Sanghavi, and M. Rabinowitz. Science, 156:1234, 1967.

JUVENILE HYPERURICEMIA WITH NEUROLOGICAL MANIFESTATIONS*

By

L. B. Sorensen and R. Y. Moore†

Primary gout is an uncommon disease of childhood. Among such cases, however, a number have been described in recent years which present not only with the manifestations of hyperuricemia but with marked neurological impairment as well (Catel and Schmidt,[1] Riley,[2] Lesch and Nyhan,[3] Nyhan, Oliver, and Lesch,[4] Hoefnagel,[5] Hoefnagel, et al,[6] Sass, et al,[7] Shapiro, et al,[8] and Seegmiller, et al[9]). These cases have been regarded as representing a syndrome as distinct metabolically from adult gout on the one hand and from other instances of juvenile hyperuricemia by their neurological manifestations on the other (Lesch and Nyhan[3]). The purpose of this communication is to present four additional cases in order to call further attention to the characteristics of the syndrome and the variations which may occur within the group. Two of these four cases were admitted to the Clinical Research Center, supported by FR-55, USPHS. The other two were studied in the Argonne Cancer Research Hospital.

CASE REPORTS

Michael I. This thirteen-year-old boy is the elder of two brothers. Little information is available regarding their past history, as he has been abandoned by his parents. For the same reason no family history is available, nor are details concerning the pregnancy or delivery. It is stated, however, that this child was said at birth by the physician attending to have cerebral palsy. Thus, he is the only one in the series whose neurologic manifestations were apparently evident at an early age. His development was consistently retarded, and he has never achieved any significant milestones in motor skills. He is able to speak, although at times is difficult to understand. He is not toilet-trained, does not walk, does not feed himself, and in no way is able to care for his own needs. It is said that he has had several urinary calculi in the past, but there is no other information available about his general health. Early in his life it was noted that he exhibited a tendency toward self-mutilation. He had bitten off the major portion of his upper and lower lips; self-mutilation also involved the upper extremities, and he had bitten off all but a small portion of the proximal phalanx of the thumb in the right hand. Because of the tendency toward self-mutilation, it was necessary to keep this child in restraints. He was usually happy and well-disposed to be cooperative and attentive, although on occasion he would spit at someone speaking to him. Self-mutilation in this boy was of particular interest in that it seems to be a compulsive rather than a voluntary activity. As noted above, when restrained he was quite happy, but if the restraints were removed he became increasingly agitated, and his hands would immediately begin to move toward his mouth, and if allowed to go on he would begin to bite him-

*This paper was presented before the 2nd International Congress on Neuro-Genetics and Neuro-Ophthalmology, Montreal, 1967. It appears in Excerpta Medica.

†Departments of Medicine, Anatomy, and Pediatrics, The University of Chicago. Holder of Career Research Development Award (K3-NB-7,389) from the National Institute of Neurological Diseases and Blindness, USPHS.

self despite the fact that he cried out in pain and was evidently greatly disturbed by his own behavior. If he were then restrained again, he would quiet down and return to his normal state. This could be repeated over and over again, and whenever he was unrestrained he became agitated, obviously fearful, and would compulsively move one member or another toward his mouth, where it would obviously have been mutilated if this were not prevented.

General physical examination was unremarkable save for the evidence of self-mutilation. Again, as noted above, very little of his upper or lower lip remained, and that which was present was heavily scarred. In addition most of his right thumb was missing and he had other scars on his hands. A well-healed scar was found along the lower midline of the abdomen.

On neurological examination this boy showed evident mental retardation. It was not clear, however, how much of this was due to his rather severely impaired motor ability and how much represented truly diminished intelligence. He would perform simple movements to command, and could answer simple questions in the affirmative or negative. He ate without difficulty, but had no accomplishments beyond apparent recognition of his surroundings and of individuals. He did become attached to certain members of the nursing staff and quite evidently interacted with some individuals on a primitive level. In addition to the retardation he showed evidence of severe disturbance of movement, and a marked choreoathetosis with an associated double hemiparesis. The deep tendon reflexes were considerably increased, and both plantar responses were extensor. There was some sustained clonus at the ankles. There was a consistent increase in muscle tone, which seemed to be a combination of both spasticity and rigidity. When up on his feet the boy made walking movements with a scissors gait, but was unable to stand or walk by himself. He showed no evidence of sensory defect.

Mark I. This is the second of the two brothers, and was born on June 2, 1960. This boy, at six years of age, was less severely afflicted than his older brother. As is the case with his brother, the history is sketchy because of the unavailability of a parent or similarly informed historian. The child was said to have been slow in his development from the beginning. It is not known, however, whether he showed any clear abnormality at birth, and nothing is known of the history of the pregnancy or delivery. He is said to have passed a kidney stone earlier in his life but the details of this are not known. He has never walked, nor has he been able to care for himself in any manner. He is not toilet-trained, he does not feed himself nor dress himself. He is able to talk and interacts more with people than does his elder brother. He recognizes things shown to him in books and will carry on rudimentary conversations with individuals. He clearly recognizes people and interacts with his surroundings. He is able to play somewhat and will catch and throw a ball. Unlike his brother he has never shown any tendency toward self-mutilation, and can be maintained without restraints. It is noted that he is usually tied into a chair or a bed, though, because with his disorder of motility he has a tendency to fall out and to injure himself.

The general physical examination was normal. On neurological examination, the findings were primarily those of mental retardation with a disorder of motility. In the case of this child the retardation seemed moderate to mild. Again it was difficult to judge this because his difficulty with movement certainly impaired his performance, and his understanding and intelligence may be greater than is apparent from this performance. In contrast to his brother, he showed no choreic movement, but had marked athetosis. He held his head in a position of hyperextension, often with rotation to the right, and there was athetotic posturing and movement of the upper ex-

tremities, which was greater on the left than on the right. He was unable to sit without support and could not walk. Deep tendon reflexes were all considerably increased and the plantar responses were extensor. He also showed a combined spasticity and rigidity which were difficult to separate one from the other. He demonstrated no sensory abnormality. The neurological syndrome in this boy, thus, was one of a combined mental retardation with athetosis and a mild double hemiparesis. He did not demonstrate any evidence of self-mutilation.

David T. This seven-year-old boy was born August 10, 1958, after an uncomplicated, full-term pregnancy. He was the second child in the family, and the family history is unremarkable except that the older brother died at the age of 3 months with a diagnosis of uremia. He was not known to have had hyperuricemia and no neurological abnormality had been noted. This child appeared normal to the mother until the age of 6 months, when she noted that he appeared to experience severe pain when touched over his back. In retrospect his development seemed retarded from the beginning. He did not recognize his mother until 4-5 months of age, and rolled over by himself at 10-11 months. He has never held his head up by himself, nor has he sat, crawled or stood. He does not speak but does make some attempts to play rudimentary games. He has attempted to feed himself but is not able to accomplish this. At the age of one year his mother noted some material in his diaper which had the appearance of sandy gravel. At the same age she also noted self-mutilating behavior, and restraint was required to prevent him from harming himself. At the age of two years he was first noted to have jerking movements of his arms and legs, and these have continued. His neurological status has been stable for some years. In 1965 he had an operation for the removal of kidney stones.

General physical examination showed a small boy who appeared younger than his reported age, but the only other abnormality was evidence of self-mutilation. Neurological examination showed findings which were predominantly those of an extrapyramidal disorder of motility. The primary manifestation of this was athetotic posturing of the arms and head with moderately severe slow athetotic movements. Some rigidity was present both in the arms and legs, and the deep tendon reflexes were increased. The plantar responses were extensor on both sides, and it was not possible to determine whether there was any sensory abnormality. He was clearly severely retarded and evidenced only slight appreciation of his surroundings and a very modest ability to obey simple commands. He showed no control over his own movements. In addition there was marked loss of the tissue of the lower lip from self-mutilation. He was kept in restraints in order to prevent mutilation of the extremities, and became quite agitated when the restraints were removed.

Carl M. This thirteen-year-old boy was first admitted to the University of Chicago Clinics on January 24, 1966. His early history was unremarkable, and he was believed to be perfectly normal until the age of three, when uric acid crystals were noted in the urine, on a routine urinalysis done when he had an upper respiratory infection. At the age of five he had abdominal pain and vomiting, and again was found to have uric acid crystals in the urine. He was relatively well until the age of ten, when he had another episode of abdominal pain and vomiting and on this occasion was found to have hematuria. Such episodes have recurred several times in the last few years. In September of 1965, during a flare-up of this difficulty he was found to have a uric acid of 26 mg% and a BUN of 56 mg%. The retrograde pyelogram done at this time showed hydroureter and hydronephrosis. In December of 1965 he had another episode of abdominal pain and vomiting and was found at this time to have a BUN of 172 mg% and a serum uric acid of 33 mg%.

Urine again showed uric acid crystals, and he was treated at that time with high fluid intake, sodium bicarbonate and Diamox. His BUN fell to 25 mg% and his uric acid to 9 mg%, at which time he was transferred to the University of Chicago Clinics from the University of Wisconsin, where the diagnosis of juvenile gout had been made.

Family history was unremarkable. General physical examination was normal except that he showed a patch of alopecia over the vertex of his skull. On neurological examination he was found to have an intact mental status, except that he seemed somewhat dull. Psychological testing (Stanford-Binet Intelligence Scale Form LM) showed an IQ of 80. The remainder of the neurological examination was normal except that he showed clear choreiform movements in his arms, but no abnormality of tone or posture. These movements were sometimes present at rest, but could be most easily elicited by having him hold his arms outstretched, when they were quite evident. The movements were clearly abnormal for a boy of his age.

METABOLIC STUDIES

The size of the miscible pool of uric acid and its rate of turnover were determined after intravenous injection of uric acid-2-^{14}C (Sorensen[10]). The incorporation of a precursor into purines was assessed by determining the concentration of ^{14}C in urinary uric acid following intravenous injection of glycine-1-^{14}C (Sorensen[11]). Plasma and urine uric acid and its immediate precursors, hypoxanthine and xanthine, were determined by enzymatic spectrophotometric methods.

Table 1 summarizes the results of the metabolic studies in the four boys and in the asymptomatic mother of D.T. Grossly excessive uric acid synthesis is evident. When the data were adjusted for the differences in body weight, the patients were found to have a daily uric acid production of from 42.8 to 62.2 mg/kg of body weight as compared to a normal value of 10 mg/kg. On a purine-free diet D.T.'s mother excreted 641 mg of uric acid per day, which is nearly twice the average value for normal women. However, uric acid production measured with isotopic uric acid was only modestly increased.

From Table 1 it can be seen that the percentage of the dose recovered as urinary uric acid-^{14}C agrees well with the estimate based on the mean daily urate excretion and the computed daily turnover. The amounts of uric acid excreted in the urine represented from 72.5 to 78.1 per cent of the total amount formed daily as indicated by the turnover rate. This relationship is consistent with the findings in normal subjects and is indicative of normal handling of uric acid at the renal level in our patients.

Intravenous injection of glycine-1-^{14}C into the four patients resulted in a rapid and excessive incorporation of precursor into urinary uric acid, maximum isotope concentration being reached within 18 hours after the administration of glycine. This pattern has been taken as evidence of a shunt pathway whereby precursor is incorporated into uric acid more promptly than in normal man by bypassing nucleic acid purines. The cumulative recovery of isotope in urinary uric acid over a seven day period after the administration of glycine was strikingly accentuated, ranging from 1.35 to 2.08 per cent of the injected dose. This represents a 10- to 15-fold increase in the utilization of glycine for production of uric acid as compared to normal control subjects.

No evidence for a shunt pathway was found in the case of the mother of D.T., and the cumulative recovery of ^{14}C in urinary uric acid was grossly normal.

Table 1

SUMMARY OF DATA ON URIC ACID METABOLISM IN FOUR PATIENTS WITH JUVENILE HYPERURICEMIA AND NEUROLOGIC MANIFESTATIONS AND IN ONE CARRIER FEMALE

Pt.	Age	Wt. kg	Uric acid							^{14}C-glycine in urine uric acid (7 days) % of dose
			Plasma	Miscible pool	Turnover		Recovery from urine			
			mg%	mg	mg/day	$\frac{\text{mg/day}}{\text{kg}}$	mg/day	% of turnover	% ^{14}C uric acid	
Ma. I.	6	20	8.85	695	1,244	62.2	907	72.9	71.5	1.60
Mi. I.	13	26	8.74	869	1,454	55.9	1,054	72.5	77.4	1.47
C. M.	13	56	12.45	2,695	2,396	42.8	1,741	72.7	76.9	1.35
D. T.	8	16	7.73	-	-	-	840	-	-	2.08
N. T.*	33	80	4.58	850	821	10.3	641	78.1	82.1	.21

*Mother of D. T.

Adult patients with gout characterized by overproduction of uric acid show a similar, but less marked pattern of incorporation of glycine into uric acid. It has been shown that in the adult type of gout the shunt pathway can be abolished by administration of the synthetic purine azathioprine (Imuran) with ensuing marked lowering of plasma and urinary uric acid (Sorensen[11]). Two of the boys (C.M. and Ma.I.) received azathioprine for a period of ten days in a daily dose of 4 mg per kg body weight. In contrast to the situation in adult gout with overproduction of uric acid, azathioprine failed to reduce either the plasma uric acid level or the urinary excretion of uric acid (Figure 1). Furthermore, the pattern and extent of glycine incorporation into urinary uric acid during treatment with azathioprine were remarkably similar to those obtained during the control period (Sorensen and Benke[12]).

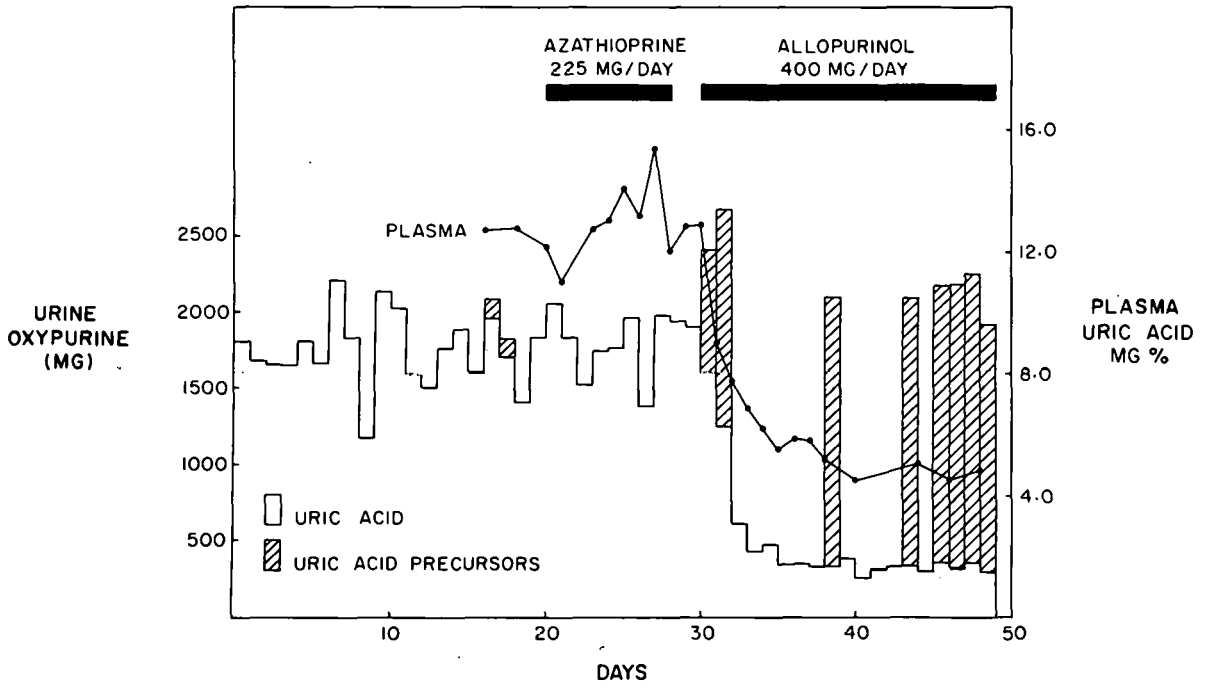

Figure 1. Plasma uric acid and urinary oxypurines during a control period and during treatment with azathioprine and allopurinol in a boy with a syndrome of a neurological disorder associated with excessive purine synthesis. Oxypurines, comprising hypoxanthine, xanthine, and uric acid, are expressed as mg of uric acid.

Allopurinol (Zyloprim®), an isomer of hypoxanthine, is a potent inhibitor of xanthine oxidase, the enzyme which catalyzes the oxidation of hypoxanthine and xanthine to uric acid. This compound produced a dramatic reduction in both plasma and urinary uric acid, but simultaneously there was an increase in the precursors of uric acid so that the total excretion of urinary oxypurines remained constant. With allopurinol, the cumulative recovery of carbon-14 in urinary uric acid was decreased, but when this figure was corrected for the simultaneous increase in hypoxanthine and xanthine, the incorporation of glycine-^{14}C into all oxypurines was comparable to the control value.

DISCUSSION

The striking neurological manifestations associated with remarkable aberration in uric acid metabolism indicate that these patients have a unique disorder. Patients with this syndrome have a four to sixfold increase in uric acid production when compared to control subjects of similar age and weight. This degree of overproduction of uric acid is far greater than that encountered in the adult type of gout. Whereas azathioprine in a dose of 4 mg per kg body weight per day abolished the shunt pathway in gouty men, this drug had no effect on uric acid metabolism in children with this disorder (Sorensen and Benke,[12] Seegmiller, et al[9]).

Recently Seegmiller, et al[9] have demonstrated virtually complete absence of the enzyme hypoxanthine-guanine phosphoribosyltransferase (E.C. 2.4.2.8.) in hemolyzates of washed erythrocytes as well as in fibroblasts grown in vitro from skin biopsies obtained from children with this syndrome. This enzyme converts the free bases hypoxanthine and guanine to their respective ribonucleotides by reaction with 5-phosphoribosyl-1-pyrophosphate. Seegmiller, et al have suggested that this enzyme plays an important role in the normal regulation of purine biosynthesis.

All patients with this syndrome have been boys. Published data on the pedigrees indicate an X-linked recessive pattern of inheritance as the most likely mode of transmission for the disorder (Hoefnagel, et al,[6] Shapiro, et al[8]). The mothers of affected children show no abnormalities on physical examination. Two carrier mothers reported by Hoefnagel, et al[6] and by Shapiro, et al[8] had elevated urinary uric acid outputs in the face of normal serum uric acids. The mother reported by us was also a hyperexcretor of uric acid. However, uric acid dynamics evaluated by the incorporation of glycine into urinary uric acid and by turnover studies with uric acid-^{14}C were not grossly abnormal, thereby excluding metabolic isotope studies as a means of detecting the carrier state.

Seegmiller, et al.[13] have demonstrated that female carriers show mosaicism for the defect in the enzyme hypoxanthine guanine phosphoribosyltransferase. They cultured fibroblasts from skin biopsies obtained from a carrier mother and found that approximately half of the cells incorporated tritiated hypoxanthine, whereas the other half did not. This suggests that abnormal chromosome distribution has occurred postmeiotically and that both abnormal daughter cells and normal cells coexist in the same person. The evidence presented supports the hypothesis proposed by Lyon[14] to explain the lack of dosage effect of X-linked genes and the unusual variability of gene expression in females heterozygous for an X-linked gene.

The uniformity of the features of choreo-athetosis, double hemiparesis, mental retardation and self-mutilation has been repeatedly emphasized (Lesch and Nyhan,[3] Hoefnagel,[5] Nyhan, et al,[4] Hoefnagel, et al,[6] Sass, et al,[7] Shapiro, et al[8]). The cases presented here are of interest in that they show a disparity in the neurologic manifestations of the syndrome. Two patients (David T. and Michael I.) are typical in most respects. Both exhibit the marked pyramidal and extrapyramidal signs, are mentally retarded, and show self-destructive biting. The latter manifestation, as noted by others (Lesch and Nyhan,[3] Shapiro, et al[8]) is unusual and deserves further mention. Although occasionally seen in nonhyperuricemic children with severe mental retardation it is rarely, if ever, as marked or as persistent. When kept restrained these children are docile and happy. If the restraints are removed, however, they become agitated and compulsively move an extremity to the mouth where it is mutilated, obviously with great pain. The genesis of such complex behavior is unclear. In addition these patients appear to have more intellectual de-

fect than, for example, the less severely affected brother (Mark I.). The more severely affected brother (Michael I.) is remarkable in that his signs were evidently sufficiently gross to be noted at birth. This would argue that the defect in purine metabolism is present and of consequence in utero. If this is the case, it would suggest that the primary defect might be an isolated enzyme defect analogous to what has been found in the neurolipidoses. Hypoxanthine-guanine phosphoribosyltransferase is present in brain normally and is especially concentrated in the basal ganglia (Seegmiller, et al[13]). Since oxypurines accumulate abnormally in the cerebrospinal fluid of these patients (Seegmiller, et al[13]), it would seem reasonable to suggest that this enzyme is absent or reduced in the brains of severely affected children. A deficiency of hypoxanthine-guanine phosphoribosyl has been established by assaying the brain of one of Dr. Nyhan's original patients, who died recently (Seegmiller, et al[13]). Two of our patients (Mark I. and Carl M.), however, demonstrated less than the full-blown neurologic picture. In one (Carl M.), only mild choreic movements were evident and he has normal intelligence. In the other (Mark I.) the disorder of motility was apparent but not as marked as in the severely involved patients and he showed borderline intelligence and no self-mutilation. It might be postulated that in these patients there is only a partial enzyme defect in the brain with concomitantly altered function. Such a concept would also be consistent with the fact that neuropathologic studies have not shown lesions consistent with the neurologic picture (Sass, et al[7]). The neurologic manifestations could, then, be viewed as the result of a functional alteration in neuronal metabolism which, since it does not involve structural elements, is not evidenced by an anatomic abnormality in the affected cells.

LITERATURE CITED

1. Catel, W., and J. Schmidt. Deutsche med. Wchnschr., 84:2145, 1959.
2. Riley, J. O. Archives of Diseases of Childhood, 35:293, 1960.
3. Lesch, M., and W. L. Nyhan. American Journal of Medicine, 36:561, 1964.
4. Nyhan, W. L., W. J. Oliver, and M. A. Lesch. Journal of Pediatrics, 67:257, 1965.
5. Hoefnagel, D. Journal of Mental Deficiency Research, 9:69, 1965.
6. Hoefnagel, D., E. D. Andrew, N. G. Mireault, and W. O. Berndt. New England Journal of Medicine, 273, 130, 1965.
7. Sass, J. K., H. H. Itabashi, and R. A. Dexter. Archives of Neurology, 13:639, 1965.
8. Shapiro, S. L., G. L. Sheppard, Jr., F. E. Dreifuss, and D. S. Newcombe. Proc. Soc. Exptl. Bio. and Med., 122:609, 1966.
9. Seegmiller, J. E., F. M. Rosenblum, and W. M. Kelley. Science, 155:1682, 1967.
10. Sorensen, L. B. The Scandinavian Journal of Clinical and Laboratory Investigation, 12, supplementum 54, 1960.
11. Sorensen, L. B. Proc. Nat. Acad. Sci., U.S., 55:571, 1966.
12. Sorensen, L. B., and P. J. Benke. Nature, 213:1122, 1967.
13. Seegmiller, J. E., F. M. Rosenblum, and W. M. Kelley. Personal communication, 1967.
14. Lyon, M. F. American Journal of Human Genetics, 14:135, 1962.

THE EFFECTS OF ESTRADIOL AND ESTRIOL ON PLASMA LEVELS OF CORTISOL- AND THYROID HORMONE-BINDING GLOBULINS AND ON ALDOSTERONE- AND CORTISOL-SECRETION RATES IN MAN*

By

F. H. Katz† and A. Kappas‡

Estriol is quantitatively the most important metabolite of estradiol, being derived from this hormone and related precursors such as estrone, via a chemical transformation which is not reversible in vivo.[1] Its production is known to increase extraordinarily in pregnancy, reaching levels of 60 mg/day or more during the last trimester of a normal human gestation.[2,3] These amounts exceed daily production of this compound in the non-gravid state by a factor of 1000 or more, thus raising the possibility that this steroid metabolite might contribute to certain of the physiological and chemical alterations known to accompany pregnancy, or participate in certain biological effects generally attributed to its precursor hormone, estradiol.

Recent studies from this laboratory have in fact demonstrated that estriol, like estradiol, was anabolic and significantly diminished spontaneous and certain secondary or experimentally induced hydroxyprolinurias in man,[4] substantially reduced the incidence and severity of experimental immune arthritis in the rat,[5] and in appropriate amounts regularly impaired liver function with respect to dye disposal in both man and the experimental animal.[6,7]

In the present study the effects of estriol on certain endocrine factors known to be altered during pregnancy were examined and compared with those effects induced by the natural hormone estradiol. The endocrine parameters chosen for study were the activities of the plasma binding proteins for thyroid hormone and for cortisol, and the secretory rate of aldosterone, all which are known to be elevated in late pregnancy,[8-10] or during estrogen treatment.[11-13] The secretory rate of cortisol was also measured during estriol and estradiol treatment and one possible mechanism of estrogen-induced hyperaldosteronism was tentatively explored.

METHODS

Patients under study were housed on a metabolic ward, and, when indicated for this or concurrent investigations, were given constant diets or maintained on fixed intakes of sodium and potassium. The short control periods shown on the charts depicting the balance studies represent the last several days of a 7-10 day period on the constant diet prior to the initiation of steroid treatment. The majority of the patients studied had musculo-skeletal diseases; none had detectable renal, hepatic, or endocrine abnormalities, except as noted. Steroids were prepared as described in an earlier study.[6] The steroid solvent vehicle alone was shown to be inert, with respect to the endocrine indices studied.

---

*This report appeared in J. Clin. Invest., 46:11, 1967. The work was supported in part by USPHS Training Grant TI AM 5445-03.

†Present address: Department of Medicine, Loyola University Stritch School of Medicine, Hines, Ill. 60141.

‡Present address: The Rockefeller University Hospital, New York, N. Y. 10021.

Analysis of urine sodium and potassium was performed by flame photometry or atomic absorption spectrometry; urine creatinine was measured by a minor modification (without heating) of the method of Bonsnes and Taussky.[14] Thyroid hormone binding globulin was measured indirectly using the tri-iodothyronine (T_3) resin uptake method of Sterling and Tabachnik,[15] or the commercial Triosorb* technique. Cortisol binding globulin was estimated by fractionation of 1 ml plasma containing 0.1 μc (1.6 μg) 4-^{14}C-cortisol on Sephadex G 50 columns,[16] a slight variation of the method of DeMoor, et al.[17] All plasma was heparinized and stored frozen until performance of the tests. Specific activities of urinary tetrahydrocortisol and tetrahydrocortisone[18] and "tetrahydroaldosterone"[19] following injections of radioactive cortisol and aldosterone were used to measure aldosterone and cortisol secretion rates concurrently by double isotope derivative methods as previously described.[20] Routine statistical methods were utilized.[21]

RESULTS

Estrogen effects on thyroid-hormone binding globulin (TBG). Thirteen patients received estriol in amounts of 5-40 mg/day for 3-10 days; 9 patients received estradiol in amounts of 5-50 mg/day for 5-14 days. A minimum of 2 control samples of plasma and 2 samples at the end of the steroid treatment period was obtained at least 2 days apart from each patient (except for one treated for only three days, and studied twice before treatment and on the morning after the last injection). All samples from each subject were tested in duplicate at the same time. Estriol did not consistently or significantly alter the mean T_3 resin uptake in the treated subjects whereas all patients treated with equivalent or substantially lesser amounts of estradiol demonstrated the expected increase in binding activity of TBG (i.e., decreased T_3 resin uptake). Figure 1 shows the difference between the estradiol and estriol effects graphically.

Estrogen effects on cortisol-binding globulin (CBG). Twelve patients received estriol, 8-40 mg/day for 5-10 days; 11 patients received estradiol 5-100 mg/day for 4-16 days. Table 1 shows the results of treatment with these steroids on plasma CBG activity, expressed as μg cortisol capacity per 100 ml plasma for each patient. Figure 2 compares these effects on CBG in each steroid treated group with the range of CBG values observed in the same patients during a control period. Estriol administration did not significantly influence plasma CBG activity, even when injected in the large amounts which are produced during late pregnancy; estradiol, as expected, produced consistent and striking increases in plasma CBG capacity. It is of interest that 5 mg of this hormone was able to evoke practically as much of an increase in plasma CBG activity as was 50-100 mg (Table 2), suggesting that the amount of this hormone excreted in pregnancy (which may exceed 5 mg/day) probably already provides the maximal estrogenic stimulus for CBG production. Evidence that CBG production is actually increased following estrogen has been reported by others.[22]

Estrogen effects on the secretion rate of cortisol (CSR). The CSR was studied before and after steroid treatment in 12 subjects, 7 of whom received estriol 10-40 mg/day for 5-10 days, and 5 of whom received estradiol 5-20 mg/day for 3-10 days (Table 2). Estradiol did not consistently or significantly alter the CSR in either direction; it is of interest that the CSR in none of the estriol treated subjects decreased and that in 2 subjects the increases noted during steroid treatment (S.B. and E.W.) exceed 50 per cent. The mean CSR increased only by 4.1 mg per

*Abbott Laboratories, Franklin Park, Ill.

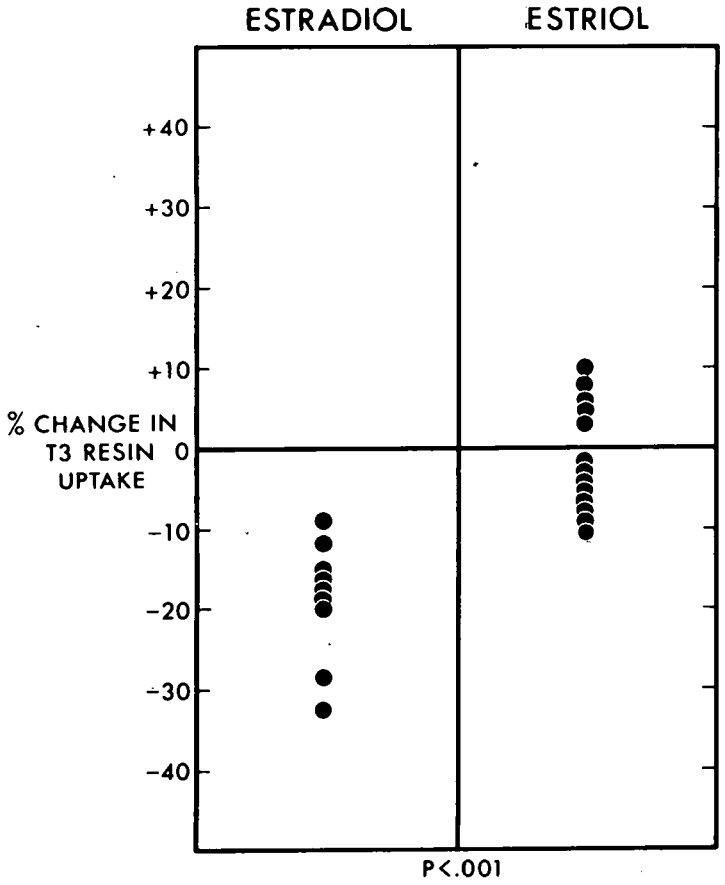

Figure 1. Estrogen effects on T_3 resin uptake. Thirteen patients received estriol, 5-40 mg/day for 3-10 days; 9 patients received estradiol, 5-50 mg/day for 5-14 days. Patients given estradiol had a diminution of their mean T_3 resin uptake while those receiving estriol had no change.

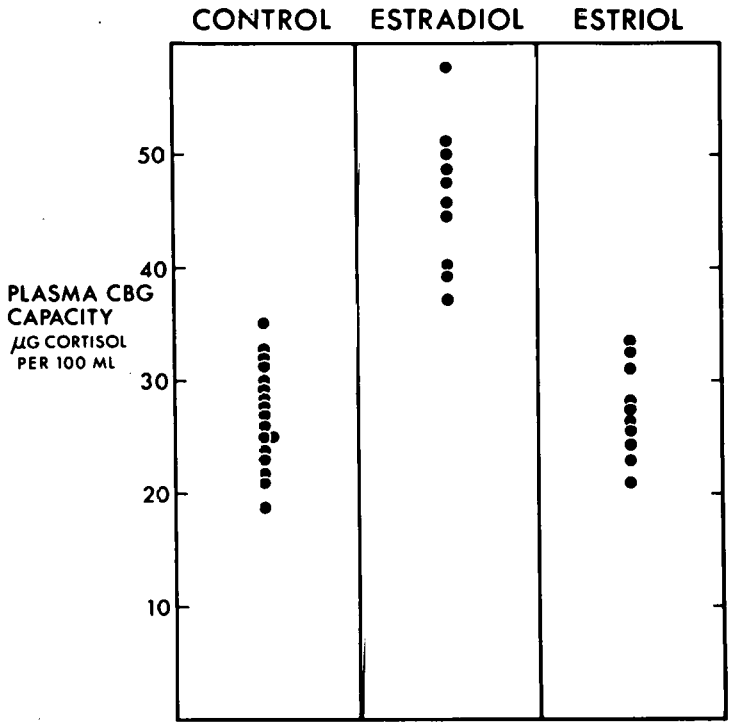

Figure 2. Estrogen effects on cortisol binding globulin (CBG). Subjects receiving estradiol had an increase in CBG capacity while those given estriol had no change.

Table 1

TREATMENT SCHEDULE AND CBG CAPACITY IN 22 SUBJECTS

Patient	Treatment		CBG cortisol capacity	
			Control	Estrogen
		mg/day x days	μg/100 ml plasma	
E. G.	Estriol	8 x 6	27	21
A. R.	Estriol	10 x 7	28	31
J. Z.	Estriol	10 x 10	22	25
E. O.	Estriol	20 x 5	22	27
J. W.	Estriol	20 x 6	23	23
R. A.	Estriol	20 x 7	25	25
J. F.	Estriol	40 x 7	29	23
E. W.	Estriol	40 x 7	31	28
L. W.	Estriol	40 x 8	29	32
S. B.	Estriol	40 x 10	31	34
M. H.	Estriol	40 x 10	27	31
L. M.	Estradiol	5 x 6	29	40
M. M.	Estradiol	5 x 7	19	37
R. B.	Estradiol	5 x 10	28	48
E. M.	Estradiol	7.5 x 12	24	52
E. C.	Estradiol	10 x 8	35	49
E. K.	Estradiol	10 x 8	31	50
A. P.	Estradiol	20 x 4	28	47
J. F.	Estradiol	20 x 7	29	49
E. W.	Estradiol	20 x 7	31	59
L. S.	Estradiol	50 x 4	25	46
M. P.	Estradiol	100 x 16	26	58

day after estriol, although this increase was highly significant ($p < 0.001$). However, the CSR values in all periods remained within the normal range.

Estrogen effects on the secretory rate of aldosterone (ASR). The ASR was studied before and after steroid treatment in 19 subjects, 11 of whom received estriol 10-40 mg/day for 5-11 days and 8 of whom received estradiol 5-40 mg/day for 3-10 days. In 6 subjects the ASR was determined twice during the control period; and in 3 subjects 2 or 3 times during the period of steroid treatment. The upper limit of normal for the ASR on a diet containing 120 mEq sodium in this laboratory is in the range of 200 μg/24 hours. The results of the treatment on the ASR in the 19 subjects are shown in Table 3. One patient in this series (E.K.) was being investigated for the presence of an aldosterone-producing tumor. S.M. had primary aldosteronism with depressed plasma renin activity due to bilateral nodular adrenocortical hyperplasia. One patient had hyperparathyroidism due to metastatic parathyroid cancer (J.F.). K.R. was a 54-year-old man with active acromegaly; four subjects (M.T., P.D., V.C., R.G.) were on 20 mEq sodium

Table 2

TREATMENT SCHEDULE AND CORTISOL SECRETION RATE IN 12 SUBJECTS

Patient	Treatment		Cortisol secretion rate	
			Control	Estrogen
		mg/day x days	mg/day	
A. R.	Estriol	10 x 6	16.5	18.0
F. C.	Estriol	20 x 5	15.0	16.0
S. B.	Estriol	40 x 5	10.3	18.3
J. F.	Estriol	40 x 7	16.0	21.5
E. W.	Estriol	40 x 7	9.3	15.1
N. M.	Estriol	40 x 8	13.5	15.5
M. H.	Estriol	40 x 10	16.4	21.4
M. M.	Estradiol	5 x 7	13.7	12.6
E. K.	Estradiol	10 x 3	8.8	9.4
S. B.	Estradiol	20 x 5	10.3	13.1
E. W.	Estradiol	20 x 7	9.3	7.5
J. F.	Estradiol	20 x 10	16.0	14.4

diets and subject V.C. had severe congestive heart failure. A.R. and V.M. were men and F.C., S.B., and A.P. had undergone hysterectomy.

The administration of estriol increased the ASR significantly (in excess of 20 per cent) in 7 out of 11 patients; these increases ranged from approximately 100 per cent to 900 per cent above control levels and occurred within the shortest time period studied (5 days) after initiation of steroid treatment. The least amount of estriol which appeared to be effective in increasing ASR was about 20 mg/day (1 subject out of 3 responded); although amounts of estriol in the higher ranges of those produced in pregnancy (40 mg/day) induced consistent and pronounced elevation in the ASR in all but one subject (J.N.). The administration of 40 mg/day of estriol for 6 days to an adrenalectomized subject, maintained on cortisol, did not lead to the urinary excretion of metabolites behaving chromatographically like tetrahydroaldosterone, thus excluding the possibility of artifact in the ASR determination after estriol treatment.

Estradiol treatment resulted in an increase ranging from about 40 per cent to 450 per cent in the ASR, in 6 of the 8 patients studied. The effect could be observed with as little as 5 mg/day (subject E.M.) and was apparent at higher doses as quickly as 2 days after injection of the steroid (subject V.M.). It is of interest that the patients with proven and suspected primary aldosteronism (S.M. and E.K.), and subject R.G. (who was on a 20 mEq/day sodium diet), responded to estradiol with significant increases in ASR; the patient with hyperparathyroidism, shown to respond to estriol, did not increase her ASR on estradiol treatment. The possibility that the estradiol effect on the ASR is mediated in part through conversion to its active metabolite estriol cannot be excluded; the converse is not possible however since the transformation estriol →

Table 3

TREATMENT SCHEDULE AND ALDOSTERONE SECRETION RATE IN 19 SUBJECTS

Patient	Treatment		Aldosterone secretion rate		
			Control	Estrogen	% change with estrogen
M. T.	Estriol	10 x 10	260,271	250	-
F. C.	Estriol	20 x 5	90	262	+326
P. D.	Estriol	20 x 5	317,346	260	- 23
A. R.	Estriol	20 x 7	150	165	-
S. B.	Estriol	40 x 5	70	145	+107
A. P.	Estriol	40 x 6	152	380	+150
J. F.	Estriol	40 x 7	179	488	-173
N. M.	Estriol	40 x 8	67	194	+190
J. N.	Estriol	40 x 9	194,189	141,111	- 32
M. H.	Estriol	40 x 10	90	900	+900
V. C.	Estriol	40 x 11	630,438	2478	+383
E. M.	Estradiol	5 x 7	87	145	+ 67
E. K.	Estradiol	10 x 3	433	617	+ 42
S. M.	Estradiol	10 x 10	360,364	547	+ 51
S. B.	Estradiol	20 x 5	70	177	+153
K. R.	Estradiol	20 x 6	262,246	262,246	-
V. M.	Estradiol	20 x 7	90,90	150,235,190	+172
J. F.	Estradiol	20 x 10	179	189	-
R. G.	Estradiol	40 x 8	432,415	2300	+445

estradiol does not occur in vivo.[1] The acromegalic subject (K.R.) also did not increase his ASR during estradiol administration.

Urinary excretion of sodium and potassium following estradiol and estriol treatment. The effects of these steroids on acute changes in urine excretion of sodium and potassium were studied in 4 patients, in a tentative exploration of the possible ways in which estrogens might evoke increases in ASR in man. The effect of estradiol on the urinary excretion of these electrolytes is depicted in Figures 3 and 4. Subject L.R. (Figure 3), a patient with emphysema, had a marked increase in sodium excretion in the first 24 hours following estradiol administration, followed by a prolonged period of sodium retention, due presumably to the increase in ASR induced by estradiol. There was little if any potassium retention in the first 2 days of estrogen treatment. Subject S.S. (Figure 4) also appeared to have a transient sodium diuresis in the first 48 hours after estradiol administration.

The injection of estriol in two patients also appeared to be associated with a very early and transient natriuresis as shown in Figures 5 and 6. The effect was marked in subject V.C. (Figure 6) who was a patient with congestive heart failure exhibiting a significantly positive sodium balance on an intake of 27 mEq/day. Although she had been excreting less than 5 of the 27 mEq of sodium intake per day during the control period, on days 1 and 3 of estriol treatment (the

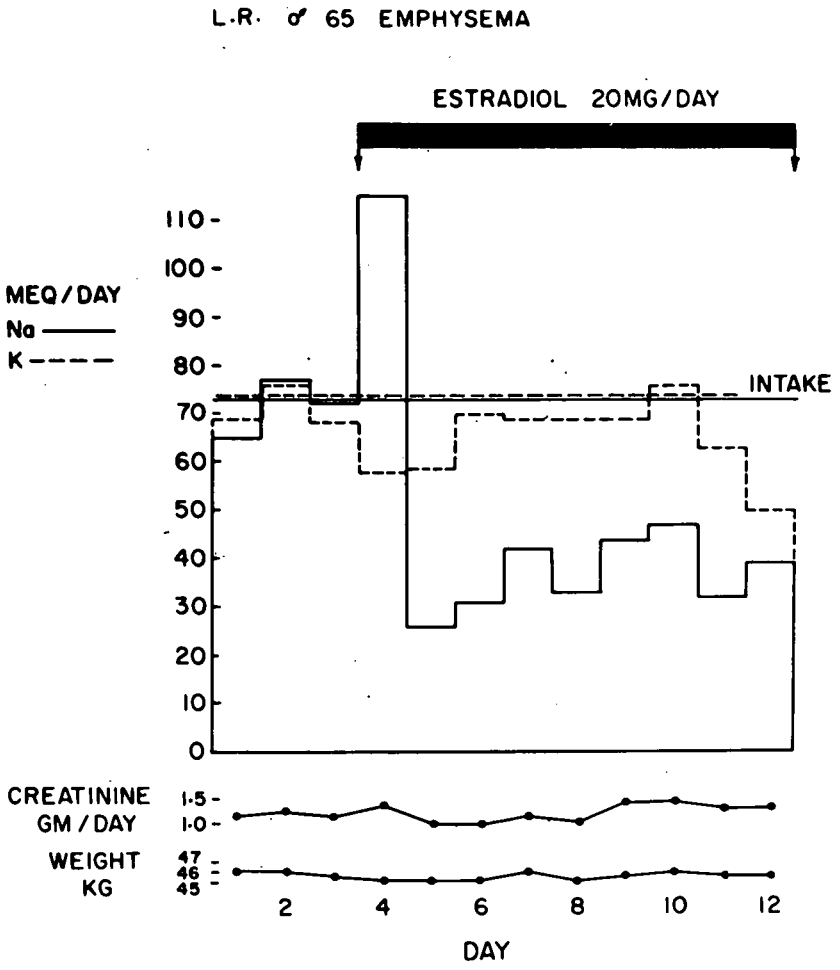

Figure 3. Urinary excretion of sodium and potassium. Urinary sodium loss was seen on the first day of estradiol administration.

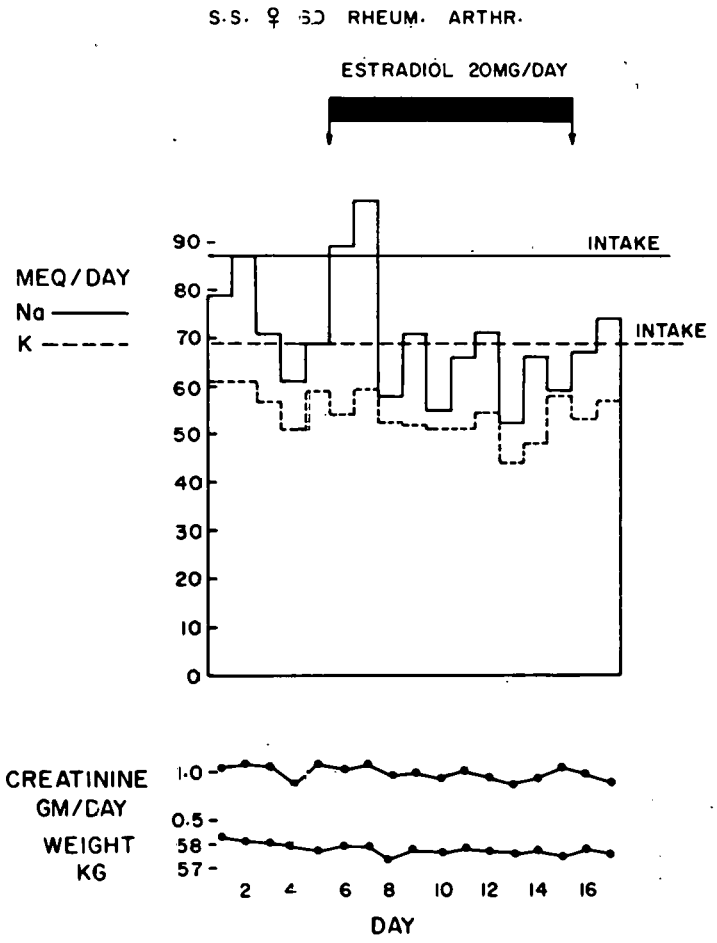

Figure 4. Urinary excretion of sodium and potassium. This subject had excretion of sodium greater than intake on first two days of estradiol.

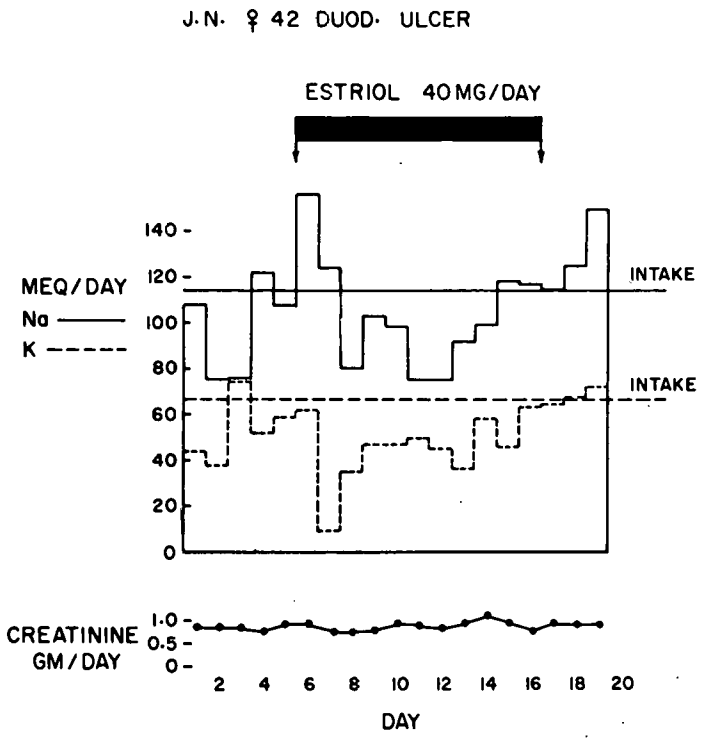

Figure 5. Urinary excretion of sodium and potassium. Estriol injections resulted in increased sodium excretion for one day followed by transient sodium retention.

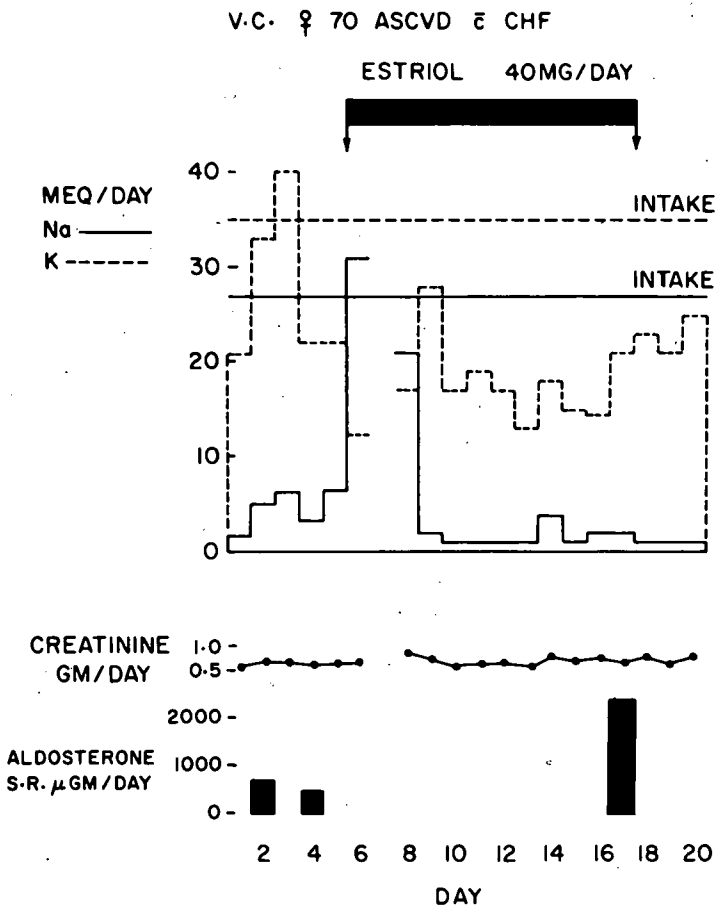

Figure 6. Urinary excretion of sodium and potassium. Estriol caused a transient increase in the very low sodium excretion in this woman with congestive heart failure. The aldosterone secretion rate rose from its already elevated levels of 630 and 438 to 2478 μg per day.

urine of the second day of estriol treatment was lost), the urine sodium rose to 32 and 20 respectively with suggestive reciprocal changes in potassium excretion. Subsequently during the remainder of the estriol treatment period, the urinary sodium returned to its previous low levels, in keeping with the measured increase in ASR.

DISCUSSION

Estriol is, under normal circumstances, i.e., in the nongravid state, derived from the in vivo biotransformation of estrone and estradiol in man. Studies of estrogen metabolism in pregnancy, however, have indicated that a considerable amount of the estriol excreted in urine may arise from other chemical pathways[23] in which 16α-hydroxydehydroepiandrosterone sulfate[24] and dehydroepiandrosterone sulfate[25] are important steroid precursors of estriol, and that the placenta is a major site of this biotransformation.[26] The activity of estriol in "classical" tests of estrogenic function is strikingly less than that of estradiol and estrone;[27] nevertheless its extraordinary production rate during gestation raises the possibility that any biological properties which it might be shown to possess could contribute to certain of the physiological alterations which accompany normal human pregnancy.

The present studies show that with respect to elevation of cortisol and thyroid-hormone binding globulin activity in man the metabolite estriol does not possess more than a small fraction of the activity of its ovarian precursor hormone estradiol. With due consideration of the fact that this conclusion is drawn on the basis of only short term studies, this difference in potency between estriol and estradiol indicates that the sustained increase in CBG and TBG activity during pregnancy may result primarily from biological actions of the latter hormone - or perhaps derivatives which are structurally distinct from estriol, or which undergo different pathways of metabolism in vivo. The latter is an important consideration, since one reason why estriol did not stimulate binding protein activity effectively in this study may relate to the markedly higher rate of renal disposal of this compound, compared with estradiol.[28]

Estradiol did not consistently affect the rate of cortisol secretion in this study. As noted, 2 of the estriol treated subjects increased their CSR by 50 per cent or more during treatment with this steroid and there was a small but highly significant increase in the mean CSR of the entire estriol treated group. Since both subjects with marked increases in CSR after estriol had a low CSR during the control period, it is conceivable that estriol treatment facilitated—or possibly coincided with—a spontaneous increase of adrenal activity in these otherwise chronically ill patients. However, this did not occur in the two estradiol treated subjects with low control rates of cortisol secretion; in any case, the CSR did not exceed the normal range in any subject despite relatively intense, short-term, estrogen treatment. The results are consistent with other observations on the CSR following the administration of synthetic estrogens.[13,29]

The most noteworthy findings in this study relate to the ability of estradiol and estriol to increase—sometimes to strikingly high levels—the rate of secretion of aldosterone in man. The effect could be demonstrated at low or high levels of salt intake (high and low baseline ASR control values respectively) and in at least one patient with primary aldosteronism as well. The stimulatory action of estriol and estradiol on the ASR is of special relevance to the situation in pregnancy since the ASR is known to increase substantially at this time.

The mechanism of the increased aldosterone production which occurs during pregnancy is not clearly understood. An important stimulant to the ASR at this time is the large amount of

progesterone which is produced during gestation. This steroid has been shown to competitively inhibit aldosterone action at the renal tubular level,[30] an effect which, as would be expected, results in a compensatory increase in aldosterone.[31]

It is clear from the present study that the striking increase in estradiol and estriol production which occurs in pregnancy may also contribute to the elevated ASR which characterizes the gravid state. The mechanism(s) of this apparently paradoxical estrogen effect is not clear although it could be explained if it could be shown that these steroids, like progesterone, were natriuretic substances. The preliminary observations reported here suggest this possibility although their tentative nature is emphasized. Layne and associates,[13] who also demonstrated increased aldosterone secretion as a result of treatment with synthetic estrogens, suggested that these hormones are sodium-retaining substances, citing the detailed study of Preedy and Aitken.[32] The latter report, however, shows a small transient net average sodium chloride loss on Day 1 in the estrogen treated group; although data for individual subjects are not given. The patients reported here (Figures 3-6) also had a transient negative sodium balance in the initial period of estradiol or estriol treatment. This was generally followed by sustained sodium retention, and in one subject (J.N., Figure 5) by a clear "escape" phenomenon like that seen in the Preedy and Aitken study[32] and similar to that which is observed when aldosterone is administered to normal subjects.[33] The results strongly suggest that the apparent "salt-retaining" activity of these estrogens may in fact be sttributed to the increased aldosterone secretion which they stimulate. Lack of consistent and marked reciprocal changes in potassium balance are not at all unusual, even when large amounts of aldosterone are administered.[33]

If a transient natriuretic response consistently follows estrogen administration, the resultant stimulation of aldosterone secretion could ensue via stimulation of renal renin production. Indeed plasma renin activity is known to be elevated in human gestation[34] and has recently been found to increase after estrogen administration.[35]

In addition to its usual renal source, however, the increased plasma renin during pregnancy may be largely derived from uterine stores.[36] The enzyme can be found in amniotic fluid[37] and will form angiotensin II,[38] but apparently does not respond to the same physiologic stimuli—i.e., salt loading and hypervolemia—that suppress renal renin production.[39,40] This could provide another possible sustained stimulus to aldosterone production in pregnancy.

It is of interest that androgens, like progesterone, have also been shown to compete with aldosterone at the renal tubular level.[41,42] Indeed older studies by Kenyon and his co-workers[43] demonstrate a renal "escape" from testosterone-induced sodium retention which could well be mediated by aldosterone. More conclusive evidence of a similar property for estrogens would extend the spectrum of aldosterone antagonism to another class of natural hormones and one which, like progesterone, would have particular relevance to the alterations in ASR seen in pregnant women.

Other mechanisms than natriuresis for estrogen stimulation of aldosterone secretion are of course entirely possible and may for example include direct actions on the adrenal cortex, direct stimulation of renal renin production (and of uterine renin production as well in pregnancy, alterations in the metabolism of relevant substances such as renin, renin substrate,[44] angiotensin, progesterone, etc. Whatever this mechanism(s) proves to be, it is likely that this class of steroids—and particularly estriol—plays a significant role among the factors which evoke and sustain the striking hyperaldosteronism which characterizes the gravid state.

ACKNOWLEDGMENTS

Technical assistance during various phases of this study was rendered by Miss Evelyn Damgaard, Miss Judith Wiley, Mrs. Valentine Harrer, Miss Grace You Lin Yao, and Miss Janet Marie Cobb. Mrs. Nancy Gallagher and Miss Carmen Dominguez devised and supervised the constant diets. Mrs. Genevieve LaPinska and Mrs. Jane Kresler prepared the manuscript.

LITERATURE CITED

1. Maner, F. D., B. D. Saffan, R. A. Wiggins, J. D. Thompson, and J. R. K. Preedy. J. Clin. Endocr., 23:445, 1963.
2. Fishman, J., J. B. Brown, L. Hellman, B. Zumoff, and T. F. Gallagher. J. Biol. Chem., 237:1489, 1962.
3. Yousem, H. L., and D. Strummer. Amer. J. Obstet. Gynec., 88:375, 1964.
4. Katz, F. H., and A. Kappas. (Abstract) J. Clin. Invest., 44:1063, 1965.
5. Mueller, M. N., and A. Kappas. Proc. Soc. Exptl. Biol. (N.Y.), 117:845, 1964.
6. Mueller, M. N., and A. Kappas. J. Clin. Invest., 43:1905, 1964.
7. Gallagher, T. F., M. N. Mueller, and A. Kappas. Trans. Ass. Amer. Phycns., 78:187, 1965.
8. Slaunwhite, W. R., and A. A. Sandberg. J. Clin. Invest., 38:384, 1959.
9. Dowling, J. T., N. Freinkel, and S. H. Ingbar. J. Clin. Endocr., 16:280, 1956.
10. Watanabe, M., C. I. Meeker, M. J. Gray, E. H. Sims, and S. Solomon. J. Clin. Invest., 42: 1619, 1963.
11. Sandberg, A. A., and W. R. Slaunwhite. J. Clin. Invest., 38:1290, 1959.
12. Dowling, J. T., N. Freinkel, and S. H. Ingbar. J. Clin. Endocr., 16:1491, 1956.
13. Layne, D. S., C. J. Meyer, P. S. Vaishwanar, and G. Pincus. J. Clin. Endocr., 22:107, 1962.
14. Bonsnes, R. W., and H. H. Taussky. J. Biol. Chem., 158:581, 1945.
15. Sterling, K., and M. Tabachnik. J. Clin. Endocr., 21:456, 1961.
16. Seal, U. S., and R. P. Doe. Endocrinology, 73:371, 1963.
17. DeMoor, P., K. Heirwegh, J. F. Heremans, and M. Declerk-Raskin. J. Clin. Invest., 41: 816, 1962.
18. Peterson, R. E. Recent Progr. Hormone Res., 15:231, 1959.
19. Ulick, S., J. H. Laragh, and S. Lieberman. Trans. Ass. Amer. Phycns., 71:225, 1958.
20. Katz, F. H. Aerospace Med., 35:849, 1964.
21. Snedecor, G. W. Statistical Methods Applied to Experiments in Agriculture and Biology, 5th ed. Ames: Iowa State College Press, 1956.
22. Sandberg, A. A., M. Woodruff, H. Rosenthal, S. Nienhouse, and W. R. Slaunwhite. J. Clin. Invest., 43:461, 1964.
23. Gurpide, E., M. Angers, R. L. VandeWiele, and S. Lieberman. J. Clin. Endocr., 22:935, 1962.
24. Easterling, W. E., H. H. Simmer, W. J. Dignam, M. V. Frankland, and F. Naftolin. Steroids, 8:157, 1966.

25. Siiteri, P. K., and P. C. McDonald. J. Clin. Invest., 44:465, 1965.

26. Bolte, E., S. Mancuso, G. Eriksson, N. Wiquist, and E. Diczfalusy. Acta Endocr. (Kbh.), 45:535, 1964.

27. Miyake, T. Endocrinology, 69:534, 1961.

28. Brown, C. H., B. D. Saffan, C. M. Howard, and J. R. K. Preedy. J. Clin. Invest., 43:295, 1964.

29. Peterson, R. E., G. Nokes, P. S. Chen, and R. L. Black. J. Clin. Endocr., 20:495, 1960.

30. Landau, R. L., and K. Lugibihl. J. Clin. Endocr., 18:1237, 1958.

31. Laidlaw, J. C., J. L. Ruse, and A. G. Gornall. J. Clin. Endocr., 22:161, 1962.

32. Preedy, J. R. K., and E. H. Aitken. J. Clin. Invest., 35:423, 1956.

33. August, J. T., D. H. Nelson, and G. W. Thorn. J. Clin. Invest., 37:1549, 1958.

34. Brown, J. J., D. L. Davies, P. B. Doak, A. F. Lever, and J. I. S. Robertson. Lancet, 2:900, 1964.

35. Crane, M. G., J. Heitsch, J. J. Harris, and V. J. Johns. J. Clin. Endocr., 26:1403, 1966.

36. Ferris, T. F., P. Gorden, and P. J. Mulrow. Am. J. Physiol., 212:698, 1967.

37. Brown, J. J., D. L. Davies, P. B. Doak, A. F. Lever, J. I. S. Robertson, and M. Tree. Lancet, 2:64, 1964.

38. Gross, F., G. Schaechtelin, M. Ziegler, and M. Berger. Lancet, 1:914, 1964.

39. Brown, J. J., D. L. Davies, P. B. Doak, A. F. Lever, and J. I. S. Robertson. J. Endocr., 35:373, 1966.

40. Gorden, P., T. F. Ferris, and P. J. Mulrow. Am. J. Physiol., 212:703, 1967.

41. Kagawa, C. M., E. G. Shipley, and R. K. Meyers. Proc. Soc. Exptl. Biol. (N.Y.), 102:521, 1959.

42. Williamson, H. E. Steroids, 6:365, 1965.

43. Kenyon, A. T., K. Knowlton, I. Sandiford, F. C. Koch, and G. Lotwin. Endocrinology, 26: 26, 1940.

44. Helmer, O. M., and R. S. Griffith. Endocrinology, 51:421, 1952.

INFLUENCE OF ESTRADIOL AND ESTRIOL ON URINARY EXCRETION OF HYDROXYPROLINE IN MAN*

By

F. H. Katz† and A. Kappas‡

Hydroxyproline (hypro) is a major component of collagen and the amount of this imino acid excreted in urine is considered to reflect the rate of metabolic turnover of collagen.[1] Excessive hydroxyprolinuria characterizes certain endocrine disorders; and the exogenous administration of several natural hormones is known to increase hydroxyprolinuria in man. Thus patients with acromegaly have urinary levels of hypro which exceed the normal adult range of values, and pituitary dwarfs excrete less hypro than do normally growing children, in whom high levels of urinary hypro are characteristic. In addition to these changes attributed to greater or lesser amounts of pituitary growth hormone, alterations in urinary hypro are also observed when parathyroid or thyroid hormones are administered to man or when the relevant endocrine disorders are present. It appears, however, that adrenal glucocorticoids have little effect on urinary hypro output although it seems reasonable to suppose that the severe osteoporosis and soft tissue wasting of Cushing's syndrome may at some point be reflected in excessive hypro output.

The present study demonstrates that the natural ovarian hormone estradiol and its metabolite estriol both significantly decrease the urinary excretion of hypro following their administration to man. Estrogen suppression of hypro excretion was observed in both men and women, and in patients with primary and secondary (metastatic cancer) bone disorders characterized by profound hydroxyprolinuria. Moreover, both steroids were shown to counteract the hydroxyprolinuria associated with primary endocrine disease and the increased hypro output induced by certain natural hormones. A preliminary report has been published.[2]

METHODS

The subjects studied were housed on a metabolic ward during all study periods and maintained on diets from which gelatin desserts and candies were excluded. Most patients had rheumatoid arthritis or other musculoskeletal diseases unless otherwise noted; all served as their own controls for periods of at least one week or more before the administration of endocrine preparations, since patients with rheumatic diseases sometimes have increased urinary hypro excretion.[3] Steroids were dissolved in the solvent vehicle previously described[4] and administered by intramuscular injection; testosterone, human growth hormone (HGH)§ and parathyroid extract¶ were administered by intramuscular injection as well, and diethylstilbestrol and triiodothyronine were given by mouth.

*This paper appeared in J. Lab. Clin. Med., 71:65, 1968. The study was supported in part by USPHS Training Grant TI AM 5445-03.

†Present address: Department of Medicine, Loyola University Stritch School of Medicine, Hines, Illinois.

‡Present address: The Rockefeller University Hospital, New York, N. Y.

§Supplied through the kindness of the National Pituitary Agency, N.I.H.

¶Lilly Laboratories, Indianapolis, Indiana.

Urinary hypro was measured in 24 or 48 hour urine collections by the method of Prockop and Udenfriend.[5] Steroids and solvents added to the urine in the amounts administered to patients did not affect the hypro determinations, nor did solvent vehicle injections influence hypro excretion. Unless otherwise indicated the values for urinary hypro represent a total of both free and peptide-bound hypro. Measurements indicated as "free hypro" were made by the same technique, omitting the hydrolysis with HCl. Urinary creatinine was regularly determined to ensure complete urine collections; in several experimental periods urinary hypro was expressed, as noted, in mg/day per gram of creatinine because of incomplete collections. Urinary alpha-amino acid nitrogen was measured by the method of Rubinstein and Pryce.[6]

RESULTS

Estradiol was administered to 13 subjects in amounts of 5-20 mg/day for periods of 2-20 days. The injection of this hormone was followed by significant and consistent reductions in urinary hypro output in 11 of the 13 subjects; the results in 9 of these 11 subjects are shown in Figure 1. The decreases in urinary hypro output following this treatment reached levels as much as 60 per cent below control values (Subject E.M.), and frequently occurred on the first or second

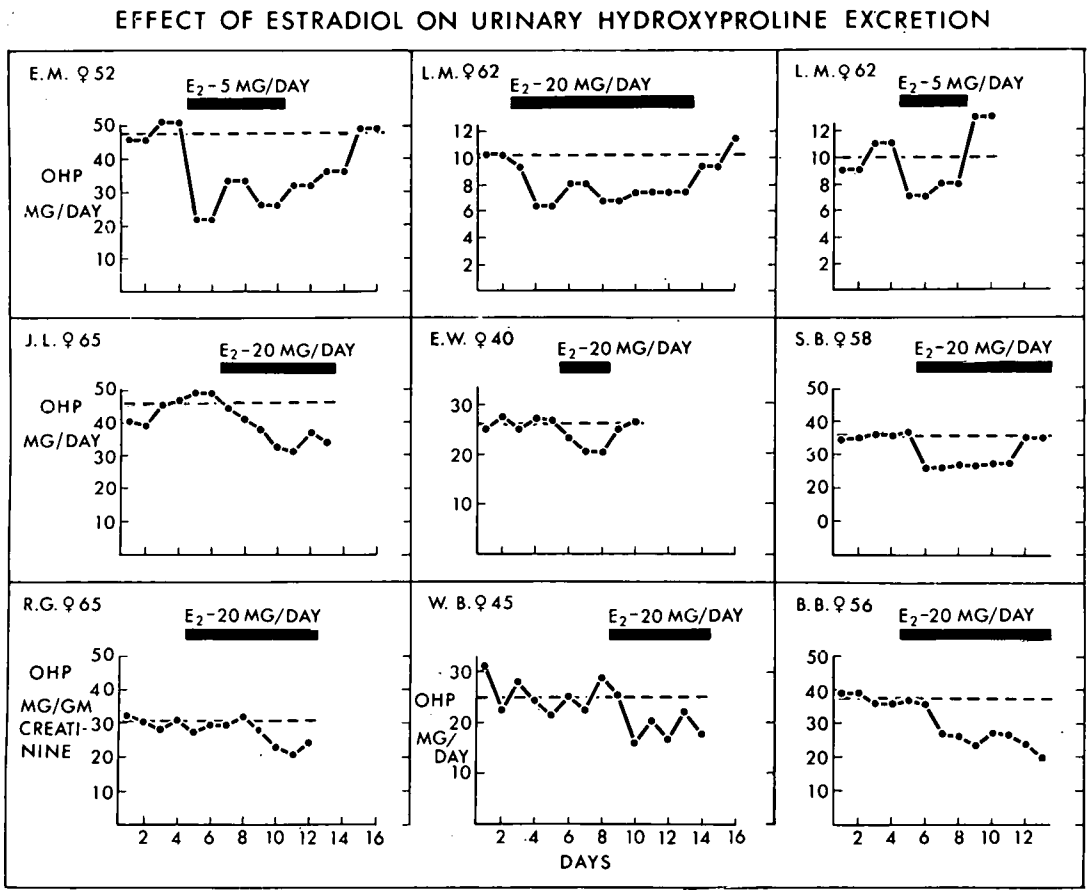

Figure 1. Effect of estradiol (E_2) on urinary total hydroxyproline (OH-P) excretion. The average value during the control period is indicated by the dashed line.

day of treatment. The response was sometimes delayed (Subjects J.L. and R.G.), however. The minimum amount of hormone required to induce this effect is not known; although most subjects received 20 mg/day, 5 mg/day was as effective as 20 mg/day in one patient (Subject L.M.). The reason why 2 out of 13 subjects did not respond is not clear. Following cessation of estradiol administration, urinary hypro usually returned to control values; but there was occasionally a return to baseline values while the estrogen was still being administered (Subject S.B.). Urinary "free hypro" excretion was studied in 3 subjects, and was also shown to decrease during estradiol treatment, 20-40 mg/day for 6-9 days. Mean control values of 2.29, 1.93, and 1.86 mg/day were diminished to mean values of 1.66, 1.46, and 1.41 respectively, during treatment.

Estriol is the principal recognized metabolite of estradiol in the non-pregnant state; it cannot undergo in vivo conversion back to its precursor hormone[7] or to the related active estrogen, estrone. Estriol also induced substantial reductions in urinary hypro output in man (9 out of 14 experiments). The results of studies in 6 subjects are shown in Figure 2. As with its precursor hormone, injection of this metabolite could rapidly decrease urinary hypro excretion (Subject W.W.); and urinary hypro quickly returned to control levels following its discontinuation or even before (Subject M.H.). The effect was observed in both males and females as well as in hysterec-

EFFECT OF ESTRIOL ON URINARY HYDROXYPROLINE EXCRETION

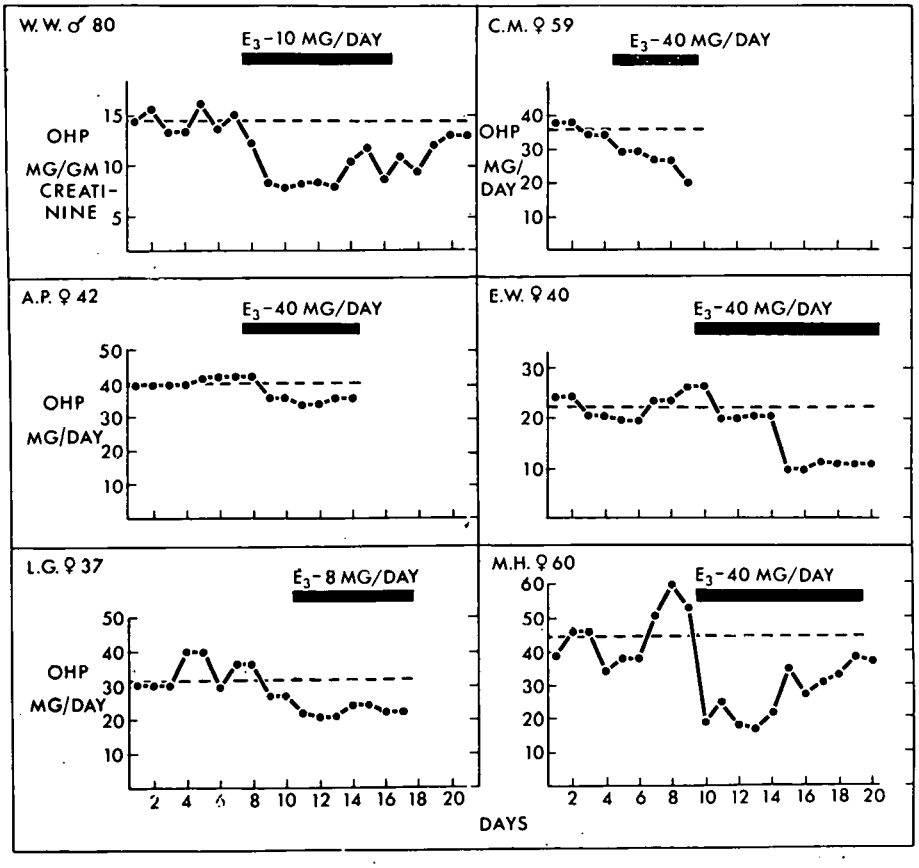

Figure 2. Effect of estriol (E_3) on urinary total hydroxyproline (OH-P) excretion. The average value during the control period is indicated by the dashed line.

tomized women. Estriol, like estradiol,[8] was also "anabolic" as reflected in consistent associated decreases in urinary alpha-amino acid nitrogen excretion shown demonstrated in one subject in Figure 3.

EFFECT OF ESTRIOL ON URINARY ALPHA AMINO NITROGEN

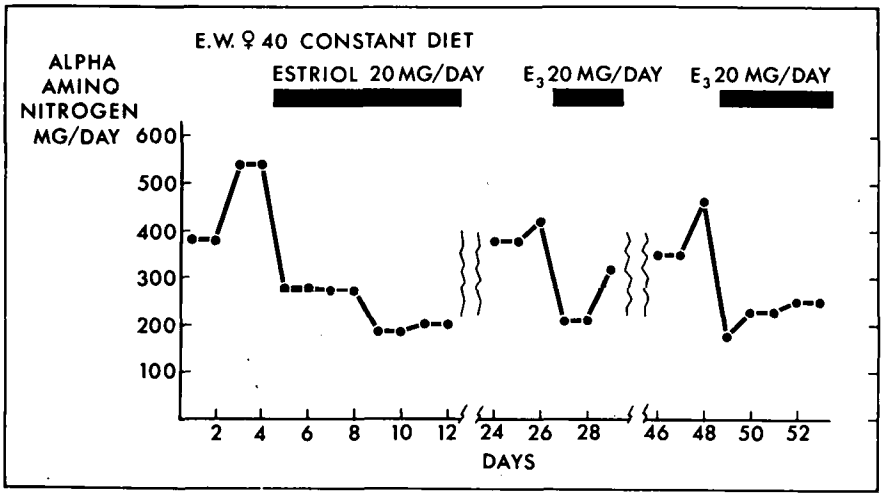

Figure 3. Effect of estriol (E_3) on urinary total alpha amino nitrogen excretion.

The levels of hypro in protein-free filtrates of blood serum were variable, even in the same individual. Studies in 6 subjects indicated that estradiol and estriol treatment was not accompanied by significant or consistent changes in serum hypro concentration. Attention has already been called by others[9] to the uncertainties regarding assays for hypro at physiologic levels, however.

The effect of combined estradiol and triiodothyronine (T_3) treatment on urinary hypro output was studied in 2 subjects. The results are shown in Figure 4. In both experiments the marked elevation in urinary hypro accompanying T_3 administration was almost entirely prevented by concurrent estradiol treatment.

The effect of combined estradiol and paratnyroid extract (PTE) treatment on urinary hypro output was also studied in 2 subjects. The results are shown in the top two sections of Figure 5. As with thyroid hormone, the excessive hydroxyprolinuria induced by PTE administration was significantly diminished by estradiol treatment. Subject J.F. (bottom of Figure 5) was a young woman with established hyperparathyroidism due to disseminated parathyroid carcinoma, in whom intensive estrogen treatment was utilized in an attempt to diminish the elevated serum calcium levels and counteract the severe catabolic effects of parathormone on bone and other tissue.[10] Estradiol significantly diminished the abnormally high hypro excretion in this patient but only when large amounts of the steroid were administered. This requirement for extremely large amounts of estrogen may reflect the excessive output of parathormone by the metastatic parathyroid cancer.

Figure 6 depicts the results of 3 studies in which estrogen (including the synthetic estrogen diethylstilbestrol) was shown to diminish the hydroxyprolinuria accompanying primary and sec-

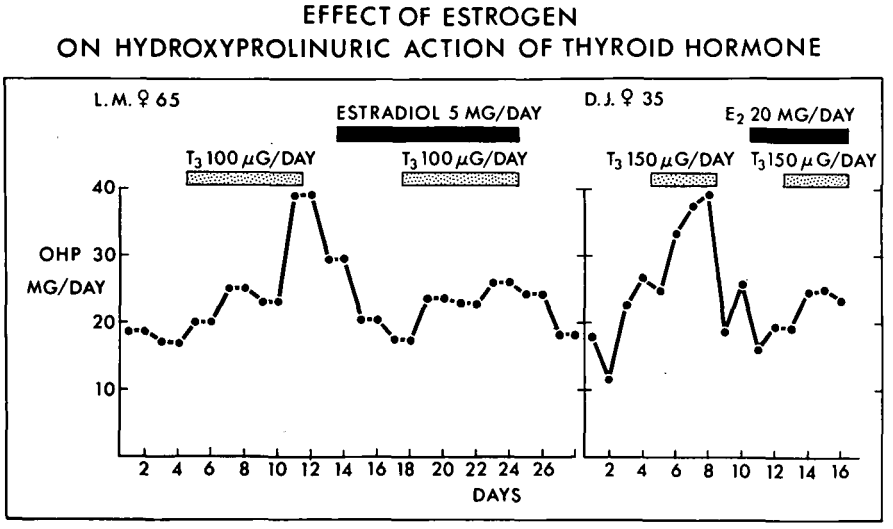

Figure 4. Effect of estradiol (E_2) on the urinary hydroxyproline (OH-P) elevation caused by the administration of triiodothyronine (T_3).

ondary bone disease (Subjects R.T. and E.W.) and that associated with excessive pituitary secretion of growth hormone (Subject L.R.). In none of these patients was estrogen in short term treatment capable of diminishing urinary hypro to normal levels however.

Estradiol was able to significantly decrease the hydroxyprolinuria of the acromegalic subject L.R. (Figure 6). In addition, 1 of 3 subjects given the metabolite estriol, 20 mg/day, together with 3 daily injections of 5 mg/day of HGH, failed to exhibit the same rise in urinary hypro which occurred when the HGH was given in the same amount alone. It is not clear why two out of the four subjects studied did not demonstrate with estrogen a diminution of the hydroxyprolinuria caused by HGH.

Total fasting, except for water and plain tea or coffee, for 6 days, resulted in a diminution of urinary hypro from control values averaging 20 mg/day to levels averaging 10 mg/day in two obese, otherwise normal women.

Testosterone also reduced urinary hypro, but the effects appeared to be less pronounced than that observed following estrogen treatment; the results of studies in 2 subjects are shown at the top of Table 1. There were similar responses seen in 3 women with metastatic breast cancer being treated with this hormone (Table 1, bottom portion). Patient B.M. in this group had soft tissue dissemination of tumor but no apparent bone metastases, thus probably accounting for her normal hypro output. Patients M.S. and A.C. both had skeletal tumor metastases and thus significantly elevated hypro excretion.[11]

DISCUSSION

This report demonstrates that estradiol and its metabolite estriol significantly decrease the output of urinary hypro in man. The effect is a rapid and almost consistent one and could frequently be observed on the first day of steroid administration. Return of hypro excretion to control levels was equally rapid and could sometimes be observed while steroids were still being

EFFECT OF ESTROGEN ON
HYDROXYPROLINURIC ACTION OF PARATHORMONE

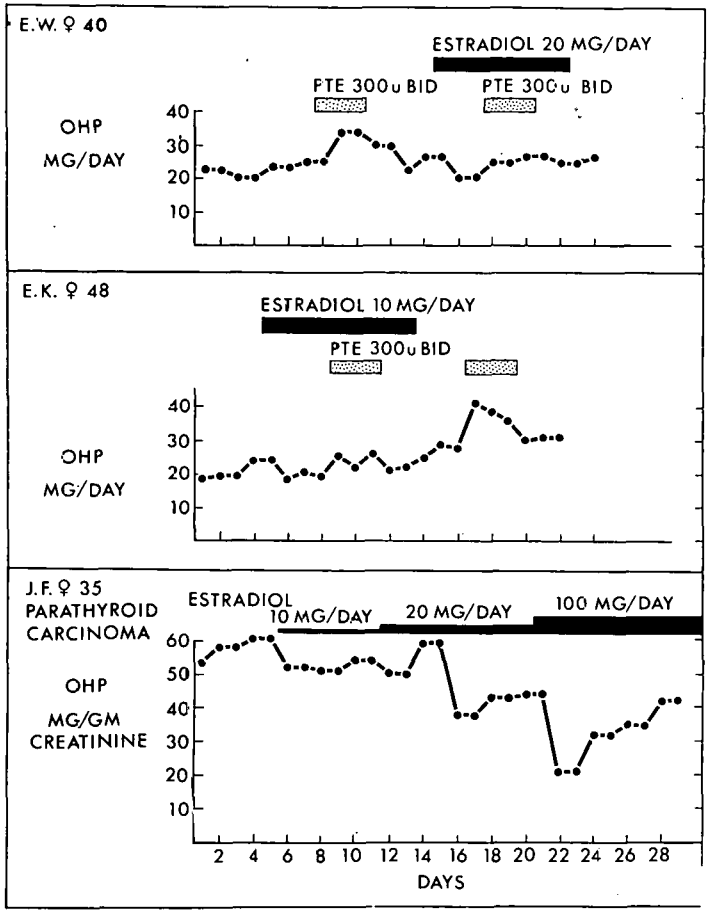

Figure 5. Effect of estradiol on the increased hydroxyproline (OH-P) excretion caused by parathyroid hormone.

EFFECT OF ESTROGEN ON
PATHOLOGICALLY ELEVATED HYDROXYPROLINURA

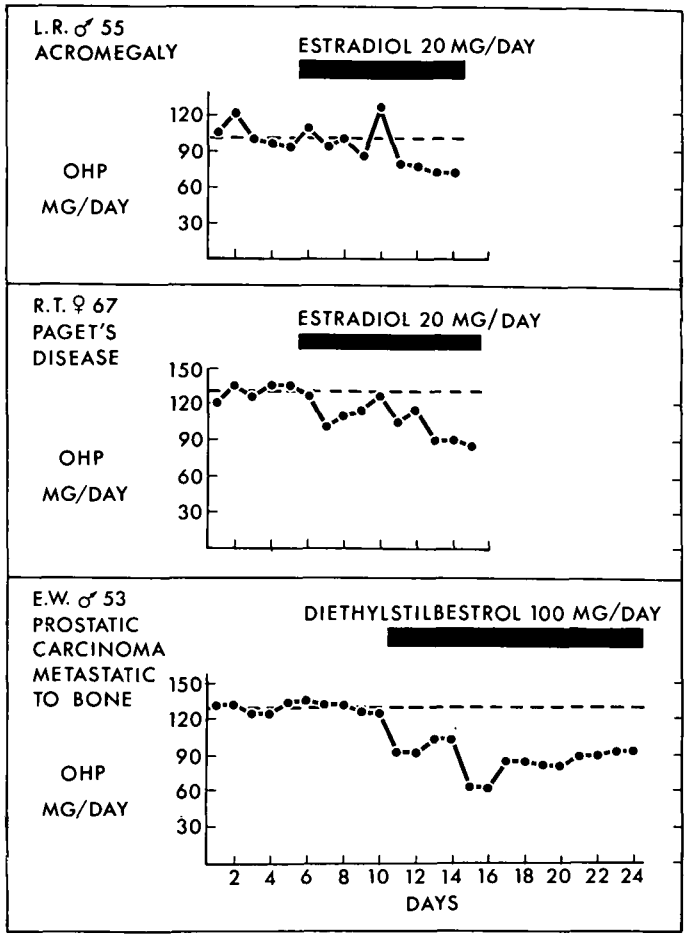

Figure 6. Effect of estrogens on pathologically elevated urinary hydroxyproline (OH-P) excretion. The average OH-P level during the control period is indicated by the dashed line.

Table 1

EFFECT OF TESTOSTERONE ON URINARY HYDROXYPROLINE (HYPRO) EXCRETION

	Control			Dose mg/day	Testosterone		
	Days	Hypro - mg/day			Days	Hypro - mg/day	
		Range	Mean			Range	Mean
Normal subjects							
M.K., ♂ 21	5	16.9 - 19.7	18.3	200	3	11.7 - 15.0	13.8
R.A., ♂ 37	4	38.4 - 49.0	43.0	100	4	25.8 - 33.9	29.8
Metastic breast carcinoma							
B.M., ♀ 55	4	28.3 - 38.3	33.5	50	2	20.8 - 23.9	22.8
M.S., ♀ 49	4	49.3 - 58.8	54.1	100	6	38.1 - 45.5	41.3
A.C. ♀ 47	4	59.6 - 71.0	68.0	100	4	43.8 - 52.9	47.3

injected. It is possible that, with respect to the latter response, compensatory mechanisms may come into play in the form, for example, of increased levels of hormones which augment urinary hypro, such as growth hormone, parathyroid hormone or thyroid hormone in some subjects. Estrogens are known to elevate plasma levels of HGH[12] and thyroid hormone, although the latter increase is due mainly to protein bound hormone, presumably the physiologically inactive moiety.[13]

The estrogen effect described in this report is not a specific one limited to classical target tissues for these sex hormones since hysterectomized women and men also had diminished urinary hypro levels after estrogen treatment. This estrogenic action on collagen metabolism could reflect in part the general "anabolic" nature of these hormones[8] since testosterone also diminished urinary hypro to some extent. Some evidence for such an "anabolic" effect of estradiol has been presented in studies from our laboratory,[14] in which injected radioactive proline was shown to disappear from human plasma more rapidly after estrogen treatment than during control periods. However an anabolic hormone (HCH) as well as catabolic hormones (thyroid and parathyroid hormones) both cause increased urinary hypro excretion.

There is some direct evidence for an "anti-catabolic" action of the estrogens, on the other hand, as reflected in their ability to counteract the increase in hypro that follows thyroid (Figure 4) and parathyroid (Figure 5) hormone treatment; and in the effects of estradiol on the specific activity of hypro extracted from skin collagen previously labeled by injected proline in rats.[15] Since estrogens have been shown to decrease bone resorption in man,[16] and most urinary hypro is derived from insoluble collagen, including bone collagen,[17,18] the anti-catabolic effect of estrogens may well explain the findings here presented.

A third possible mechanism of the estrogen-induced diminution of hypro excretion is a reduction of renal hypro clearance. Serum free hypro levels did not increase when urinary free hypro levels fell. In addition, when radioactive hydroxyproline is given intravenously, its excretion is increased after estrogen treatment rather than decreased.[14] Although this excludes an

effect of estrogens on renal handling of free hypro, an effect on the major hypro fraction, that which is peptide-bound, has not been ruled out, though it is unlikely.

In addition to the effect of estradiol on urinary hypro levels, this study has also revealed that estriol administration will reduce urinary hypro excretion. This irreversible metabolite of estradiol[7] has a largely different mode of origin in pregnancy when it also arises as a placental metabolite of dehydroepiandrosterone sulfate,[19] as well as of estradiol. Moreover, estriol shares with estradiol the property of general "anabolism" as shown by the diminished excretion of alpha amino nitrogen by patient E.W. (Figure 3) on three occasions when the metabolite was administered. Thus, during pregnancy, estriol, which is produced in extraordinarily large amounts,[20] could act as a "growth hormone" for the fetus in a manner analogous to that of the recently described placental lactogen;[21] the estriol effect on collagen metabolism may have special importance in this regard. Estriol has now been shown to share several other biological properties of estradiol in non-sexual tissues, including its ability to impair hepatic bromsulfophthalein excretion,[4] suppress experimental immune polyarthritis[22] and stimulate aldosterone secretion in man;[23] these observations thus provide several new experimental contexts in which it is shown that steroid metabolites may possess unique or at least distinct biological properties as compared with their precursor hormones.

The ability of estrogens to lower the elevated urinary hypro in acromegaly and in at least one HGH treated subject cannot at this point be easily explained. These hormones have been thought to be useful in the treatment of acromegaly although paradoxically they increase the plasma concentration of immunoreactive HGH in normal subjects.[12]

It is of interest that complete fasting, in this study, distinctly reduced hypro excretion although the increased plasma HGH levels associated with fasting[24] might have been expected to lead to increased urinary hypro output.

It has been suggested that Paget's disease is an inflammatory or auto-immune disorder.[25] The effect of estrogens on urinary hypro in the patient with this condition may have resulted from an anti-inflammatory action of these hormones analogous to their ability to suppress inflammation in certain immune reactions.[26]

The effect of diethylstilbestrol on urinary hypro in the patient with carcinoma of the prostate metastatic to bone (Figure 6) may have resulted in part from a specific action of the estrogen on the tumor, leading to some healing of the bony lesions. The alkaline phosphatase rose significantly during estrogen treatment in this patient, suggesting increased osteoblastic activity. A similar mechanism would account for the reduced hypro in the patients with metastatic breast cancer treated with testosterone (Table 1). Testosterone in two men, however, also reduced urinary hypro (Table 1), thus indicating that this hormone may have an action on collagen similar to that of the estrogens.

Finally, the positive correlation between urinary hypro excretion and serum alkaline phosphatase previously discussed by others[27] does not pertain to patients receiving estrogen treatment, since, despite the almost consistent diminution in hypro excretion, alkaline phosphatase values rise in about 50 per cent of estrogen treated subjects.[4]

ACKNOWLEDGMENTS

Helpful discussions about the results with Drs. Darwin J. Prockop and John L. Skosey are gratefully acknowledged.

Technical work for this study was performed by Miss Evelyn Damgaard, Miss Judith Wiley, Mrs. Valentine Harrer, and Miss Grace You-Lin Yao. Mrs. Genevieve LaPinska, Mrs. Jane Kresler, and Miss Patricia Keenan prepared the manuscript.

LITERATURE CITED

1. Smiley, J. D., and M. Ziff. Physiol. Rev., 44:30, 1964.
2. Katz, F. H., and A. Kappas. J. Clin. Invest., 44:1063, 1965. (Abstract)
3. Ziff, M., A. Kibrick, E. Dresner, and H. J. Gribetz. J. Clin. Invest., 35:579, 1956.
4. Mueller, M. N., and A. Kappas. J. Clin. Invest., 43:1905, 1964.
5. Prockop, D. J., and S. Udenfriend. Anal. Biochem., 1:228, 1960.
6. Rubinstein, H. M., and J. D. Pryce. J. Clin. Path., 12:80, 1959.
7. Maner, F. D., B. D. Saffan, R. A. Wiggins, J. D. Thompson, and J. R. K. Preedy. J. Clin. Endocrinol., 23:445, 1963.
8. Knowlton, K., A. T. Kenyon, I. Sandiford, G. Lotwin, and R. Fricker. J. Clin. Endocrinol., 2:671, 1942.
9. Keiser, H. R., J. R. Gill, A. Sjoerdsma, and F. C. Bartter. J. Clin. Invest., 43:1073, 1964.
10. Landau, R. L., and A. Kappas. Ann. Int. Med., 62:1223, 1965.
11. Platt, W. D., L. H. Doolittle, and J. W. S. Hartshorn. New Engl. J. Med., 271:287, 1964.
12. Frantz, A. G., and M. T. Rabkin. J. Clin. Endocrinol., 25:1470, 1965.
13. Sterling, K., and M. Brenner. J. Clin. Invest., 45:153, 1966.
14. Katz, F. H. J. Lab. & Clin. Med., 68:886, 1966. (Abstract)
15. Skosey, J. L., and A. Kappas. Fed. Proc., 26:426, 1967. (Abstract)
16. Gordan, G. S., and E. Eisenberg. Proc. Royal Soc. Med., 56:1027, 1963.
17. Prockop, D. J. J. Clin. Invest., 43:453, 1964.
18. Avioli, L. V., and D. J. Prockop. J. Clin. Invest., 46:217, 1967.
19. Siiteri, P. K., and P. C. McDonald. J. Clin. Invest., 44:465, 1965.
20. Fishman, J., J. B. Brown, L. Hellman, B. Zumoff, and T. F. Gallagher. J. Biol. Chem., 237:1489, 1962.
21. Josimovich, J. B., and B. L. Brande. Trans. N. Y. Acad. Sci., 27:161, 1964.
22. Mueller, M. N., and A. Kappas. Proc. Soc. Exptl. Biol. & Med., 117:845, 1964.
23. Katz, F. H., and A. Kappas. J. Clin. Invest., 46:1768, 1967.
24. Roth, J., S. M. Glick, R. S. Yalow, and S. A. Berson. Science, 140:987, 1963.
25. Maurice, P. F., T. N. Lynch, C. H. Bastomsky, T. A. Dull, L. V. Avioli, and P. H. Henneman. Trans. Ass. Amer. Physcns., 75:208, 1962.
26. Kappas, A., H. E. H. Jones, and I. M. Roitt. Nature, 198:902, 1963.
27. Klein, L., F. W. Lafferty, O. H. Pearson, and P. H. Curtiss. Metabolism, 13:272, 1964.

STAFF PUBLICATIONS

Charleston, D. B. Radiation Detectors in Nuclear Medicine. In Year Book of Nuclear Medicine, Vol. 2. Edited by J. L. Quinn, III. Chicago, Ill.: Year Book Publishers, Inc., 1967, p. 7.

DeGowin, R. L. Effect of Erythropoietin on the Recovery of Erythropoiesis After Partial-body Irradiation. (Abstract.) J. Lab. Clin. Med., 70:869, 1967.

DeGowin, R. L. Inhibition of Erythropoiesis During Stem Cell Proliferation. (Abstract.) Clin. Res., 15:275, 1967.

DeGowin, R. L. Postirradiation Sensitivity of Endogenous Stem Cells to Erythropoietin. (Abstract.) Exptl. Hematol., 15:93, 1968.

DeGowin, R. L., and S. Johnson. Effect of Endogenous Erythropoietin on Replicating Hemopoietic Stem Cells. Proc. Soc. Exptl. Biol. Med., 126:442, 1967.

Dukes, P. P. Erythropoietin. Its Nature and Mechanism of Action. 18. Colloquium der Gesellschaft für physiologische Chemie, 5-8 April 1967, Mosbach. Berlin: Springer-Verlag, 1967, p. 198.

Fitch, F. W., and D. A. Rowley. Mechanisms of Homeostasis of Antibody Formation in the Rat. Proc. 10th Congr. europ. Soc. Haemat., Strasbourg 1965; part II. Basel: S. Karger, 1967, p. 959.

Foft, J. W., W.-T, Hsu, and S. B. Weiss. Detection of T4-Specific 4S RNA by Sulfur Labeling. (Abstract.) Federation Proc., 27:341, 1968.

Goldwasser, E. Erythropoietin Induction of Red Cell Differentiation. In Experimental Biology and Medicine, Vol. 1. Edited by E. Hagen, W. Wechsler, and P. Zillikin. Basel: S. Karger, 1967, p. 234.

Gottschalk, A. Radioisotope Scintiphotography with Technetium-99m and Gamma Scintillation Camera. In Year Book of Nuclear Medicine, Vol. 2. Edited by J. L. Quinn, III. Chicago, Ill.: Year Book Publishers, Inc., 1967, p. 36.

Gottschalk, A., P. V. Harper, F. F. Jiminez, and J. P. Petasnick. Quantification of Respiratory Motion Artifact in Radioisotope Scanning with Rectilinear Focused Collimator Scanner and Gamma Scintillation Camera. In Year Book of Nuclear Medicine, Vol. 2. Edited by J. L. Quinn, III. Chicago, Ill.: Year Book Publishers, Inc., 1967, p. 273.

Griem, M. L., J. T. Ernest, M. L. Rozenfeld, and F. W. Newell. Eye Lens Protection in the Treatment of Retinoblastoma with High-Energy Electrons. Radiology, 90:351, 1968.

Griem, M. L., L. S. Skaggs, L. H. Lanzl, and F. D. Malkinson. Experience in Radiobiological Dosimetry with High Dose Rate Electrons. (Abstract.) Conference on High Energy Radiation Therapy Dosimetry, sponsored by the New York Academy of Sciences and the American Association of Physicists in Medicine, 15-17 June 1967.

Gross, M., and E. Goldwasser. Effect of Erythropoietin on RNA Synthesis. (Abstract.) Federation Proc., 27:394, 1968.

Gross, N. J., and M. Rabinowitz. Turnover of Mitochondrial and Nuclear DNA in Rat Liver. (Abstract.) J. Clin. Invest., 45:1064, 1967.

Harper, P. V., Jr., A. Gottschalk, and R. N. Beck. Recent Advances in Scanning. In Progress in Atomic Medicine, Vol. 2, Chap. 6. Edited by J. H. Lawrence. New York: Grune & Stratton, Inc., 1968, p. 168.

Hayward, R. S., J. L-Demare, and S. B. Weiss. Applications of RNA Polymerase in the Detection of Base Sequence Relationships Between Ribonucleic Acids. In Current Aspects of Biochemical Energetics. Edited by N. O. Kaplan and E. P. Kennedy. New York: Academic Press Inc., 1966, p. 227.

Hoffer, P. B., W. B. Jones, R. B. Crawford, R. Beck, and A. Gottschalk. Fluorescent Thyroid Scanning: A New Method of Imaging the Thyroid. Radiology, 90:342, 1968.

Hsu, W.-T., J. W. Foft, and S. B. Weiss. Effect of Bacteriophage Infection on the Sulfur-Labeling of SRNA. Proc. Natl. Acad. Sci., 58:2028, 1967.

Katz, F. H., and A. Kappas. Influence of Estradiol and Estriol on Urinary Excretion of Hydroxyproline in Man. J. Lab. Clin. Med., 71:65, 1968.

Katz, F. H., and A. Kappas. The Effects of Estradiol and Estriol on Plasma Levels of Cortisol and Thyroid Hormone-Binding Globulins and on Aldosterone and Cortisol Secretion Rates in Man. J. Clin. Invest., 46:1768, 1967.

Katz, F. H. Primary Aldosteronism with Suppressed Plasma Renin Activity Due to Bilateral Nodular Adrenocortical Hyperplasia. Ann. Int. Med., 67:1035, 1967.

Kingdon, H. S. Evidence for Partial Proteolysis During Factor IX Activation. (Abstract.) Federation Proc., 27:374, 1968.

Krantz, S., and V. Kao. Red Cell Aplasia: Demonstration of Plasma Inhibitor to Heme Synthesis and Antibody to Erythroblast Nuclei. (Abstract.) Clin. Res., 15:283, 1967.

Krantz, S. B. In Vitro Study of Polycythemia Vera. (Abstract.) Blood, 30:848, 1967.

Lanzl, L. H., and J. S. Laughlin. Dosimetry: High-Energy Radiation Therapy. Science, 158: 1499, 1967.

Lanzl, L. H. Magnetic and Threshold Techniques for Energy Calibration of High-Energy Radiations. (Abstract.) Conference on High Energy Radiation Therapy Dosimetry, sponsored by the New York Academy of Sciences and the American Association of Physicists in Medicine, 15-17 June 1967.

McKay, R., R. Druyan, and M. Rabinowitz. Intramitochondrial Loci for δ-Aminolevulinic Acid Synthetase and Ferrochelatase. (Abstract.) Federation Proc., 27:774, 1968.

Mosier, D. E. A Requirement for Two Cell Types for Antibody Formation in Vitro. Science, 158:1573, 1967.

Mosier, D. E., F. W. Fitch, and D. A. Rowley. Cellular Interaction During the Primary Immune Response in Vitro. (Abstract.) Federation Proc., 27:317, 1968.

Nair, K. G., A. F. Cutilletta, R. Zak, and M. Rabinowitz. RNA Polymerase Activities in Hypertrophied and Normal Rat Heart. (Abstract.) Clin. Res., 15:217, 1967.

Nakamoto, T., and E. Hamel. The Activation of 50S and 30S E. coli Ribosomes for Polyphenylalanine Synthesis. Proc. Natl. Acad. Sci., 59:238, 1968.

Nakamoto, T., E. Hamel, E. Klem, and R. Nyako. Activation of the 50S and 30S Ribosomal Subunits of E. coli for Polypeptide Synthesis. (Abstract.) Federation Proc., 27:459, 1968.

Palmer, R. H. The Formation of Bile Acid Sulfates: A New Pathway of Bile Acid Metabolism in Humans. Proc. Natl. Acad. Sci., 58:1047, 1967.

Palmer, R. H., and M. G. Bolt. Sulfate Esters of Lithocholic Acid and Its Conjugates: A New Pathway of Bile Acid Metabolism in Humans. (Abstract.) J. Lab. Clin. Med., 70:873, 1967.

Petasnick, J. P., and A. Gottschalk. Spleen Scintiphotography with Technetium-99m Sulfur Colloid and the Gamma Ray Scintillation Camera. In Year Book of Nuclear Medicine, Vol. 2. Edited by J. L. Quinn, III. Chicago, Ill.: Year Book Publishers, Inc., 1967, p. 183.

Pierce, C. W. The Effects of Endotoxin on the Immune Response in the Rat. Lab. Invest., 17: 380, 1967.

Rieselbach, R. E., L. B. Sorensen, W. D. Shelp, and T. H. Steele. Tubular Secretion of Urate per Unit GFR in Gout. (Abstract.) J. Clin. Invest., 46:1108, 1967.

Rimpila, J. J., S. C. Kraft, and F. W. Fitch. Differences in Colonic Staining with Technical Variations in Fluorescent Antibody Conjugation. Proc. Soc. Exptl. Biol. Med., 126:704, 1967.

Rowley, D., and F. Fitch. Clonal Selection and Inhibition of the Primary Antibody Response by Antibody. Scientific Memo: #147, Proc. Symp. Reg. Antibody Resp., Information Exchange Group No. 5, 1966, p. 1.

Rowley, J. D., and R. K. Blaisdell. Abnormal Marrow Karyotype in Chloramphenicol-Associated Aplastic Anemia. (Abstract.) Clin. Res., 15:287, 1967.

Rozenfeld, M. L., L. H. Lanzl, and H. Vetter. Determination of Radiation Isodose Levels Using a Semi-Automatic Isodensity Plotter. (Abstract.) Conference of the Society of Photographic Scientists & Engineers, 15-19 May 1967.

Rozenfeld, M. L., and L. H. Lanzl. Use of Film in Radiation Accident Re-enactment. (Abstract.) Conference of the Society of Photographic Scientists & Engineers, 15-19 May 1967.

Schaer, L. R., H. O. Anger, and A. Gottschalk. Gallium Edetate-^{68}Ga Experiences in Brain Lesion Detection with the Positron Camera. In Year Book of Nuclear Medicine, Vol. 2. Edited by J. L. Quinn, III. Chicago, Ill.: Year Book Publishers, Inc., 1967, p. 254.

Sinclair, J. H., B. J. Stevens, N. Gross, and M. Rabinowitz. The Constant Size of Circular Mitochondrial DNA in Several Organisms and Different Organs. Biochim. Biophys. Acta, 145: 528, 1967.

Tarlov, A. Turnover of Mitochondrial Phospholipids by Exchange with Soluble Lipoproteins in Vitro. (Abstract.) Federation Proc., 27:458, 1968.

Tarlov, A. R., and E. Mülder. Phospholipid Metabolism in Rat Erythrocytes: Quantitative Studies of Lecithin Biosynthesis. (Abstract.) Blood, 30:853, 1967.

Thompson, J. S., E. L. Simmons, M. K. Crawford, and C. D. Severson. Effect of Donor Strain on the Acquisition of Mutual Tolerance. Exptl. Hematol., 15:39, 1968.